Spring 4-23-2018

CHARACTERIZATION AND UTILIZATION OF HOT-WATER EXTRACTED LIGNIN FOR FORMALDEHYDE-FREE RESIN APPLICATIONS

Prajakta Dongre
pdongre@syr.edu

CHARACTERIZATION AND UTILIZATION OF HOT-WATER EXTRACTED LIGNIN FOR FORMALDEHYDE-FREE RESIN APPLICATIONS

by

Prajakta Dongre

A dissertation submitted in partial fulfillment of the requirements for the Doctor of Philosophy Degree
State University of New York
College of Environmental Science and Forestry
Syracuse, New York
April 2018

Department of Paper and Bioprocess Engineering

Approved by:
Biljana Bujanovic, Major Professor
Thomas Amidon, Co-Major Professor
Robert W. Malmsheimer, Chair, Examining Committee
Bandaru V. Ramarao, Faculty Chair
S. Scott Shannon, Dean, The Graduate School
Gary M. Scott, Director, Division of Engineering

Acknowledgements

I would like to thank my advisor Dr. Biljana Bujanovic for her constant guidance and continually encouraging me to push boundaries. Dr. Amidon, for his ever-ready helping hand and understanding. I appreciate Dr. Arthur Stipanovic for his support on thermal analysis, Dr. Mark Driscoll for his continued support on the hot-press and adhesive testing, Dr. Gary Scott for help on statistical analysis, and Dr. Robert Malmsheimer for feedback on the thesis. I would be remiss not to mention Debbie Dewitt for her words of reassurance, and the many times we solved the world's problems in your office, shall always be fond memories for me. Lynn Mickinkle, without whom we would all come to a standstill at PBE – thank you.

I would also sincerely appreciate the generous support of SUNY-ESF for the raw materials for this work, Dave Kiemle for support with NMR analysis, Mr. Burry and George Westby for continued assistance on the tensile tester, and Sean Hohm and Mr. Appleby for Pilot plant operations. I appreciate Fred Matt from USDA-FPL for carbohydrate analysis, and Paul Elsesser, Dr. Deanna Higgins and Dr. Feng Dong from Borgwarner Inc. for consultation on friction paper tests.

This work is funded by the USDA-McIntire-Stennis "Novel Green Adhesives from the ESF Biorefinery" Project.

I would like to thank my colleagues and friends Aditi Nagardeolekar, Chris Wood, Cher Jing, Kuoting Wang, Jake Finkelstein and Mathew Ovadias for helping me in some of my experiments. I would also like to acknowledge the many friends that I have made over the years in Syracuse – Chen, Gina, Jenny, Alan, Derek, Neil, Mangesh, Ericka, Dan, Shraddha, Sravani, Jennifer, Shama, Nidhi, Parvathy and so many more. Your support has been invaluable.

Finally, my family, Aai, Baba and Amu, have been a source of continuous support and encouragement for me, and I am most grateful for their belief in me.

Table of Contents

CHAPTER I: INTRODUCTION 1
1.1 Biorefineries/Lignocellulosic biomass 1
1.2 Outline 4
CHAPTER II: OBJECTIVES 5
CHAPTER III: LITERATURE REVIEW 7
3.1 Chemical composition 7
3.2 Cellulose 8
3.3 Hemicelluloses 9
3.4 Lignin 16
3.4.1 Biosynthesis of lignin 18
3.5 Lignin-carbohydrate complex (LCC) 22
3.6 Pretreatment methods 23
3.6.1 Acid Pretreatment 25
3.6.2 Alkaline Pretreatment 26
3.6.3 Organosolv Pretreatment 26
3.6.4 Biological Pretreatment 27
3.6.5 Electron beam irradiation treatment (EBI) 27
3.6.6 Hydrothermal treatment 28
3.7 Quantitative Studies and Qualitative Studies of Lignin Isolation 31
3.7.1 Lignin content determination 31
3.8 Lignin in Polymer Applications 33
3.8.1 Resins 33
CHAPTER IV: MATERIALS AND METHODS 44
4.1 Materials 45
4.2 Methods (Experimental): 45
4.2.1 Lignin Isolation and Characterization 45
4.2.2 Ash 46
4.2.3 Molecular Weight Distribution 47
4.2.4 Nuclear Magnetic Spectroscopy (NMR) 47
4.2.5 Acetylation 48
4.2.6 Free Phenolic Hydroxyl Group Content (PhOH) 48
4.2.7 Kappa number 49
4.2.8 Thermogravimetric Analysis (TGA) 49
4.2.9 Differential Scanning Calorimetry (DSC) 49
4.2.10 Electron beam irradiation (EBI) 49
4.2.11 Preparation of lignin based resins 50

4.2.12 Mechanical testing on glass fiber filters 53
4.2.13 Mechanical testing on friction paper 55
4.2.14 Mechanical testing on kraft paper 55
CHAPTER V: RESULTS AND DISCUSSION 56
5.1 Characterization of Crude Lignins 56
5.1.1 Chemical Composition of Crude Lignins 56
5.1.2 Molecular Weight Distribution of Biorefinery Lignins 62
5.1.4 Thermal Behavior of Biorefinery Lignins 66
5.2 Lignin based resins 70
5.2.1 Initial Scouting Studies 71
5.2.2 Effect of Higher Furfural Contents 76
5.2.3 Evaluation of Mechanical Properties of Biorefinery Lignins and their Resin Blends 78
5.2.4 Effect of Curing Agents on Mechanical Properties of Resin Reinforced Glass Fibers 90
5.2.5 Reinforcement applications 93
5.2.5.1 Reinforcement of friction paper 94
5.2.5.2 Reinforcement of kraft paper 99
CHAPTER VI: CONCLUSIONS 104
CHAPTER VII: RECOMMENDATIONS FOR FUTURE WORK 107
REFERENCES 109
APPENDIX 121
RESUME 132

List of Figures

Figure 1 Schematic of the different levels of the formation of a wood microfibril (a) minisheet cross-section believed to form from a single subunit, (b) elementary fibril cross-section, the assembly of 6 minisheets into a cellulose crystal. The consolidation of multiple elementary fibrils forms a microfibril, (c) microfibril cross-section composed of 6 elementary fibrils, (d) microfibril lateral section showing the series configuration of crystalline and amorphous regions [33]..... 8
Figure 3: O-acetyl-4-O methylglucuronoxylans, the main hemicelluloses found in hardwoods. Adapted from [39]..... 14
Figure 4: Glucomannan in hardwoods. Adapted from [39] 14
Figure 5: O-acetyl galactoglucomannans, main hemicelluloses found in softwoods. Adapted from [39] 14
Figure 6: Arabino-4-O-methylglucuronoxylan in softwoods. Adapted from [39]..... 15
Figure 7: Simplified Structure of Ferulic Acid (FA) Cross-Linking Arabinoxylan (AX) in Grass Cell Walls. The 1,4-β-linked xylan backbone is represented by dotted lines and the side sugars, arabinose (Ara), are shown in circles. Ester and ether bonds are shown by arrows as follows: (1) acetyl group, (2) ester linked FA to AX, (3) arabinose-lignin (4) 5–5 –ester linked FA dimer cross-linking AX chains, (5) FA ether linked to lignin. Adapted from [42]. 15
Figure 8: Representative lignin structure (poplar). Adapted from [49]. 17
Figure 9: Lignin precursors, *p*-coumaryl alcohol, coniferyl alcohol and sinapyl alcohol. Adapted from [49]. 17
Figure 10: Resonance stabilized monolignol phenoxy radicals [29]. 19
Figure 11: The structures that are produced during dimerization (bulk polymerization) and lignification (end-wise polymerization) have certain differences. Dimerization of coniferyl alcohol produces only three dimers, cross-coupling of coniferyl alcohol with a G unit gives only two main products [47]**.**... 20
Figure 12: Typical linkages found in lignin. Adapted from [54,55] 20
Figure 13: Formation of erythro and threo forms of β-O-4 structures by the addition of water to the quinone methide intermediates. Only the syn isomer of the quinone methide intermediate (R_1=H) is illustrated here, although this structure must contain syn and anti isomers [60]. 22
Figure 14: Common LCC structures found in lignocellulosic biomass [64]. 23
Figure 15: Desired effects of pretreatment on lignocellulosic biomass [68]. 24
Figure 16: Synthetic route of phenol-formaldehyde (PF) resins. Figure adapted from [112]..... 34
Figure 17: Step 1 of novolac formation: Formaldehyde reacts with phenol to form methylol phenol. Figure adapted from [112]..... 34
Figure 18: Step 2 of novolac formation: methylol phenol and phenol self-condense to form linear polymers. Figure adapted from [112]..... 35
Figure 19: Step 3 of novolac formation: Mechanism of HMTA crosslinking novolac resin during curing process. Figure adapted from [112]..... 35
Figure 20: Step 1 of resole formation: Formaldehyde reacts with phenol to form methylol phenol. Figure adapted from [112]. 36
Figure 21: Step 2 of resole formation: Methylol phenol forms dimethylene ether bridges. Figure adapted from [112]..... 36

Figure 22: Proposed scheme for LPF resins in alkaline conditions. Adapted from [133]. 38
Figure 23: Mechanism that governs the presence of higher electron density on Position 2 and 6 on lignin phenylpropanoid units in acidic medium: (**a**) the induction effect of the alkyl group at Position 1; and (**b**) the resonance effect of the electron pairs on the methoxy oxygen [136]. 40
Figure 24: Proposed mechanism of lignin-furfural condensation products: (**A**) xylose based carbohydrates breakdown to furfural; (**B**) lignin-lignin condensation takes place; and (**C**) lignin-lignin-furfural condensation product (adapted from [22,142–144]. 41
Figure 25: Classical reaction mechanism, as proposed in various sources. Adapted from Root (1956) [147]. 42
Figure 26: Reaction pathway through cyclic intermediates, proposed by Antal et al (1991) [148]. Adapted from Yang et al (2012) [149]. A is the pyranose form of xylose, and D is furfural. 43
Figure 27: Scheme showing the origin of SM, SMAH SMAH_IRR50 and SMAH_IRR100 lignins. Sugar maple wood chips undergo HWE at 160°C for 2 hours. The extract undergoes membrane separation 1 to produce SM lignins. The permeate from this membrane separation (Phase 1) undergoes membrane separation 2. The permeate from this membrane separation (Phase 2) is subjected to acid hydrolysis (1.5% H_2SO_4, 130°C and 45 minutes). The precipitate collected is SMAH lignin. SMAH lignin was subjected to two levels of EBI – 50 and 100 kGy producing SMAH_IRR50 and SMAH_IRR100..... 44
Figure 28: Scheme showing the origin of W, NHW, MS and WS lignins. The respective biomass undergoes HWE at 160°C for 2 hours. The extract is subjected to acidification, precipitation and the supernatant decanted. The precipitate is collected to give W, NHW, MS or WS lignins. 44
Figure 29: Representative stress-strain curves of PF and lignin-based resins. 54
Figure 30: Normalized molecular weight distribution of lignin samples isolated from different species from the SUNY-ESF biorefinery: sugar maple before acid hydrolysis (SM), sugar maple after acid hydrolysis (SMAH) hot-water extract, willow (W), miscanthus (MS) and wheat straw (WS) 63
Figure 31: Normalized molecular weight distribution of lignin samples isolated from different species from the SUNY-ESF biorefinery: sugar maple after acid hydrolysis (SMAH), SMAH electron beam irradiated at, 50 kGy (SMAH_IRR50) and 100 kGy) SMAH_IRR100). 64
Figure 32: TGA of biorefinery and technical lignins: SM, SMAH, W, NHW, MS, WS, KL, PL 67
Figure 33: TGA of SMAH lignin and its corresponding irradiated fractions of 50 and 100 kGy (SMAH IRR50 and SMAH IRR100) 68
Figure 34: Effect of curing temperature (150°C and 180°C) on tensile properties of resin blends with 5% furfural at curing pressure of 1.9MPa and reaction pH = 0.3 and 1. All samples are compared to PF resin which was cured at 180°C and 1.9MPa. Tensile strength per gram (N/m·g) was determined using Equation (2). 73
Figure 35: Effect of curing pressure (1.9MPa and 3.8MPa) on tensile properties of resin blends with 5% furfural at curing temperature of 180°C and reaction pH = 0.3 and 1. All samples are compared to PF resin which was cured at 180°C and 1.9MPa. Tensile strength per gram (N/m·g) was determined using Equation (2). 73
Figure 36: Effect of pH on tensile properties (tensile strength and elastic modulus) resin blends at curing temperature and pressure of 180°C and 1.9MPa. Tensile strength per gram (N/m·g) was determined using Equation (2). 75

Figure 37: Mechanical properties (tensile strength and Young's modulus) of resin blends prepared from MS lignin at 0% furfural at pH 0.65 (MS F0 0.65) and 50%, 100% and 200% furfural at pH 1 (MS_F50_1, MS_F100_1, and MS_200_1). The results are compared to SMAH_F0_0.65 and SMAH_F50_1. All resins were cured at of 180°C and 1.9MPa. Tensile strength per gram (N/m·g) was determined using Equation (2). 78
Figure 38: Mechanical properties of crude lignin fractions (SMAH, W, NHW, MS, WS, PL, KL, SMAH IRR 50 and SMAH IRR 100). All resins were cured at of 180°C and 1.9MPa. Tensile strength per gram (N/m·g) was determined using Equation (2). 80
Figure 39: Mechanical properties (tensile strength and elastic modulus) of resin blends at curing temperature and pressure of 180°C and 1.9MPa. All blends were prepared at pH 0.65 with 0% furfural. Tensile strength per gram (N/m·g) was determined using Equation (2). 80
Figure 40: Mechanical properties (tensile strength and elastic modulus) of resin blends at curing temperature and pressure of 180°C and 1.9MPa. All blends were prepared at pH 1 with 50% furfural. Tensile strength per gram (N/m·g) was determined using Equation (2). 81
Figure 41: Normalized molecular weight distribution of resins blends prepared at 0% furfural and pH 0.65. Normalized molecular weight distribution of SMAH crude lignin from Figure 30 lignin is used as a reference. 87
Figure 42 Normalized molecular weight distribution of resins blends prepared at 50% furfural and pH 1. Normalized molecular weight distribution of SMAH crude lignin from Figure 30 is used as a reference. 88
Figure 43: Effect of curing agents (HMTA and furfural) on the mechanical properties of MS F50 and W F50 reinforced glass fibers. All resins were cured at 180°C and 1.9MPa. Tensile strength per gram (N/m·g) was determined using Equation (2). 91
Figure 44: Thermal degradation behavior of select crude lignins (MS, SMAH and SMAH_IRR100), corresponding resins (MS_F50_1 and SMAH_IRR100_F0_065) and PF. All resins tested are prior to curing. 95
Figure 45: Effect of heat aging on the mechanical properties of PF, MS_F50_1, SMAH_F0_1, and SMAH_IRR100_F0_1 reinforced glass fibers. All resins were cured at 180°C and 1.9MPa. Tensile strength per gram (N/m·g) was determined using Equation (2). PF T, MS_F50_1 T, SMAH_F0_065 T and SMAH_IRR100_F0 065 T represent the mechanical properties of the respective resins after being exposed to 150°C for 22 hours. 96
Figure 46: Effect of heat aging on the mechanical properties of PF and MS_F50_1 reinforced friction paper. All resins were cured at 180°C and 1.9MPa. Tensile strength per gram (N/m·g) was determined using Equation (2).MS F50 T and PF T represent the mechanical properties of the resins after being exposed to 150°C for 22 hours. 96
Figure 47: Effect of hot oil exposure on the mechanical properties of PF and MS_F50_1 reinforced friction paper. All resins were cured at 180°C and 1.9MPa. Tensile strength per gram (N/m·g) was determined using Equation (2). MS F50 ATF and PF ATF are representative of the resins exposed to automatic transmission fluid (ATF) and 110°C for 22 hours. 97
Figure 48: Effect of HMTA on the mechanical properties of MS F50 and W F50 reinforced softwood kraft paper. All resins were cured at 180 °C and 1.9 MPa. Tensile strength per gram (N/m·g) was determined using Equation (2). 101

Figure 49: Effect of HMTA on the mechanical properties of MS F50 and W F50 reinforced hardwood kraft paper. All resins were cured at 180°C and 1.9MPa. Tensile strength per gram (N/m·g) was determined using Equation (2). 102

List of Tables

Table 1: Three major constituents of selected species based on oven dried mass. [1][29] [2][30] [3][31] [4][32] 7
Table 2: The types of hemicelluloses in hardwoods, softwoods and gramineae and their backbones, side chains and linkages [41]. 12
Table 3: Frequency of linkages typically found in lignin. Structures are shown in Figure 12. 21
Table 4: Lignin-based resin blends studied in these experiments with their furfural content and reaction pH condition – design of experiment matric. The lignin sample used in these experiments: SMAH (the fraction separated from sugar maple hot-water extract after acid hydrolysis). Kraft lignin (KL) was used as a control..... 51
Table 5: Lignin-based resin blends studied in these experiments with their furfural content and reaction pH condition. The lignin sample used in these experiments: miscanthus (MS). 52
Table 6: Lignin-based resin blends studied in these experiments with their furfural content and reaction pH condition. The lignin samples used in these experiments: willow (W), Northern hardwoods (NHW), wheat straw (WS) and PL..... 52
Table 7: The pH and curing conditions at which the experiments were carried out with 5% furfural and 0% furfural – design of experiment matrix. Additional blends with 8% and 16% furfural prepared at pH = 1 were pressed at 1.9 MPa and 180 °C. The tensile strength per gram of the resin is calculated using Equation (2). 54
Table 8: Lignin content and ash content of biorefinery and technical lignins based on oven-dried mass (SM, SMAH, NHW, W, MS, WS, KL and PL) 58
Table 9: Carbohydrate composition of biorefinery and technical lignins: SM, SMAH, MS, WS, KL and PL (based on oven-dried mass) 59
Table 10: Free phenolic hydroxyl groups (PhOH) content and S/G ratios of biorefinery lignins. Reference values of PhOH and S/G ratios are also provided. 60
Table 11: Number average molecular weight (Mn), weight average molecular weight (Mw) and polydispersity (PD) of biorefinery lignins..... 63
Table 12: Glass transition temperature of biorefinery and technical lignins (SM, W, MHW, SMAH, SMAH_IRR50, SMAH_IRR100, MS, WS, KL and PL). [1] [185] 68
Table 13: Number average molecular weight (Mn), weight average molecular weight (Mw) and polydispersity (PD) of crude biorefinery lignins and their resins prepared at 0% furfural and pH 0.65. 87
Table 14 Number average molecular weight (Mn), weight average molecular weight (Mw) and polydispersity (PD) of crude biorefinery lignins and their resins prepared at 50% furfural and pH 1. . 88
Table 15: Kappa number of softwood and hardwood kraft paper used for reinforcement applications 101
Table 16: Data of 6 lignins (W, SMAH, SMAH_IRR50, SMAH_IRR100, MS, WS)..... 127
Table 17: p values: Tensile strength column is in bold to showcase no value is <0.05..... 129
Table 18*:* Values of improved strength at F0 and F50 as calculated by Equations (6) and (7), respectively. 131

List of Abbreviations

AGX: Arabinoglucuronoxylan
AISL: Acid-insoluble lignin
ASL: Acid-soluble lignin
AX: Arabinoxylan
ATF: Automatic transmission fluid
DHP: Dehydrogenative polymer
DMSO: Dimethylsulfoxide
DSC: Differential Scanning Calorimetry
EBI: Electron beam irradiation
EPA: Environmental Protection Agency
F0_03: Resin blend at 0% furfural and pH 0.3
F0_065: Resin blend at 0% furfural and pH 0.65
F0_1: Resin blend at 0% furfural and pH 1
F5_03: Resin blend at 5% furfural and pH 0.3
F5_065: Resin blend at 5% furfural and pH 0.65
F5_1: Resin blend at 5% furfural and pH 1
F8_1: Resin blend at 8% furfural and pH 1
F16_1: Resin blend at 16% furfural and pH 1
F50_1: Resin blend at 50% furfural and pH 1
F100_1: Resin blend at 100% furfural and pH 1
F200_1: Resin blend at 200% furfural and pH 1
FA: Ferulic acid
FTIR: Fourier transform infrared spectroscopy
G-unit: Guaiacyl unit
GAX: Glucuronoarabinoxylan
H-unit: *p*-hydroxyphenylpropanoid unit
HMTA: Hexamethylenetetramine
HSQC: Heteronuclear single quantum correlation
HWE: Hot water extraction
KL: Kraft lignin
LCB: Lignocellulosic biomass
LCC: Lignin carbohydrate complex
LMW: Low molecular weight
LPF: Lignin-phenol-formaldehyde
MeGlcA: 4-O-methyl-α-D-glucuronic acid
Mn: Number average molecular weight
MS: Miscanthus
Mw: Weight average molecular weight
MWL: Milled wood lignin
NHW: Northern hardwoods
NMR: Nuclear magnetic resonance
PD: Polydispersity
PF: Phenol formaldehyde
PhOH: Free phenolic hydroxyl groups
PL: “Pure lignin”
S-unit: Syringyl unit
SEC: Size exclusion chromatography
SEM: Scanning electron microscopy
S/G ratio: Syringyl-to-Guaiacyl ratio
SM: Sugar maple

SMAH: Lignin isolated from the hot water extract of SM
SMAH_IRR50: SMAH lignin irradiated at 50 kGy
SMAH_IRR100: SMAH lignin irradiated at 100 kGy
Tg: Glass transition temperature
TGA: Thermogravimetric analysis
THF: Tetrahydrofuran
UDPG: Uridine diphosphate glucose
W: Willow
WS: Wheat straw

P. Dongre, Characterization and utilization of hot-water extracted lignin for formaldehyde-free resin applications

Abstract: Phenol formaldehyde (PF) is found across a wide variety of applications, from wood adhesives in plywood and particleboard, to friction materials in automotive break parts and as a coating material in several markets. However, it is a petrochemical product and formaldehyde has also been classified as a carcinogen by the Environmental Protection Agency (EPA). Lignin-furfural resins are proposed as sustainable and safe formaldehyde-free alternatives.

Lignins recovered from hydrolysates of the hot water extraction (HWE) process of select angiosperms; sugar maple (SM), willow (W), mixture of northern hardwoods (NHW), miscanthus, (MS) and wheat straw (WS) were used as raw materials. In addition, crude lignin recovered after acid hydrolysis of sugar maple hot water extract (SMAH) and SMAH after electron-beam irradiation (EBI) at 50 kGy (SMAH_IRR50) and at 100 kGy (SMAH_IRR100), were also used. The biorefinery lignins were characterized for their chemical composition and inherent properties via wet chemistry and instrumental techniques (HSQC, SEC, TGA and DSC). Two technical lignins, kraft (KL) and a lignin from dilute acid treatment (PL) were also selected for control purposes.

The effect of reaction pH, furfural content, curing conditions (180°C and 1.9 MPa) and curing agents (HMTA and furfural) on the mechanical properties of the lignin based resins is determined. Testing of mechanical properties was conducted on resin reinforced glass fiber filters. Glass fiber filters were chosen for their inert nature and any improvement in strength was assumed to be of the resin itself.

Based on the results obtained from the tests performed on glass fiber filters, select resins were tested for their mechanical properties on friction paper, and softwood and hardwood kraft papers for their reinforcement ability. Commercially available novolac-type PF resin was used as a control for all mechanical testing.

Resins prepared from MS and SMAH lignin show better mechanical properties compared to other biorefinery lignins and are also comparable with PF resin. The good mechanical strength of resins prepared from MS and SMAH is attributed to higher S/G ratio and free phenolic hydroxyl group content – features that determine reactivity of the lignin.

Keywords: lignin; hot-water extraction; formaldehyde-free lignin resin blend; furfural; phenol-formaldehyde (PF), glass fiber filters, friction paper, softwood kraft paper, hardwood kraft paper, Angiosperms

P. Dongre
Candidate for the degree of Doctor of Philosophy, April 2018
Biljana Bujanovic, PhD
Thomas Amidon, PhD
Department of Paper and Bioprocess Engineering
Division of Environmental and Resource Engineering, State University of New York College of Environmental Science and Forestry, Syracuse, NY

CHAPTER I: INTRODUCTION

1.1 Biorefineries/Lignocellulosic biomass

The lignocellulosic biorefinery based on wood, agricultural residues or paper waste may be the most important endeavor to replace fossil fuels in the future. These raw materials undergo several operations, including pretreatment, separation, purification, hydrolysis, and fermentation to produce a broad palette of products, including alternative fuels, bioplastics, chemicals, materials and sorbents [1]. The main polymer constituents of lignocellulosic biomass are cellulose, lignin, and hemicelluloses. When lignocellulosics undergo pretreatment processes, the degradation of at least one polymer occurs, depending on the reagents and conditions used. One approach is to use a method that degrades the hemicellulose constituent and keeps the other two, lignin and cellulose, largely intact [2]. Hot-water extraction, a pretreatment method based on autohydrolysis, utilizes this approach. It is recommended as an environmentally benevolent process, with limited corrosion, no sludge generation, and low capital and operational costs [2]. This process does not use any mineral acids or bases possibly preventing extensive degradation of lignin and cellulose, making separation processes less complex. A relatively large part of hemicelluloses (~80% of total hemicelluloses in hardwoods, mostly xylans) is degraded to shorter chains, oligomers, and monosaccharides with limited degradation to furfural (pentoses) and hydroxymethylfurfural (hexoses) [1,2]. These carbohydrates can be used as a substrate for fermentation to produce various compounds, such as ethanol, butanol, polyhydroxyalkanoates, succinic acid, and xylitol. High value added chemicals can be produced from the undegraded lignin and cellulose such as resins, bioplastics, activated carbon and nanocellulose, which in turn increase the value of the biorefinery.

Phenol formaldehyde (PF) resins are routinely used in wood products, such as particle boards, plywood, finger-jointing fields, cement mold boards, container boards as well as composite

materials, thermal insulating materials, surface coatings, friction materials and laminated resins. Almost two-thirds of the wood industry currently employs phenol-formaldehyde (PF) as the commercial adhesive [3–6]. PF resins are produced from petro-chemicals, phenol and formaldehyde and are divided into two classes – novolacs and resoles. Novolacs are produced in the presence of an acid catalyst, with a phenol to formaldehyde ratio greater than 1 and require a curing agent such as hexamethylenetetramine (HMTA). Resoles are prepared in alkaline conditions with phenol to formaldehyde ratio less than 1 and do not require a curing agent [7]. PF resins have several advantages, such as high mechanical strength to prevent delamination, resistance to moisture, weather resistance, and excellent temperature stability [8–10]. Despite the advantages of PF resins, the oil-dependent price of phenol restricts their broad applications. [7,11]. Furthermore, phenol and formaldehyde are environmentally unfriendly and toxic substances [11], with LD_{50} (lethal dose, 50%) values in rats of 317 mg/kg and 65 mg/kg, respectively. In addition, formaldehyde has been classified as a carcinogen by the Environmental Protection Agency (EPA) since 2008, requiring removal of formaldehyde from consumer products. Therefore, there is a need to develop a replacement which is expected to be environmentally friendly, safer for human use, economical (preferably independent of oil prices), and possess comparable mechanical properties to those of PF resin. An alternative which has been investigated in this study is a hot-water extracted lignin-based resin.

Utilization of lignin for PF resin applications has long been studied. However, most of the work aims to replace phenol with lignin to produce lignin-phenol-formaldehyde (LPF) resins [12–15]. Sulfur containing kraft lignin which is the most readily available source of lignin currently, also is the subject of most research. Moreover, the application of these LPF resins is predominantly for resole-type products [7,14,16]. Comparatively lesser work has been done in novolac-type applications.

In this study, lignin isolated from hot water extracts of select Angiosperms such as sugar maple (SM), willow (W), miscanthus (MS) and wheat straw (WS) has been used as a raw material for producing resins. Lignin after acid hydrolysis of sugar maple hot water extract (SMAH), electron beam irradiated SMAH lignin at two intensities - 50 kGy (SMAH_IRR50) and 100 kGy (SMAH_IRR100) and lignin from hot water extract of a mixture of northern hardwoods (aspen, maple and red oak; NHW) were also used as raw materials. Electron beam irradiation was performed as it was expected that the molecular weight of lignin would decrease. Some preliminary results showed that low molecular weight lignin was a better candidate for resin production. Therefore, the effect of irradiation on lignin structure is also investigated.

Hot water extraction trials were performed in the State University of New York, College of Environmental Science and Forestry (SUNY-ESF) pilot plant 65 ft^3-digester. Technical lignins such as kraft lignin (KL) from Sigma Aldrich and "pure lignin" (PL) obtained from Pure Lignin Environmental Technologies have been used as controls in this investigation. PL was isolated from sugar maple wood shavings after a "weak acid treatment." Furfural, which is also designed as a biorefinery product [2], has been investigated as a potential crosslinking agent for lignin. Therefore, this study aims to produce formaldehyde-free lignin based resins.

Furfural has several uses in the plastics, food and pharmaceutical industries, as a solvent in the chemical industry, and even as a precursor for other high value products. It can be produced by conversion of 5-carbon sugars in the presence of acid catalyst via dehydration [17–22]. Furfural has been shown to be a potential cross-linking agent which can form lignin-furfural condensation products [23].

Factors such as reaction pH, curing conditions (curing agent, temperature and pressure) were varied, to produce resins from biorefinery lignins: SM, W, MS, WS, SMAH, NHW, SMAH_IRR50, and SMAH_IRR100, and technical lignins KL and PL. The resins were characterized for molecular weight distribution by size exclusion chromatography (SEC),

thermal degradation behavior by thermogravimetric analysis (TGA). The mechanical properties of the resins were tested for both resole (adhesives) and novolac-type (reinforcement) applications.

1.2 Outline

This document is broken in to seven chapters each contributing to an overall understanding of the work done. Chapter 1 briefly introduces some key concepts covered, and provides the initial motivation for this work. Chapter 2 lists the objectives to be achieved. Chapter 3 provides an extensive, but not exhaustive, literature review. Chapter 4 details the materials and methods used to perform the experiments. Chapter 5 discusses the results obtained, in-depth. Section 5.1 details the characterization of the lignin samples for its chemical composition (lignin content, ash content and carbohydrate content), inherent properties (free phenolic hydroxyl groups, S/G ratio and molecular weight distribution), and thermal behavior (thermal degradation and glass transition). Section 5.2 discusses the mechanical properties of the lignin based resins produced. The various sub-sections of Section 5.2 explore the effects of various parameters and conditions varied during resin preparation, including potential applications in friction paper and softwood and hardwood kraft papers. A summary of conclusions is encompassed in Chapter 6. Recommendations for future work are provided in Chapter 7.

CHAPTER II: OBJECTIVES

The main aim of this study is to determine the viability of lignin, obtained from hot water extracts of selected Angiosperms to produce formaldehyde-free resins as alternatives to phenol-formaldehyde resins. The key objectives of this work were to:

- Characterize biorefinery and technical lignins - SM, W, MS, WS, SMAH, NHW, KL, and PL for chemical composition (lignin, carbohydrates, and ash), including also properties such as S/G ratio and free phenolic hydroxyl groups (PhOH), and glass transition temperature (Tg), thermal degradation behavior, and molecular weight distribution by wet chemistry and instrumental techniques (DSC, TGA, HSQC, SEC).
- Determine the effect of electron beam irradiation (EBI) on the structure of SMAH lignin of two irradiation intensities – 50 kGy (SMAH_IRR50) and 100 kGy (SMAH_IRR100).
- Produce resins from biorefinery and technical lignins - SM, W, MS, WS, SMAH, SMAH_IRR50, SMAH_IRR100, NHW, KL, and PL.
- Determine the amount of additional furfural required to form a condensation product with properties comparable to PF.
- Understand the effect of reaction pH, curing conditions (temperature and pressure), species difference (sugar maple, willow, northern hardwoods, miscanthus and wheat straw) and curing agent (HMTA) on mechanical properties of the resins prepared.
- Determine applicability of the resins for resole-type applications of adhesives for wood veneers and novolac type- applications for reinforcement of glass fiber filters, softwood and hardwood kraft paper, and friction paper.

The lignins used in this study were recovered from different operations of the hot-water extraction pretreatment process proposed for a hardwood-based biorefinery. Due to the increased interest in the biorefinery, autohydrolysis lignin has been extensively studied. However, most literature reports on the lignin fraction remaining in the lignocellulosic material after hydrothermal pretreatment [24–27]. Comparatively, lesser work has been done on the lignin that is dissolved in the by-product stream; which is the subject of this study. Furfural is a projected product of the hardwood biorefinery [1,2], however, furfural used as a cross-linking agent in this study was a commercially available product. The lignin used in this study is unpurified and unmodified which is referred to as the "catch all pathway" in literature [28]

CHAPTER III: LITERATURE REVIEW

3.1 Chemical composition

Lignocellulosic biomass consists of three major polymeric constituents, cellulose, hemicelluloses, and lignin, and minor low-molecular weight constituents of organic (extractives) and inorganic (ash) nature. The amounts of cellulose, lignin, and hemicelluloses vary in species as shown in Table 1 [29]. Chemical composition of biomass also varies based on the environment in which it is grown, morphology and nutrition during growth.

Table 1: Three major constituents of selected species based on oven dried mass. [1][29] [2][30] [3][31] [4][32]

Species	Cellulose (%)	Hemicelluloses (%)	Lignin (%)
Hardwoods			
Acer rubrum[1]	42.0	25.2	25.4
Acer saccharum[1]	40.7	27.3	25.2
Betula verrucosa[1]	41.0	29.8	22.0
Betula papyrifera	39.4	33.1	21.4
Eucalyptus camaldulensis[1]	45.0	17.2	31.3
Eucalyptus glubulus[1]	51.3	21.3	21.9
Salix sp.[4]	44.1	20.4	21.8
Softwoods			
Abies balsamea[1]	38.8	25.8	29.1
Pseudotsuga menzeisii[1]	38.8	22.9	29.3
Pinus radiata[1]	37.4	28.9	27.2
Pinus syvestris[1]	40.0	24.9	27.7
Picea abies[1]	41.7	24.9	27.4
Picea glauca[1]	39.5	27.6	27.5
Graminae			
Corn cobs[2]	45.0	35.0	15.0
Wheat straw[2]	30.0	50.0	20.0
Sugarcane bagasse[2]	40.0	24.0	25.0
Miscanthus giganteus[3]	50.3	24.8	12.0
Miscanthus sinensis[3]	43.2	33.1	9.3
Miscanthus sacchariflorus[3]	49.1	27.4	12.1

3.2 Cellulose

Cellulose is a homopolysaccharide with β-D-glucopyranose units bound together with β (1→4) glycosidic bond. The glucopyranose units polymerize by the condensation reaction where water is expelled and the glycosidic bond is formed in a reaction catalyzed by glycosyltransferase/cellulose synthase enzymes; organized in higher plants in rosettes containing 36 subunits and producing simultaneously 36 cellulose chains called elementary fibrils [33]. Alternating glucopyranose molecules along chains in crystalline cellulose are rotated by 180°, meaning that the disaccharide (cellobiose) is considered the repeating unit. Intra and intermolecular hydrogen bonds combine cellulose chains to form elementary fibrils which bundle in the form of microfibrils which further combine to form cellulose fibers (Figure *1*).

Cellulose contains regions that are highly ordered (crystalline) as well disordered (amorphous) [34]. Cellulose content can range from 40~45% in most species (Table 1) and the degree of polymerization can vary from 500-15000 [35]. The crystallinity and high degree of polymerization adds to the recalcitrance of biomass and impedes enzymatic digestibility [36].

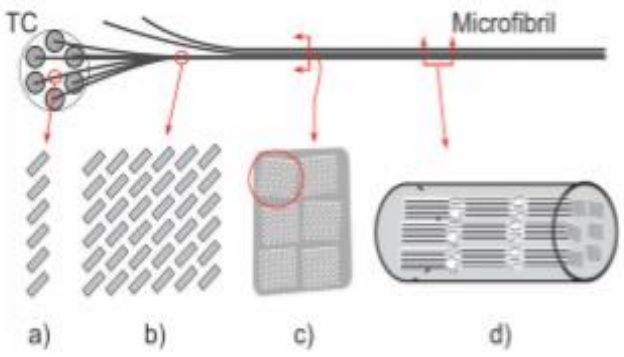

Figure 1 Schematic of the different levels of the formation of a wood microfibril (a) minisheet cross-section believed to form from a single subunit, (b) elementary fibril cross-section, the assembly of 6 minisheets into a cellulose crystal. The consolidation of multiple elementary fibrils forms a microfibril, (c) microfibril cross-section composed of 6 elementary fibrils, (d) microfibril lateral section showing the series configuration of crystalline and amorphous regions *[33]*.

3.3 Hemicelluloses

Hemicelluloses are heteropolysaccharides built from C5 and C6 sugars and a low degree of polymerizarion of 100-200. The function of hemicelluloses in woods is that as a supporting material in the cell wall [37]. In acidic conditions, hemicelluloses can relatively easily hydrolyze to monomeric building monosaccharides, including D-glucose, D-mannose, D-galactose, D-xylose, L-arabinose, and small amounts of L-rhamnose, along with D-glucuronic acid, 4-O-methyl-D-glucuronic acid, and D-galacturonic acid [29] (**Error! Reference source not found.**).

The content of hemicelluloses varies in hardwoods (25~35%), softwoods (25~30%) and grasses (20~40%) [29–31,38]. Individual species are listed in Table 1. The hemicelluloses types in hardwoods, softwoods, and gramineae (*Poaceae*) differ in sidechains and linkages and a summary is shown in Table *2*.

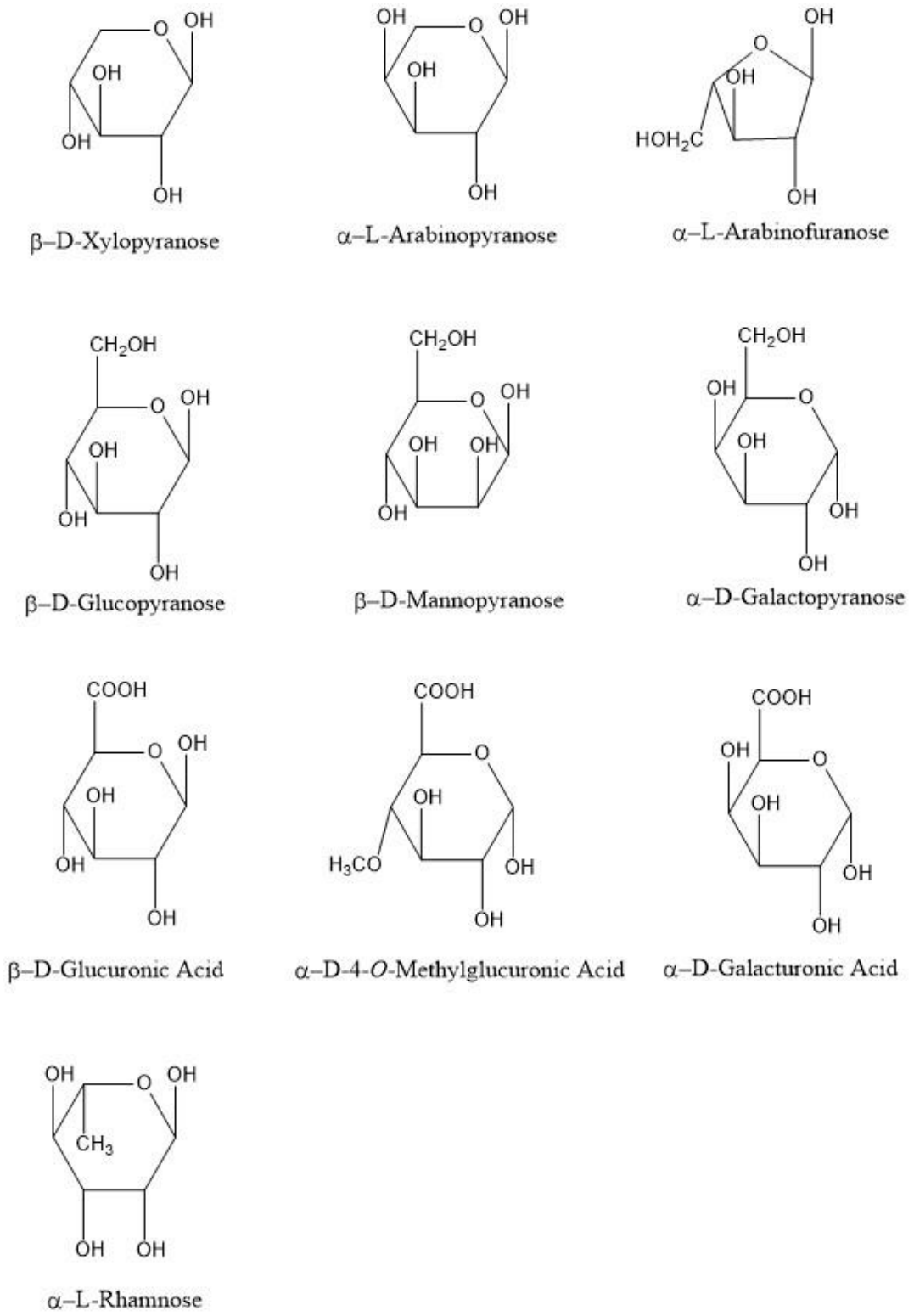

Figure 2: Monomeric building monosaccharides Adapted from *[40]*.

The hemicelluloses in hardwoods predominantly consist of glucuronoxylan (15~35%), with small amounts of glucomannan (2~5%). Glucuronoxylan in hardwoods is partially acetylated with approximately 4~7 acetyl groups per 10 xylopyranosyl residues. It also consists of side groups of 4-O-methyl-α-D-glucuronic acid (MeGlcA) sidechains on the C2 position with approximately one MeGlcA side group per 8~20 xylopyranosyl residues. Figure 2 shows the structure of O-acetyl-4-O-methylglucuronoxylans found in hardwoods. Glucomannans (Figure 3), on the other hand, are partially O-acetylated on the 2- or 3- positions of the mannopyranosyl unit [39].

Softwood hemicelluloses comprise of galactoglucomannan, with the galactopyranose at the 6-O position of mannopyranose (Figure *4*) (5~8%), glucomannan (10~15%) and arabinoglucuronoxylan (AGX) (with arabinofuranose on the 3-O position of xylopyranose, Figure *5*) (7~15%). Approximately, one acetyl group per 3~6 backbone hexose units is found in native galactoglucomannans and glucomannans in softwoods. Xylans in softwoods are not acetylated but contain an average of one MeGlcA per 5~6 xylose units in the 2-O position (Figure *5*) [39].

Table 2: The types of hemicelluloses in hardwoods, softwoods and gramineae and their backbones, side chains and linkages *[41]*.

Polysaccharide	**Biological origin**	**Amount**	**Units**			**DP**
			Backbone	**Side chains**	**linkages**	
Arabinogalactan	Softwoods	5–35	β-D-Gal*p*	β-D-Galp α-L-Araf β-L-Arap	β-(1 → 6) α-(1 → 3) β-(1 → 3)	100–600
Xyloglucan	Hardwoods, softwoods, and grasses	2–25	β-D-Glc*p* β-D-Xyl*p*	β-D-Xylp β-D-Galp α-L-Araf α-L-Fucp Acetyl	β-(1 → 4) α-(1 → 3) β-(1 → 2) α-(1 → 2) α-(1 → 2)	
Galactoglucomannan	Softwoods	10–25	β-D-Man*p* β-D-Glc*p*	β-D-Galp Acetyl	α-(1 → 6)	40–100
Glucomannan	Hardwoods	2–5	β-D-Man*p* β-D-Glc*p*			40–70
Glucuronoxylan	Hardwoods	15–30	β-D-Xyl*p*	4-*O*-Me-α-D-GlcpA Acetyl	α-(1 → 2)	100–200
Arabinoglucuronoxylan	Grasses and softwoods	5–10	β-D-Xyl*p*	4-*O*-Me-α-D-GlcpA α-L-Araf	α-(1 → 2) α-(1 → 3)	50–185
Glucuronoarabinoxylan	Grasses	15–30	β-D-Xyl*p*	α-L-Araf 4-*O*-Me-α-	α-(1 → 2) α-(1 → 3)	

				D-GlcpA Acetyl		
Homoxylan	Algae		β-D-Xyl*p*			
β-(1 → 3, 1 → 4)-glucan	Grasses	2–15	β-D-Glc*p*		β-(1 → 3) β-(1 → 4)	

*Gramineae hemicelluloses predominantly comprise of arabinoxylans (AX). In AX, the linear xyl*opyranose *backbone is xyl*opyranose *backbone is substituted by arabinofuranose units in the 2-O and/or 3-*O *(*Table 2*). In addition, the AX are also substituted by glucopyranosyl uronic unit or MeGlcA in the position 2-*O *such as in wheat straw, bagasse and bamboo [41]. The amount of glucuronic acid and arabinose determines whether the AXs are classified as arabinoglucuronoxylan (AGX) or glucuronoarabinoxylan (GAX), respectively [37]. The GAX consist of an AX backbone which contains about ten times fewer contains about ten times fewer uronic acid side chains than arabinose, in contrast to AGX. The GAX also contains xylan which GAX also contains xylan which is double-substituted by uronic acid and arabinose units [41]. In addition, gramineae also In addition, gramineae also have ferulic acid (FA) and p-coumaric acid present, both of which are not commonly present in are not commonly present in hardwoods and softwoods. FA is esterified (feruloylation) with AGX or GAX at the C5 position AGX or GAX at the C5 position of the arabinose side chain and simultaneously covalently forms an ether linkage with lignin forms an ether linkage with lignin (*

Figure *6*). This may serve the purpose bridging hemicelluloses and lignin. It is further proposed that feruloylation adds to the strength of the cell wall by forming a network between the hemicelluloses and lignin. This may be a nucleation site for lignin formation, making grasses indigestible by ruminant microbes and enzymes, and also providing protection from pathogens. Another proposed consequence of feruloylation is that it causes cell wall stiffening and growth deceleration. [42].

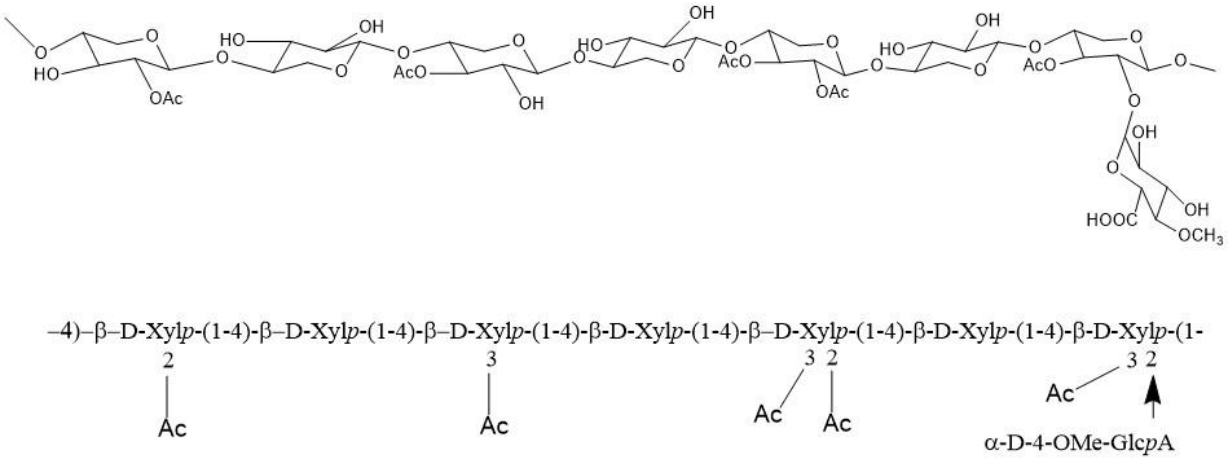

Figure 2: O-acetyl-4-O methylglucuronoxylans, the main hemicelluloses found in hardwoods.

Adapted from [39]

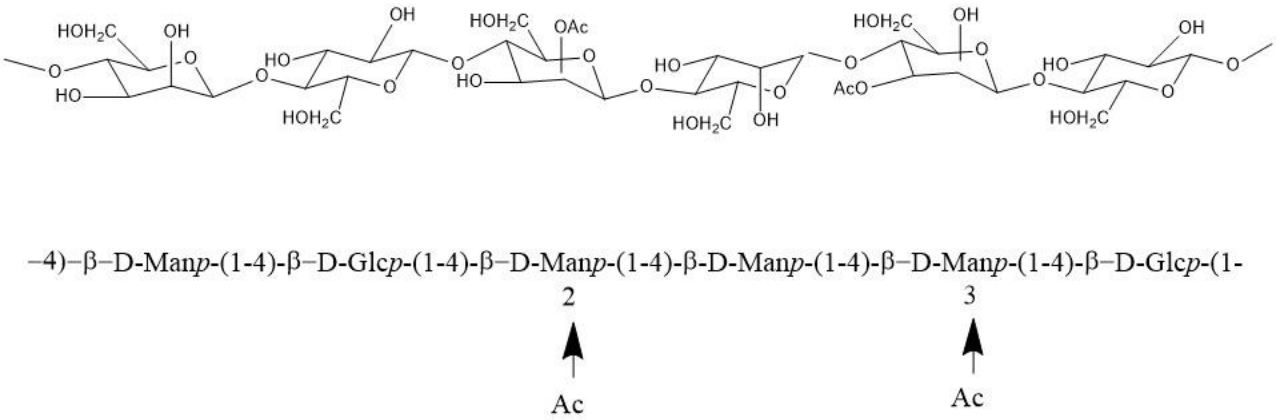

Figure 3: Glucomannan in hardwoods. Adapted from *[39]*

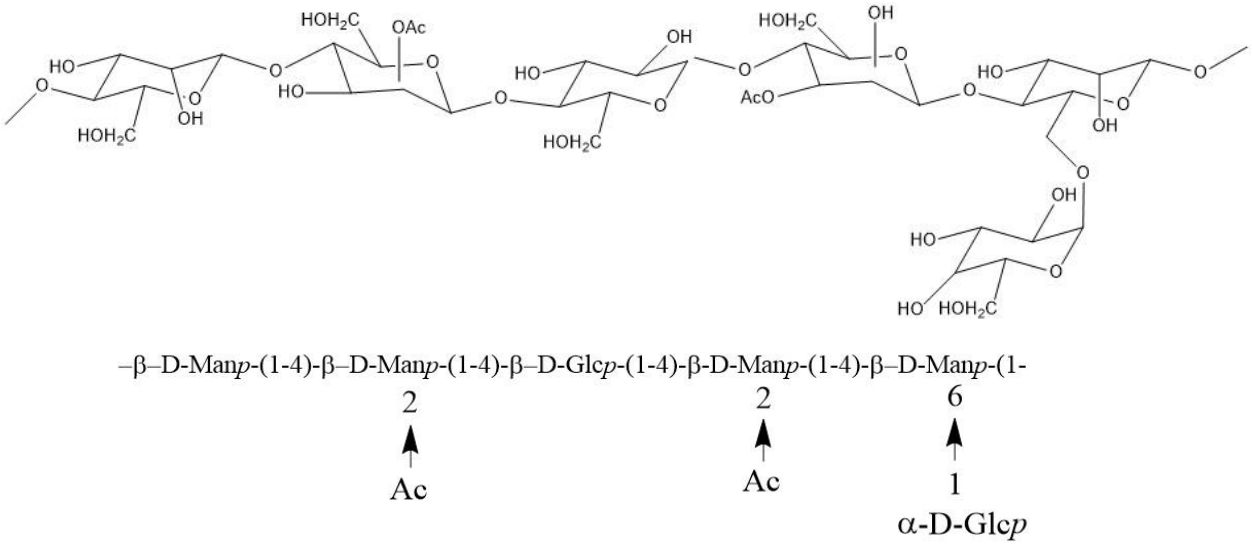

Figure 4: O-acetyl galactoglucomannans, main hemicelluloses found in softwoods. Adapted from *[39]*

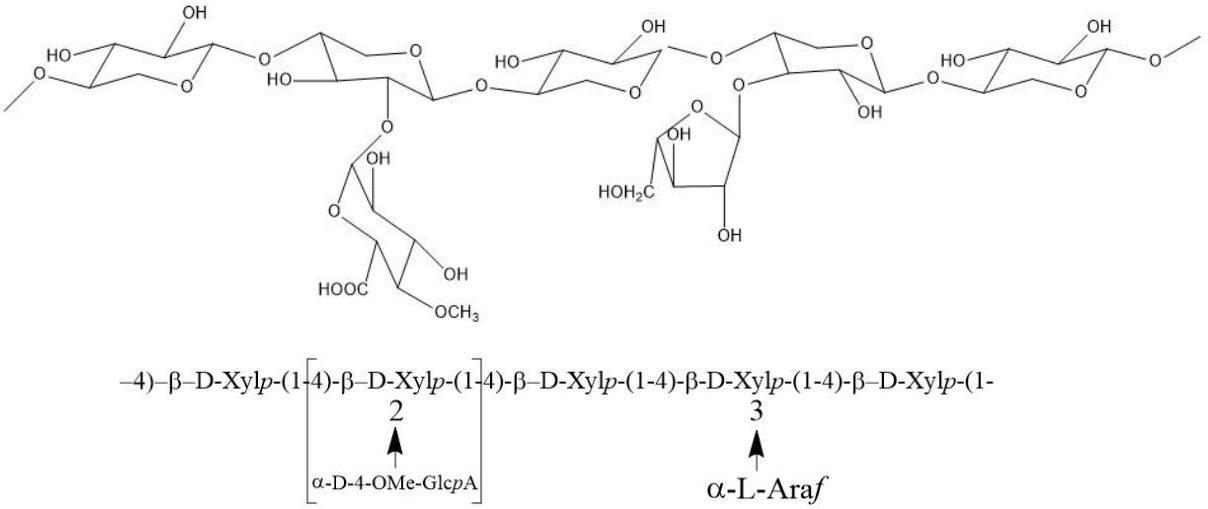

Figure 5: Arabino-4-O-methylglucuronoxylan in softwoods. Adapted from *[39]*

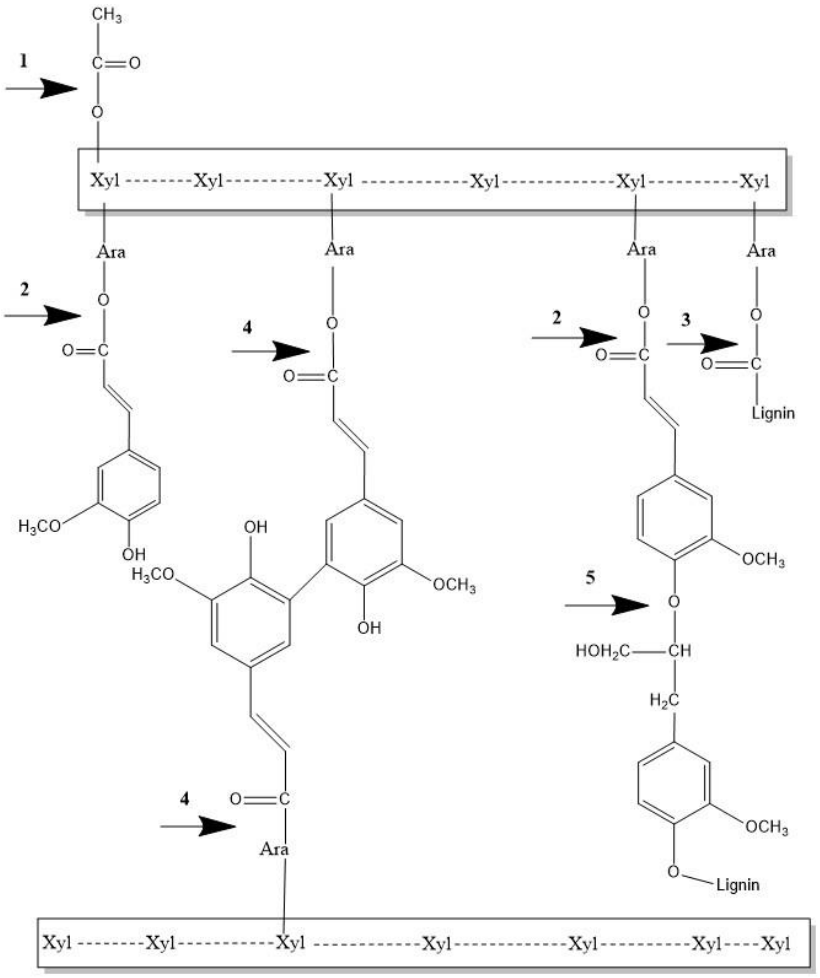

Figure 6: Simplified Structure of Ferulic Acid (FA) Cross-Linking Arabinoxylan (AX) in Grass Cell Walls. The 1,4-β-linked xylan backbone is represented by dotted lines and the side sugars, arabinose (Ara), are shown in circles. Ester and ether bonds are shown by arrows as follows: (1) acetyl group, (2) ester linked FA to AX, (3) arabinose-lignin (4) 5–5 –ester linked FA dimer cross-linking AX chains, (5) FA ether linked to lignin. Adapted from *[42]*.

Reactivity of xylans: Both acid and alkaline conditions can result in the hydrolysis of acetyl groups, generating acetic acid with a pKa of 4.8 [43]. Acidic conditions cause hydrolysis of various glycosidic linkages (with furan structure of arabinose being least stable) resulting in xylan degradation. Pentose sugars such as xylose and arabinose further degrade to furfural under severe acidic conditions where as MeGlcA is relatively stable [39]. Therefore, the reactivity of xylans largely depends on the amount of acetyl groups, arabinose, and MeGlcA side groups.

3.4 Lignin

Lignin (

Figure *7*) is a natural three dimensional amorphous polymer found in lignocellulosic biomass consisting of phenylpropanoid units linked by C–O–C and C–C bonds. It is the most abundant aromatic polymer and accounts for 12%–33% of lignocellulosic biomass [44,45] (Table 1). It is derived from three hydroxycinnamyl alcohol monomers, referred to as lignin monomers or monolignols: *p*-coumaryl alcohol, coniferyl alcohol, and sinapyl alcohol (Figure 8). These monolignols, differing in their degree of methoxylation on the aromatic ring, produce *p*-hydroxyphenyl (H), guaiacyl (G) and syringyl (S), respectively. Softwood, hardwood and gramineae lignins differ from each other based on the phenylpropanoid units present. Softwood consists of G-lignin which contains some H-units, hardwoods consist of SG-lignin with traces of H-units, and gramineae consist of HSG-lignin with common presence of *p*-coumaroylated and feruloylated units [46]. G and H units tend to undergo condensation more readily due to the $C_{3,5}$ open positions [29,38]. All lignins are acetylated at position Cγ to a variable extent and the presence of “uncommon” lignin end units such as cinnamaldehydes and benzaldehydes

have been detected. It has been also found that FA may participate in the last step of lignin biosynthesis, dehydrogenative polymerization along with cinnamyl alcohols, especially in gramineae [46,47].

The role of lignin in plants mainly consists of providing structural integrity to the cell wall, stiffness and strength to the stem and protection against pathogens. Lignin also provides hydrophobicity to plants which enables transport of water and solutes through vascular systems [48].

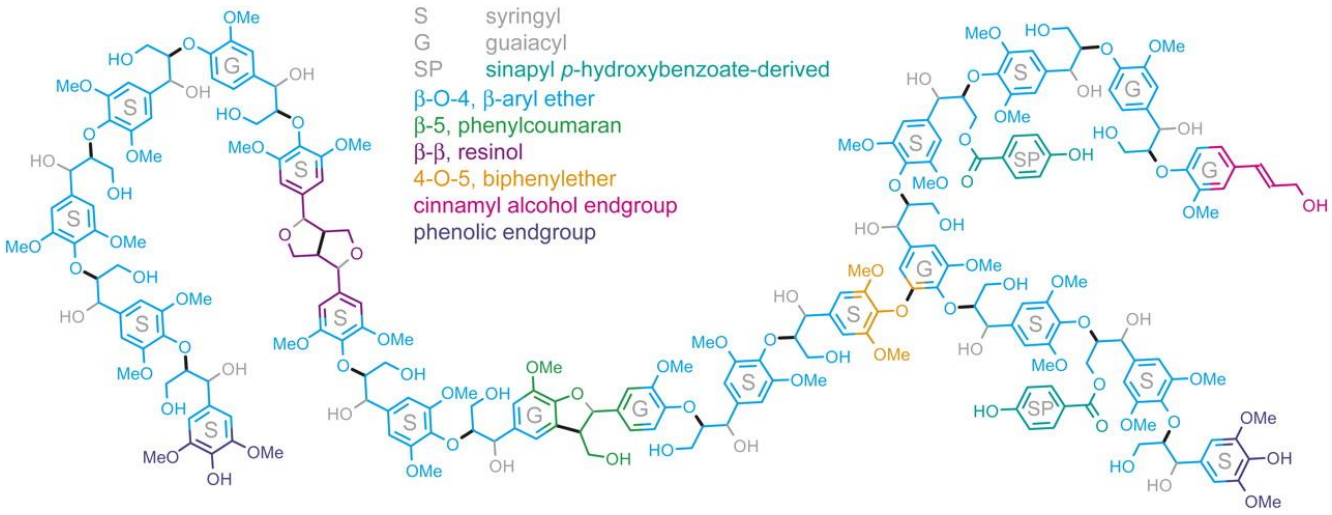

Figure 7: Representative lignin structure (poplar). Adapted from *[49]*.

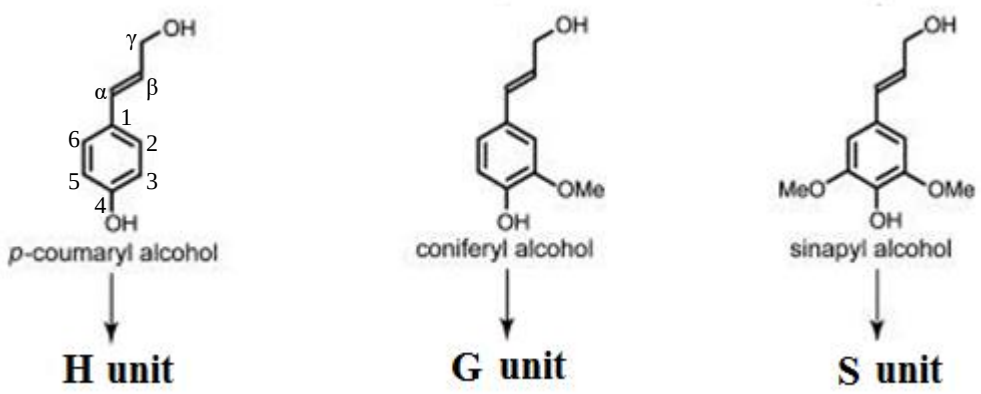

Figure 8: Lignin precursors, *p*-coumaryl alcohol, coniferyl alcohol and sinapyl alcohol. Adapted from [49].

3.4.1 Biosynthesis of lignin

The monolignols or building blocks of lignin are derived via various biosynthetic pathways from phenylalanine. Phenylalanine is a product of the Shikimate pathway and synthesized in the plant plastids [50].The Shikimate pathway will not be covered in this text but the details are well documented in literature [51].

The pathway of monolignol biosynthesis begins with the deamination of phenylalanine followed by several hydroxylation steps of the aromatic ring. The phenolic hydroxyl groups are *O*-methylated and finally the carboxyl group on the side chain is reduced to an alcohol group. [46,47].

After the monolignols synthesis is complete, they are transported to the cell wall where they can be oxidized and polymerized. It is suggested that monolignols are transported in the form of monolignol 4-*O*-*β*-D-glucosides as evidenced by the high amounts found in the cambial tissue. Enzymes like uridine diphosphate glucose (UDPG) coniferyl alcohol glucosyl transferase and coniferin-*β*-glucosidase (CG) may also regulate storage and mobilization of monolignols. [47][46]. Other theories include monolignol transport to the plasma membrane assisted by Golgi-derived vesicles, and the use of "transporters". However, both these models demonstrate inconsistencies. [52,53].

Lignin polymerization occurs via a two-step process of oxidative radicalization followed by radical coupling. Oxidative radicalization is the oxidation or dehydrogenation of *p*-hydroxycinnamyl alcohols to form phenoxy radicals (Figure 9). This process is enzymatically controlled by peroxidase or laccase in the presence of H_2O_2 or O_2, respectively [47]. Radical coupling is the random coupling of the phenoxy radicals which can be achieved either via bulk polymerization (dimerization) or end-wise polymerization (lignification) (Figure 9 and Figure

10). The structures of the linkages found in lignin are shown in Figure 11. The frequency of these linkages in softwood, hardwood and gramineae is shown in

Table *3*.

Bulk polymerization is the mechanism of lignin synthesis *in vitro* experiments where precursors are added in a single batch with dimerization being the dominant result. The linkages that are formed are mostly β-β (most abundant), β-O-4, and β-5 (Figure 9, Figure 10 and Figure 11). The polymer that is formed in this process is called dehydrogenation polymer (DHP).

Endwise polymerization is the mechanism of lignin biosynthesis which is believed to occur *in vivo*. In this process monomeric precursors are added to the growing polymer. The linkages that occur are β-O-4 (most abundant), β-5, 5-5, 4-O-5 (β-β) (Figure 9, Figure 10 and Figure 11). In natural lignin, in addition to the structures above there are two more structures that are seen which are α-O-4 and β-1 [29]. Ether linkages dominate over carbon-carbon linkages to a ratio of almost 2:1. The *in* vitro experiments indicate that the lignin polymerization depends on supply rate of monomers, rate of radical generation, presence of polysaccharides and the presence of the growing lignin polymer [47].

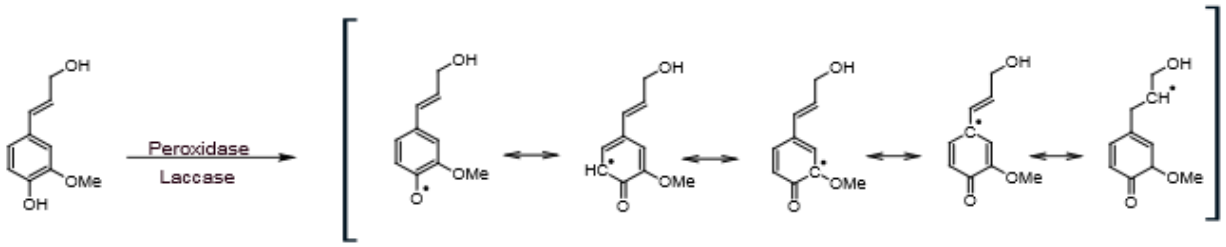

Figure 9: Resonance stabilized monolignol phenoxy radicals *[29]*.

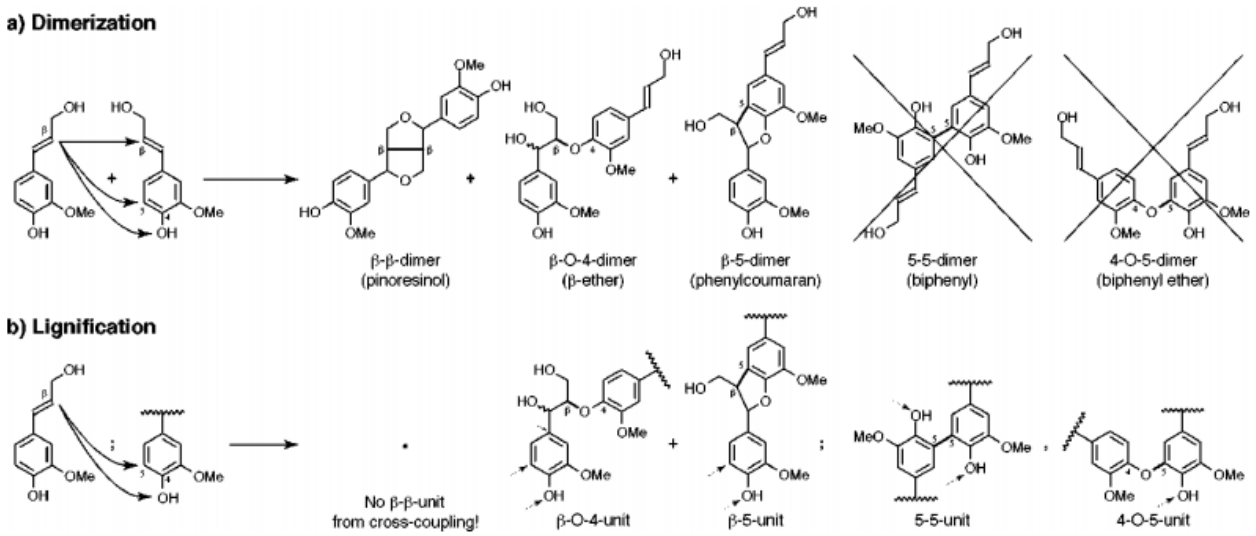

Figure 10: The structures that are produced during dimerization (bulk polymerization) and lignification (end-wise polymerization) have certain differences. Dimerization of coniferyl alcohol produces only three dimers, cross-coupling of coniferyl alcohol with a G unit gives only two main products *[47]*.

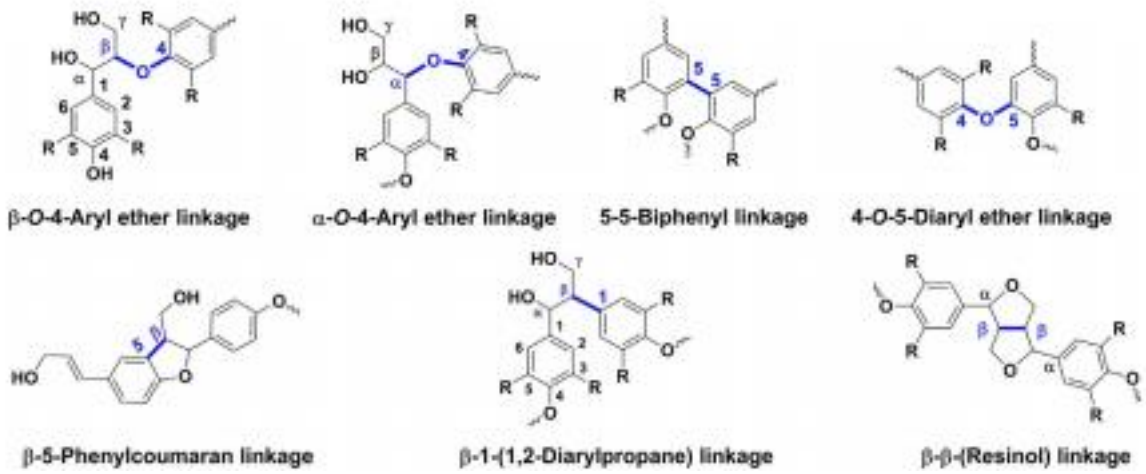

Figure 11: Typical linkages found in lignin. Adapted from [54,55]

Table 3: Frequency of linkages typically found in lignin. Structures are shown in Figure 11.

Linkage type	**Percent of total linkages**		
	Softwood	**Hardwood**	**Graminae (Wheat straw)[3]**
β-O-4’	35-50[1]	50-70[1]	75
β-5’/α-O-4’	9-12[1]	6[1]	11
β-β’	2-3[1]	3-4[1]	4
5-5’	10-11[1]	5[1]	-
4-O-5’	4[1]	7[1]	-
β-1’	1-3[2]	1[2]	-
Dibenzodioxocin (β-O-4’, α-O-4’,5-5’)	4-5[2]	1-2[2]	3
Spirodienone (β-1’, α-O-α’)	1-3[2]	2-3[2]	3

[1][56]
[2][57]
[3][58]

The β position is the most reactive and therefore drives the selectivity of the cross coupling. Other factors include redox potential and number of methoxy groups on the aromatic ring. Product formation is favorable when the difference in redox potentials of the phenol is smaller or the concentrations are relatively high. Cross coupling is likely to occur if the monolignols and the dilignols have the same number of methoxy groups on the aromatic ring. [59].

The cross-coupling reaction to form β-O-4 (most common linkage, Table *3*) can result in two steroisomers – the *erythro* and the *threo*. The *erythro* form occurs if the addition of the water molecule takes place from the top face of the quinone methide intermediate, and *threo* form occurs if the addition of the water molecule takes place at the bottom face (Figure 12). The final product is determined by the nature of cinnamyl alcohol

(monolignol) lignin precursor and hence by the nature of the non-quinone methide ring. A mono-methoxylated ring (coniferyl alcohol resulting in G-units) results in a 50:50 *erythro:threo* mixture and a dimethoxylated ring (sinapyl alcohol resulting in S-units) results in a 75:25 *erythro*:*threo* mixture. This has been corroborated by studies, hardwoods lignins contain higher quantities of the *erythro* form, whereas, almost equal amounts of *erythro* and *threo* forms are present in softwood lignins. The *erythro* to *threo* ratio can be used to characterize different lignin types [60].

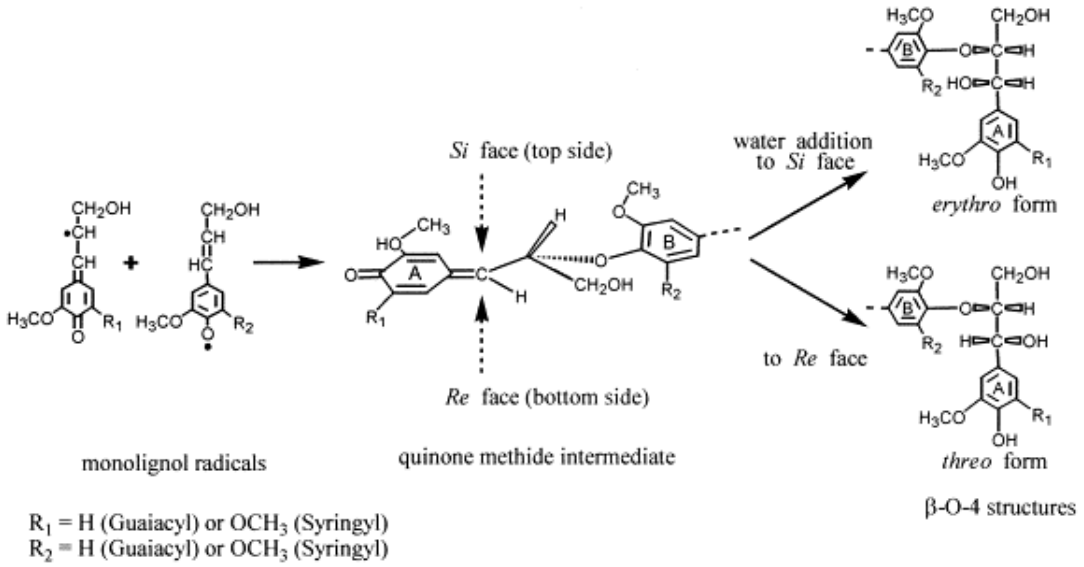

Figure 12: Formation of *erythro* and *threo* forms of β-O-4 structures by the addition of water to the quinone methide intermediates. Only the *syn* isomer of the quinone methide intermediate (R_1=H) is illustrated here, although this structure must contain *syn* and *anti* isomers *[60]*.

New tools and technology have enabled scientists to analyze the lignin structure more thoroughly leading to the discovery of new linkages. Internal trapping can result in the formation of the spirodienone structure at position 1 when preformed β-ether cross-couples with a quinone methide intermediate. Similarly, an eight membered cyclic ether structure, dibenzodioxocin, is formed when a preformed 5-5' coupled units combine with a quinone methide [61].

3.5 Lignin-carbohydrate complex (LCC)

Lignin and carbohydrates can be linked together either by the benzyl ether bonds, benzyl ester or phenyl glycosides bonds [62]. Ether linkages are more common and stable than ester linkages especially in alkaline conditions [63]. The presence of LCC has often made it difficult to separate lignin efficiently from plant material [64,65].

Benzyl ether LCC structures are subdivided as follows: (a) C1-linkages between the α-position of lignin and primary OH groups of carbohydrates (at C-6 of Glc, Gal and Man and C-5 of Ara) and (b) C2-linkages between the α-position of lignin and secondary OH groups of carbohydrates, mainly of lignin-xylan type [64]. Lawoko et al. (2005) showed that spruce wood contains four types of LCC bonds – Galactoglucomannan-glucomannan-lignin-pectin, glucomannan-lignin, glucomannan-lignin-xylan and xylan-lignin-glucomannan. Toledano et al (2010) [63] attempted lignin separation and fractionation by ultrafiltration and claim that the fraction greater than15kDa is that of LCCs. The various representative LCC linkages and their structures are shown in Figure 13.

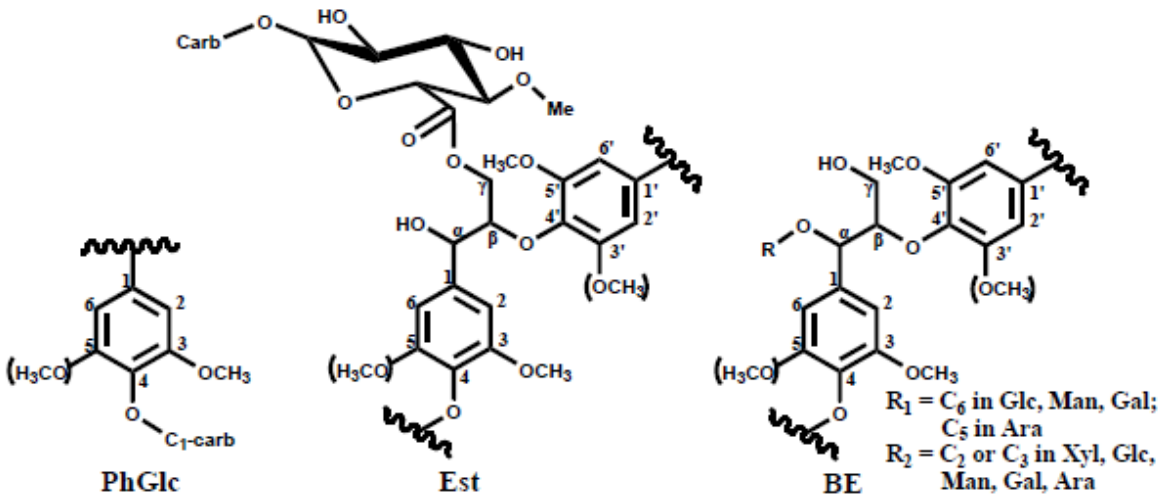

Figure 13: Common LCC structures found in lignocellulosic biomass *[64]*.

3.6 Pretreatment methods

Lignocellulosic biomass is highly recalcitrant due to lignin structure, and crystallinity and degree of polymerization of cellulose. Therefore, a pretreatment step is required prior to its conversion to high value products. The objective of pretreatment is to increase reactivity and/or accessibility of specific components present in the biomass. This can improve efficiency and lower the chemical demand for further processing. Usually, lignin or hemicelluloses are removed during this process to be used as raw material for fermentation products such as ethanol, butanol and bioplastics. In addition, cellulose processability is also increased.

Figure *14* depicts the desired effect of pretreatment for increasing accessibility of lignocellulosic biomass.

The type and severity of pretreatment used is determined by the intended end-product(s) and the technology/chemistry that will be employed during downstream processing. Some factors that are considered when selecting a pretreatment method include high yields and harvesting times for a variety of crops, digestibility of pretreated solids (e.g. cellulose), stability of sugars, minimal amounts of toxic compounds produced, accessible surface area, and recovery of lignin [66–68]. Some pretreatment methods are discussed in this section. The lignin used in this study was isolated from hydrolysates produced during hot water extraction. Therefore, special focus has been given to hot water extraction as one type of hydrothermal pretreatment.

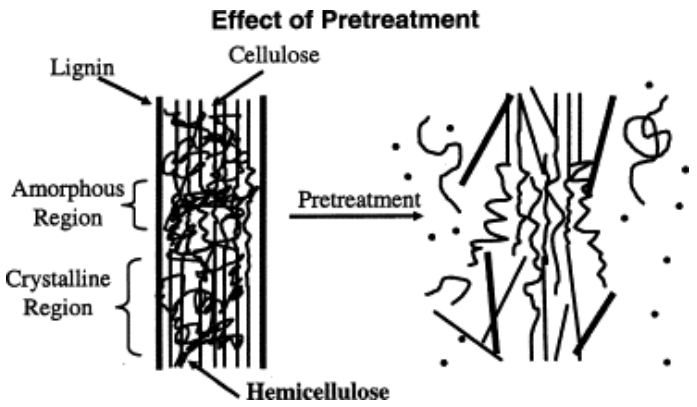

Figure 14: Desired effects of pretreatment on lignocellulosic biomass *[68]*.

3.6.1 Acid Pretreatment

Acid pretreatment can be of two types – strong acid at low temperatures and dilute acid at high temperatures. The main lignocellulosic constituent targeted during this pretreatment process is the hemicelluloses, mainly xylans. Glucomannans are relatively more acid stable and dissolves during the process making cellulose more accessible [67,69].

Strong mineral acids (30%-70%) such as sulfuric acid, hydrochloric acid and nitric acid can be used to pretreat biomass [70,71]. Strong acids most effectively remove cellulose and hemicelluloses and leave a solid enriched in lignin. However, this lignin is extensively modified due to the occurrence of condensation reactions in acidic conditions. Strong acid pretreatment does have disadvantages due to the corrosive nature of acids. Cellulose and hemicellulose can be degraded at higher temperatures in acidic environments and under some processing temperatures, degradation of pentoses and hexoses to furfural and hydroxymethyl furfural, respectively has been observed. These compounds are inhibitory to enzymatic treatment during further processing [66]. In addition, capital costs tend to be high as special corrosive resistant equipment is required for this pretreatment. It is also essential that the acid is recovered to keep costs low, as the cost of a continuous purchase, use, and waste discard system, including neutralization and environmental safety considerations is very high [70,71].

In dilute acid pretreatments, acid concentrations can range from ~0.5 - 1%, and temperatures can range from 120 and 160ºC [70]. Mineral acids such as hydrochloric acid and sulfuric acid or, organic acids such as acetic acid, formic acid, maleic acid, or carbonic acid can be used. A sugar yield from hemicelluloses and a decrease in cellulose crystallinity is observed during

dilute acid treatment [71]. However, when compared to alkaline pretreatment, the remaining cellulose hydrolyzability is inferior [71]. An advantage of dilute acid treatment is that organic acids used can be produced during autohydrolysis from the wood itself, making it a self-sustaining process [72].

3.6.2 Alkaline Pretreatment

Due to lignin solubilization in alkali, alkaline pretreatment is most effective if delignification is of interest. Bases such as sodium hydroxide, potassium hydroxide, and lime are commonly used in alkaline pretreatments. The treatment can be carried out at low temperatures but longer residence times are necessary [73].

Alkaline treatment causes cellulose swelling, which increase surface area and porosity [73]. This is an added advantage over This is an added advantage over other pretreatment methods as it disrupts the structure and makes the biomass more accessible makes the biomass more accessible to enzymes and bacteria [67,70]. Sodium hydroxide is attributed to increasing hardwood attributed to increasing hardwood digestibility from 14% to 55% and also reducing lignin content in the biomass from 24-content in the biomass from 24-25%. Furthermore, this process is shown to have a higher effect on gramineae than on woody on gramineae than on woody biomass [66]. This is attributed to the saponification of ferulates present in agricultural residues. present in agricultural residues. Ferulic acids are linked to arabinoxylan via an ester bond and linked to lignin with an ether linked to lignin with an ether bond (

Figure *6*). During the pretreatment, the alkali attacks lignin from both these directions resulting in a higher amount of lignin being removed [42].

3.6.3 Organosolv Pretreatment

Organic solvents such as, but not limited to, ethanol, methanol, acetone, and ethyl acetate are used to dissolve lignin in this pretreatment, whereas cellulose remains insoluble [70]. Selectivity of the pretreatment can be improved by addition of catalysts such as oxalic, salicylic, and acetylsalicylic acid. Temperatures for this pretreatment range from 150-200ºC

[71]. This method can yield relatively pure low molecular weight lignin, which can be isolated as a raw material for value-added products [74]. However, recovery of products from this method can be complex due to environmental and economic concerns.

3.6.4 Biological Pretreatment

In this method, microorganisms are used to metabolize and degrade lignocellulosic material. Prominent microorganisms used for this purpose are the Basidiomycota (previously called Basidiomycetes) fungi which can fall into three classes - white-rot, brown-rot, and soft-rot [75]. An advantage of using white rot fungi is that its specificity for lignin degradation can be quite high, virtually leaving cellulose and hemicelluloses unmodified. The fungi employ enzymes like peroxidases and laccases for lignin degradation. In addition, conditions are mild, compared to other pretreatment methods and energy investment is low. However, residence time can be in terms of day or weeks, as degradation is extremely slow [71,75].

3.6.5 Electron beam irradiation treatment (EBI)

In electron beam irradiation pretreatment (EBI), electromagnetic energy such as gamma rays, electron beams, and microwaves, is targeted at the lignocellulosic biomass with the aim to reduce its recalcitrance. No chemical reagents or high temperature and pressures are used, which reduces the inhibitory byproducts such as furanic aldehydes (furfural/hydroxymethyl furfural) from sugar decomposition [76]. During EBI, free-radicals can be formed due to the rapid localized absorption of energy by the material. This initiates various reactions in the lignocellulosic biomass, which can be either chain cleavage and/or polymerization reactions (condensation/cross-linking) [76].

Currently, research is focused on increasing efficiency of enzymatic hydrolysis for the production of fermentable monomeric sugars [76–79]. The effects of EBI include reduction in the degree of crystallinity of cellulose, thus reducing degree of polymerization [77], and decrease in the mechanical strength of wood chips [80]. The decrease in mechanical strength is thought to be a result of degradation of the lignin matrix [76].

The effect of EBI on lignin structure has been studied [80–82]. A study on model compounds resulted in the cleavage of β-O-4 bonds [82]. Studies on softwood milled wood lignin resulted in cleavage and condensation reactions occurring simultaneously, due to irradiation [80].

EBI is proposed as a step that would enhance the effectiveness of other chemical pretreatment methods such as enzymatic hydrolysis, and research is currently ongoing in this area [76,83].

3.6.6 Hydrothermal treatment

Hydrothermal pretreatment uses water, generally ranging from 150˚C to 230˚C [66,68,70] for the purpose of targeting hemicelluloses in lignocellulosic biomass. Below these temperatures the reactions do not provide adequate results in terms of increasing lignocellulosic processability as assessed through different parameters such as increase in porosity. Above this temperature range cellulose degradation begins to take place which is counterproductive to the goal [69]. No chemicals or reagents are used in hydrothermal pretreatment and catalysis for hydrolysis and dissolution of the lignocellulosic constituents are derived solely from the lignocellulosic biomass itself – often referred to as autohydrolysis. Hydrothermal pretreatment has many practical advantages compared to other pretreatment technologies making it attractive as the first step in an biorefinery processes [70]. Hydrothermal pretreatment is also most effective on Angiosperms due to the high xylan present.

Hot Water Extraction Pretreatment

Research on using liquid water to dissolve lignocellulosic biomass had been on-going since the 1960s, and a wide range of reaction parameters have been studied [1,84,85]. However, the most optimal conditions that demonstrate efficient hemicellulose removal, high cellulose retention and minimal furfural production are 160°C and 2 hours [1,86].

Hydrothermal pretreatment at these specific conditions is referred to as hot water extraction (HWE) and is being developed for commercialization by Applied Biorefinery Sciences, LLC [72]. It is recommended as an environmentally benevolent process, with limited corrosion, no sludge generation, and low capital and operational costs [2]. Currently, HWE is widely being explored for various biorefinery applications and/or technologies [1,2,72,87–95].

The lignocellulosic constituents that are targeted during hot water extraction are hemicelluloses, as water's dielectric constant facilitates ionic substances to disassociate and dissolve hemicellulose [96]. Dielectric constant is taken as a measure of a polarity of a substance; higher dielectric constant implies higher polarity and ability to stabilize charges.

In HWE, as the hemicelluloses are removed, the pore size of the substrate becomes larger, cellulose becoming more accessible [66,67]. Hydrolysis occurs in the presence of the hydronium ions which act as catalysts and are produced by auto-ionization of water. Deacetylation occurs and lowers the pH of the extraction liquor. Acetic acid can be isolated from the extract and represents an important co-product of HWE [69]. Other acidic constituents

such as aromatic acids and 4-O-methyl-glucuronic acid, contribute to the increasing acidity during HWE as well [2,86]. The pH of the extract can range from 3.5-4, depending on the species. Due to the high temperatures, pressure and the drop in pH, the most susceptible bonds – glycosidic bonds in the hemicelluloses – are attacked and produce oligosaccharides. This process produces a slurry which is filtered and contains lignin and hemicelluloses. Cellulose remains in the solid portion. Maintaining the pH of the extract, between 4 to 7 has shown to retain hemicellulosic sugars in their oligomeric form and prevent the formation of monomers.

Removal of hemicelluloses, inorganics and partial removal of lignin, during hot water extraction, facilitates cellulose accessibility in the biomass. Cellulose crystallinity may be reduced and the accessible surface area of cellulose increases. Therefore, cellulose becomes more susceptible to hydrolytic enzymes or pulping chemicals, thus increasing the efficiency and reducing chemical demand for further treatments including delignification [74,92,97].

Hot water extraction removes approximately 10-15% of the original lignin present in the lignocellulosic biomass [98]. Since acid conditions render ether bonds susceptible, inter-unit alkyl aryl ether bonds may be attacked during hot water extraction resulting in lignin dissolution. Lignin removal is a favorable outcome of hot water extraction, as delignification is a necessary step in subsequent processing. Furthermore, hot water extraction has shown to facilitate delignification of the extracted biomass [91].

The purity of lignin recovered from hot water extraction is relatively high >80% but carbohydrates are always present in amount usually of up to 15% [25,95]. This may pose a problem for applications that require high purity lignin, such as carbon fibers and thermoplastics [99,100]. However, this work uses lignin recovered from the hot water extraction for resin applications, in “as-is” form without a purification step. It has been suggested that lignin removed by hot water extraction is of higher value than most technical lignins currently available. This is attributed to its low sulfur content, typically low inorganic

content, and relatively low degree of condensation [98]. Typically, isolated lignins or technical lignins have higher PhOH content due to the cleavage of aryl ether bonds [98].

Recovery of solubilized lignin is achieved by acidifying the HW extract to pH 2, followed by centrifugation, ultrafiltration or precipitation over several days and decanting the supernatant. This yields a relatively pure lignin fraction of ~85% purity [90,98] and is one of the lignins utilized in this current study. The lignin has shown to have high S/G ratio and free phenolic hydroxyl group content [98]. HW extract can be further acidified by acid hydrolysis producing another lignin with even higher purity ~90% [90] - also investigated in the current work.

Inorganic compounds that are present in lignocellulosic biomass are mostly water soluble. It is expected that minimal amounts will be present in the lignin isolated from the extract as they should remain in the aqueous phase during lignin recovery via precipitation.

3.7 Quantitative Studies and Qualitative Studies of Lignin Isolation

3.7.1 Lignin content determination

Lignin isolation poses challenges as the components of the cell wall are closely associate and the lignocellulosic matrix has evolved to resist degradation. Furthermore, the existence of covalent bonds between lignin and hemicelluloses (LCC ether, ester and phenyl glycosidic bonds) prevent efficient lignin isolation [57]. One of the main challenges of lignin isolation is preserving the structure of native lignin to be studied. Lignin is extremely prone to forming inter unit bonds (condensation) during chemical treatment and most methods will alter the structure. Therefore, different methods for quantitative and qualitative purposes have been developed.

Numerous methods for lignin determination have been proposed. The most widely used method is the Klason lignin procedure [101,102]. There have been additional modifications that have been made at SUNY-ESF and is the preferred method used at the institution [89,91,95,98,103] to solubilize and hydrolyze carbohydrates in the laboratory sample. Lignin remains mostly insoluble in acid and is determined by gravimetric method.

The Klason lignin method utilizes concentrated sulfuric acid and treatment at high temperatures. The method was developed for determining lignin content in wood samples and targets to completely hydrolyze carbohydrates in the wood matrix, made possible by the strong acid conditions. The remaining insoluble lignin residue is determined by gravimetric quantification (acid-insoluble lignin, AISL). Lignin is substantially modified due to the strong acid environment, primarily via cleavage of aryl ether bonds and condensation reactions. Therefore, a certain amount of lignin dissolves in the acid (acid-soluble lignin, ASL) which is determined by UV-vis spectroscopy (reading at 205 nm), made possible by lignin's aromatic nature [104]. Prior to determining lignin content in lignocellulosic biomass, pre-extraction is required, in order to remove extractives that may interfere with UV-vis reading [104].

Due to increased interest in various pretreatment methods, a wide variety of lignins, is being investigated for their properties and possible uses, and the Klason and UV-vis method are used to determine lignin purity. The UV-vis method employs the Lambert-Beer's law (A=abc) where an absorptivity of $110 Lg{-}1 cm{-}1$, based on literature [101] is used. Absorptivity of lignin can vary based on the type and must be determined. Furthermore, absorbance is measured at 205nm instead of 280nm, which is the typical wavelength for lignin. Certain carbohydrate degradation products also absorb at 280nm and therefore may cause potential interference. In order to overcome some of these challenges, an alternative – acetyl bromide method was developed [105]. However, this method requires a well-defined lignin standard for calibration purposes [101].

Since lignin is substantially modified during Klason treatment, it is not representative of native lignin and methods that would keep the structure of lignin intact were required to be developed; for structural characterization.

The Björkman milled wood lignin (MWL) is one such method which produces lignin that is minimally altered [106]. First, wood is ground to a fine powder using a vibratory ball mill, followed by extraction in dioxane: water (96:4) to solubilize lignin. There is consensus that MWL originates from the middle lamella, with an increased amount of lignin originating from the secondary wall with increasing MWL yield. In order to obtain high MWL yields, extended ball milling time (up to several days) is required [104].

All lignin purity data reported in the current work was obtained using the conventional Klason and UV-vis method (reading at 205nm for ASL), detailed in the Materials and Methods Section.

3.8 Lignin in Polymer Applications

Lignin is a potential byproduct of the biorefinery and is gaining attention due to its projected abundant production in the future. According to the Global Renewable Fuel Alliance, 85 billion liters of ethanol were produced in 2014 which is only expected to increase in the future, resulting in large quantities of lignin-rich byproduct streams from the biorefinery. Lignin is increasingly studied for the production of different high-value, low volume products, such as resins, thermoplastics, carbon fibers, and activated carbon to increase the profitability of biorefineries [99,100,107–109].

3.8.1 Resins

Resins serving as binding materials in plastics undergo competing reactions of depolymerization and polymerization during their preparation. PF resins are synthetic polymers

produced in either acid or alkaline conditions (Figure 15) and are widely used in adhesive and coating applications. PF demonstrates excellent properties in terms of chemical resistance, electrical insulation, and water resistance, chemical and dynamic stability [110]. PF resins are of two types – novolac and resoles. Novolacs are prepared in acid conditions and have phenol to formaldehyde ratio greater than 1. Novolacs require a curing agent due to the smaller amount of formaldehyde present. The most common curing agent used in industry is HMTA ($(CH_2)_6N_4$; HMTA) [111]. In contrast, resoles are prepared in alkaline conditions and have a phenol to formaldehyde ratio less than 1. No curing agent is required as there is sufficient formaldehyde in the mixture for curing to occur [111]. The reaction mechanisms of novolac and resole production are detailed below.

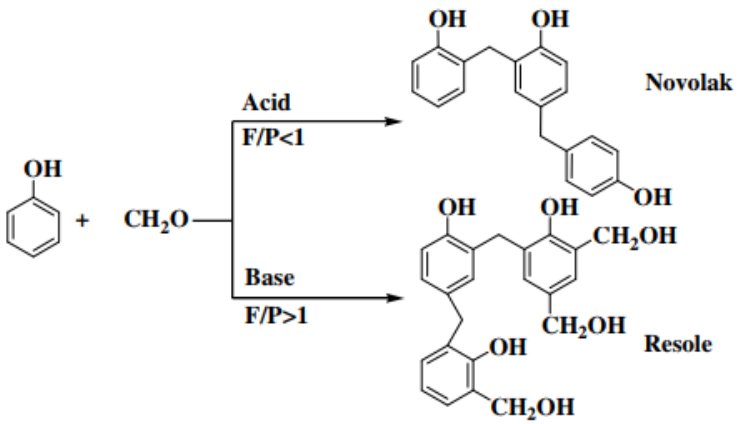

Figure 15: Synthetic route of phenol-formaldehyde (PF) resins. Figure adapted from [112].

Novolacs

An acidic catalyst and a molar excess of phenol to formaldehyde are conditions used to make novolac resins. Novolacs are typically used in binder or fiber reinforcement applications. The initial attack can occur at the 2-, 4- or 6- positions. The initial reaction is between formaldehyde and phenol [113].

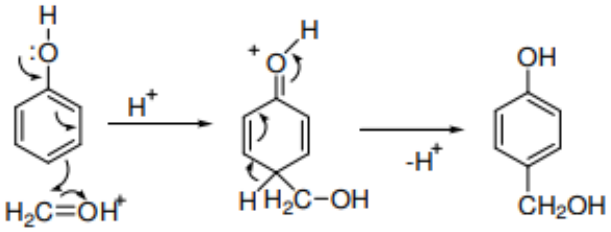

Figure 16: Step 1 of novolac formation: Formaldehyde reacts with phenol to form methylol phenol. Figure adapted from [112].

This is followed by the methylol phenol reacting with phenol or other methylol phenol moieties to form a linear polymer [113]. Methylene bridges are formed via this reaction and due to the three potential sites for polymerization, branching occurs. As the reaction progresses, the random orientations and branching produce a complex polymer network. The reaction is terminated when the formaldehyde reactant is quenched.

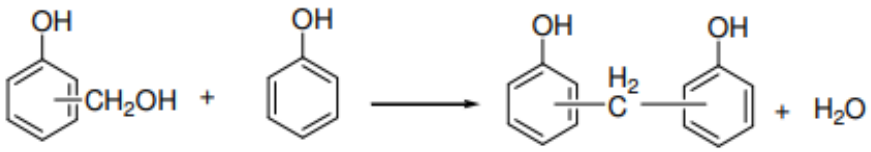

Figure 17: Step 2 of novolac formation: methylol phenol and phenol self-condense to form linear polymers. Figure adapted from [112]

For further crosslinking to occur a curing agent that will provide excess formaldehyde such as HMTA, is required.

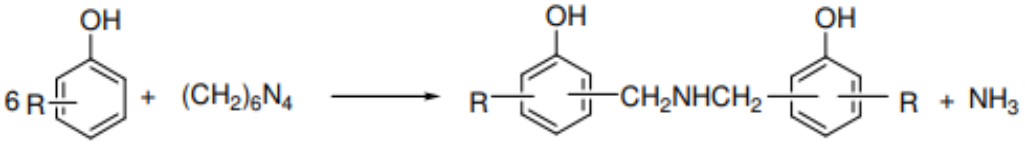

Figure 18: Step 3 of novolac formation: Mechanism of HMTA crosslinking novolac resin during curing process. Figure adapted from [112].

Resoles

A basic (alkaline) catalyst such sodium hydroxide, and a molar excess of formaldehyde are requirements to make resole resins [113]. Resoles are typically used as wood adhesives for plywood and particle board applications. First, phenol reacts with formaldehyde to form methylene glycol:

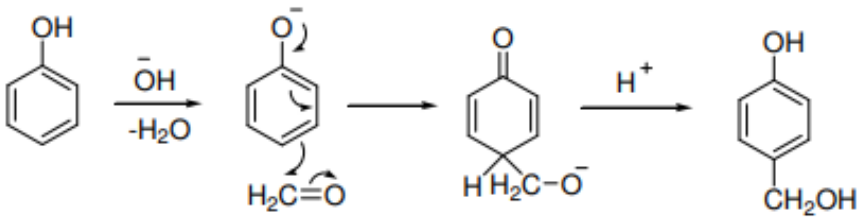

Figure 19: Step 1 of resole formation: Formaldehyde reacts with phenol to form methylol phenol. Figure adapted from [112].

In the second step, methylol phenol can either react with itself (Figure 16) or form dimethylene ether bridges with release of water:

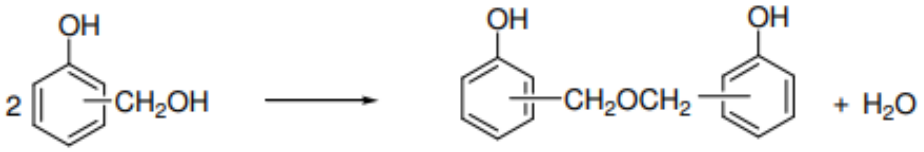

Figure 20: Step 2 of resole formation: Methylol phenol forms dimethylene ether bridges. Figure adapted from [112].

Lignin Based Resins

Lignin has been explored for both thermoplastic and thermoset applications due to its diverse thermal behavior. However, lignin is brittle and has shown to have poor flow properties which limits its use as a thermoplastic [114]. Therefore, research has focused on attempting to blend lignin with other polymers such as polypropylene, polyethylene and polyvinyl chloride [115].

On the other hand, lignin has shown to form crosslinked structures at elevated temperature and is also investigated as a thermoset material, specifically in PF applications [99,115,116].

Thermosets and thermoplastics are the two classes of polymers which manly differ in behavior when exposed to heat. Upon exposure to heat, thermoplastics will soften into a mobile liquid but can return to its original state when cooled [117]. It is possible to soften and reshape thermoplastics multiple times [118,119]. The polymer chains of these polymers are categorized into two states – random (amorphous) and ordered (crystalline). Thermoplastics generally demonstrate high impact strength, high reform ability and are easily recyclable [120]. Thermoset polymers, on the other hand, are malleable prior to curing but form extensively cross linked 3D networks post-curing. These materials are used as binders and are more difficult to recycle [121]. Thermoset polymers demonstrate resistance to solvents and corrosives, excellent thermal stability, fatigue strength, tailored elasticity and adhesion [121].

Lignin based resins have been extensively studied in the literature. Most research in literature attempts to substitute certain amounts of phenol in PF resins to produce LPF resins. Research for resole-type applications of these LPF resins, as wood adhesives in plywood and particle board, is also more abundant [15,16,112,122–124]. However, recent attempts in novolac-type applications have also been reported [13,125,126]. Kraft lignin and/or lignosulfonates, which are the traditionally produced sulfur-containing technical lignins, are the primary sources of lignin in most studies. Currently, large quantities of lignin without sulfur are not readily available for use. The lignin that is available can be extremely diverse depending on the species, pretreatment and recovery methods. At present, traditional pulping processes produce over 25 $\times 10^6$ tons of sulfur-containing lignin in the United States, annually. The sulfur-free lignin that is a potential product of emerging lignocellulosic biorefineries may only be a fraction of this amount [1].

Current literature reports two methods to synthesize lignin-based resins—the first method involves purifying lignin [6] and then modification by methylolation (hydroxymethylation) [127,128], phenolation [8,122,129], and demethylation [110]. Modification is performed to improve reactivity of the lignin and the resulting highly pure and active products are used in the preparation of phenolic resins. However, performing modification procedures on lignin increases production costs making it a less viable option [7]. The Wooten method is one of the most widely used methods where lignin and formaldehyde react for 5 hours at 553°C in the presence of sodium hydroxide [130].

The second method is called the "catch all" pathway [129], which utilizes unpurified lignin [8,131]. The lignin that is used in this study is not modified or purified; therefore the method used here may be considered as the "catch all" pathway.

The mechanism for lignin polymerization for resole-type resin (alkaline conditions) has been proposed to occur at the *ortho* position, specifically G_5 position as shown in Figure 21. Therefore, lignin rich in G units is often proposed as a better raw material for producing lignin based resins for resole-type resins [14,132]. Lignins with high S units cannot participate in this reaction as the G_5 position is occupied by the methoxy group (Figure 8). H units contain two active sites and G units contain one active site (Figure 8) to create highly crosslinked structures. Thus it has been suggested that softwood lignin may be more suitable for adhesive applications [14].

Figure 21: Proposed scheme for LPF resins in alkaline conditions. Adapted from [133].

Lignin for novolac-type resins has been less researched but has been gaining attention. Similar to resole-type resins, these also are LPF resins – where most efforts are dedicated to replacing phenol. Literature on novolac-type LPF resins is also limited to characterization of the resin for its chemical structure and little data is available for its mechanical properties. Comparison of pine kraft, soda-anthraquinone flax and hardwood organosolv lignin showed that lignins with relatively high PhOH group content were better candidates for LPF resin as they provided more active sites. Similar to resole-type LPF resins, higher G content also proved to be beneficial. The kraft lignin studied was also more polydisperse which was a favorable characteristic for resin production [123]. Another study tested enzymatic hydrolysis lignin for its viability in novolac-type LPF resins. Up to 55% phenol could be replaced with this lignin without compromising any structural properties determined by FTIR, SEC, ^{1}H NMR, and SEM [125]. Another application of novolac-type resins with HMTA is seen in brake friction materials [134]. Novolac type resin acts as a binder in the friction material and the purpose is to maintain structural integrity when exposed to mechanical and thermal stresses. Brake friction materials contain several other components such as reinforcing fibers, abrasives, lubricants, and fillers. The amount of binders in brake friction materials can range from 20-40% [135]. An environmentally friendly LPF resin with methanol soluble soda lignin was produced for use in brake friction material [13].

Overall, when comparing other technical lignins, a lignin that is of low molecular weight, more polydisperse, low Tg, high PhOH and low S/G ratio proved to be a better candidate for resin production.

Proposed Lignin-Furfural Based Resins in this Study

In the lignin-furfural resin system, lignin and furfural are proposed to replace phenol and formaldehyde used in PF resins, respectively. The lignin and furfural undergo reactions in acidic conditions. Under acidic conditions, higher electron density is created on the C2 and C6 carbons of the phenylpropanoid units. Two mechanisms are responsible for this phenomenon: The induction effect of the alkyl group at position 1 and the resonance effects of the electron pairs on the methoxy oxygen Figure 22 [136]. Therefore, the C2 and C6 positions on the ring represent reactive sites toward electrophilic substitution and will condense with the electrophilic aldehyde carbonyl carbon. A proposed mechanism of lignin-lignin condensation and lignin-furfural condensation is shown in Figure 23. However, acidic conditions also result in depolymerization (acidolysis) of lignin. A carbonium ion at the β position is formed under acidic conditions by the proton-induced elimination of water (ether) from the benzylic position. The cleavage of the β-ether linkage in the glycerol-aryl-β-ether structure results in the carbonium ion reacting further to form Hibbert ketones, analogous to an acidolysis reaction. This may lead to competing reactions of depolymerization and repolymerization of lignin [24,26,137–141]. Under acidic conditions, it is also expected that the xylose/xylose based oligomers/polymers which are likely to be present in the hardwood biorefinery lignin are converted to furfural to form a resin blend (Figure 23).

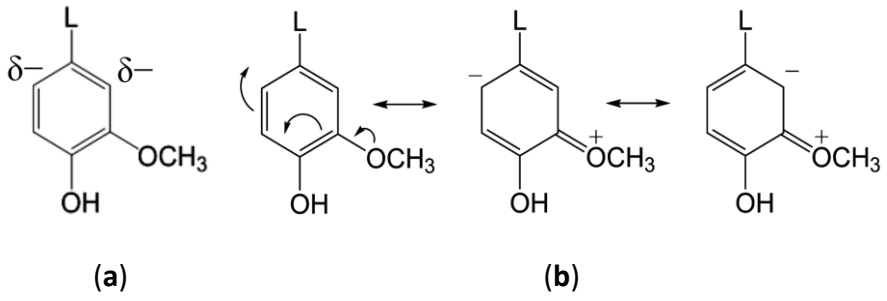

Figure 22: Mechanism that governs the presence of higher electron density on Position 2 and 6 on lignin phenylpropanoid units in acidic medium: (**a**) the induction effect of the alkyl group at Position 1; and (**b**) the resonance effect of the electron pairs on the methoxy oxygen *[136]*.

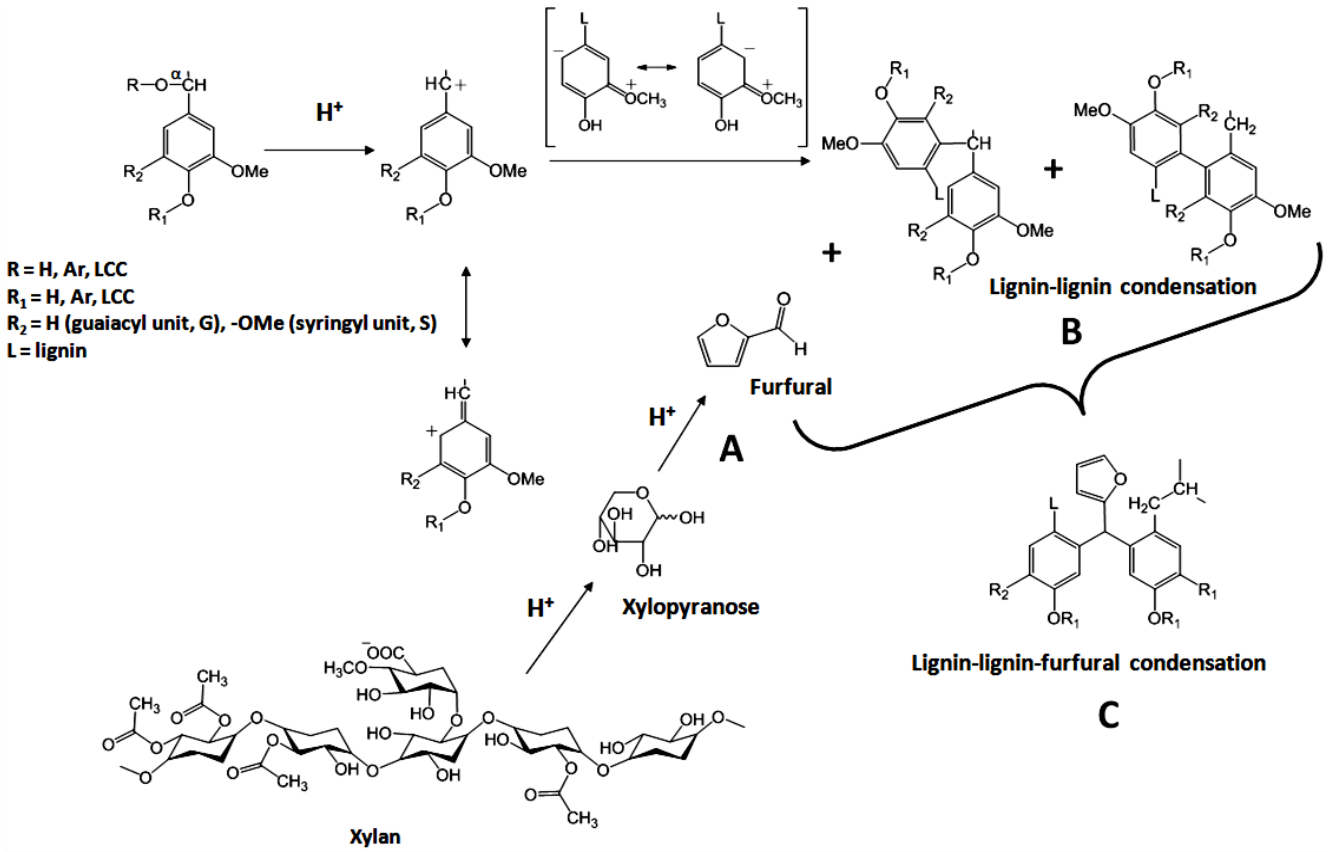

Figure 23: Proposed mechanism of lignin-furfural condensation products: (**A**) xylose based carbohydrates breakdown to furfural; (**B**) lignin-lignin condensation takes place; and (**C**) lignin-lignin-furfural condensation product (adapted from [22,142–144].

Furfural as a Biorefinery Product

The added advantage of using furfural as a crosslinking agent is that it is a potential biorefinery product, as it can be generated from pentoses. Furfural is formed during acid catalyzed dehydration of xylose and arabinose [145]. The classical reaction mechanism of xylose conversion to furfural is show in Figure 24, and Figure 25 shows an alternate mechanism proposed in literature. HWE targets mainly xylan based hemicelluloses, these sugars can be used as raw materials for furfural production. Research is ongoing in this area [146]. Currently, furfural is mainly used to produce furfuryl alcohol (industrial chemical) and tetrahydrofuran (THF). Other applications include use as a chemical intermediate solvent, fungicide, nematocide, and even a scenting and flavoring agent.

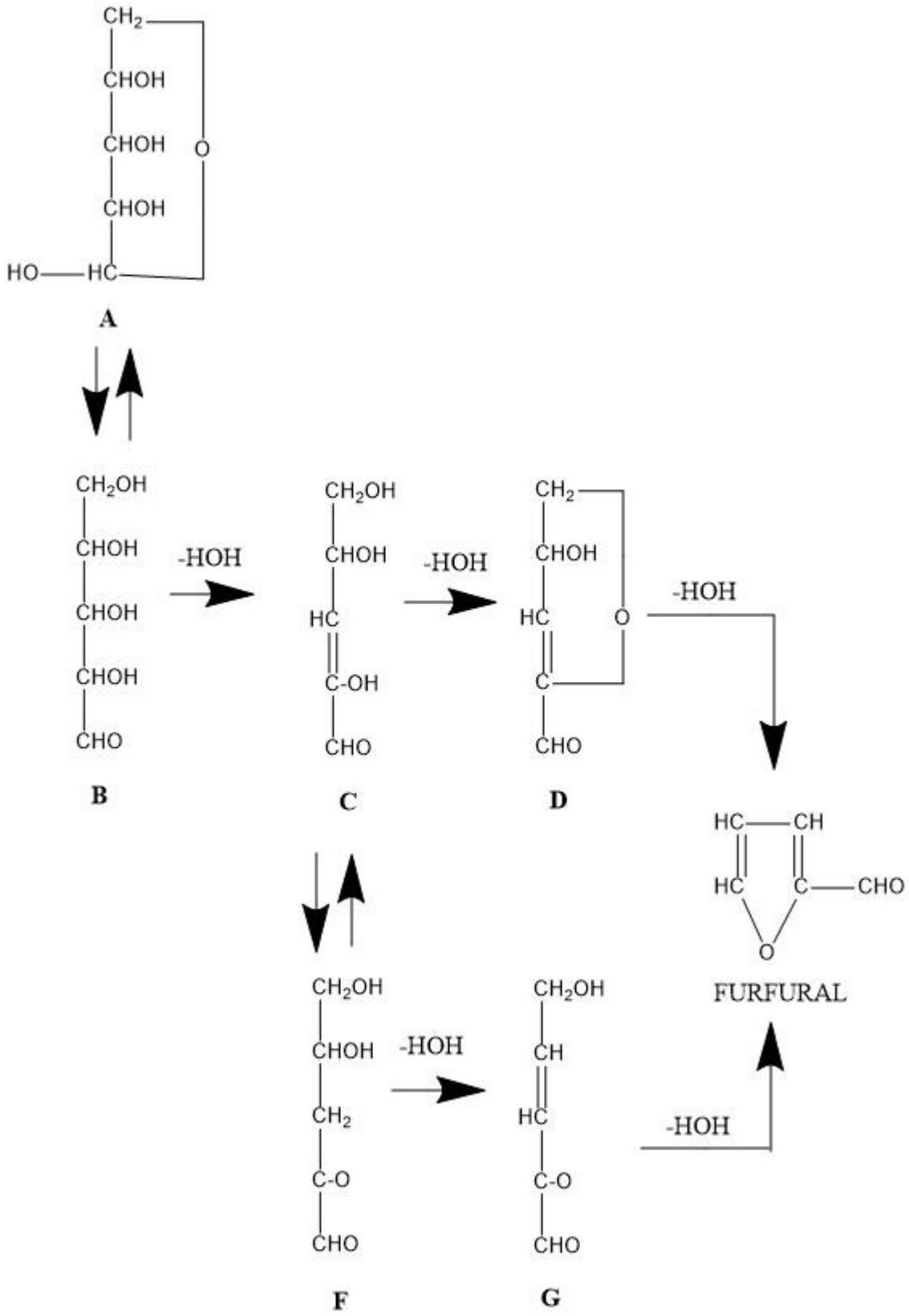

Figure 24: Classical reaction mechanism, as proposed in various sources. Adapted from Root (1956) [147].

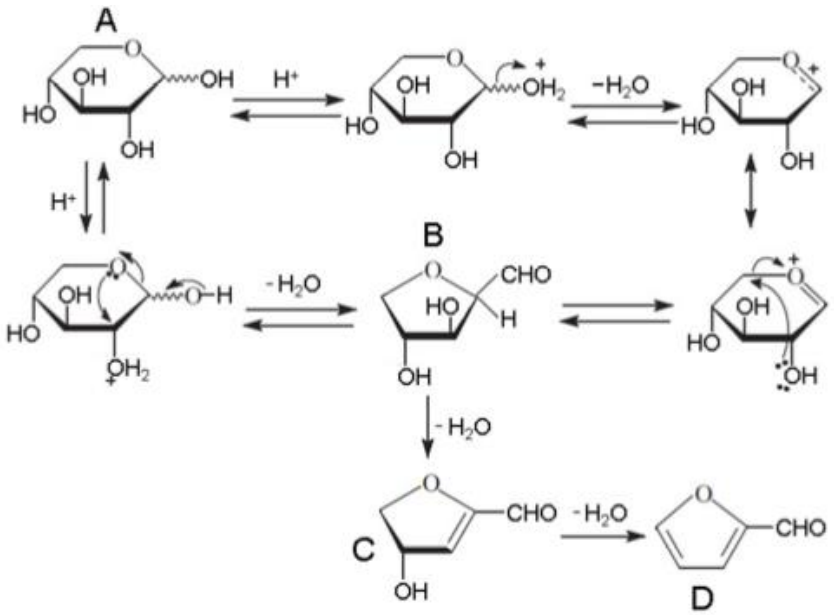

Figure 25: Reaction pathway through cyclic intermediates, proposed by Antal et al (1991) [148]. Adapted from Yang et al (2012) [149]. A is the pyranose form of xylose, and D is furfural.

CHAPTER IV: MATERIALS AND METHODS

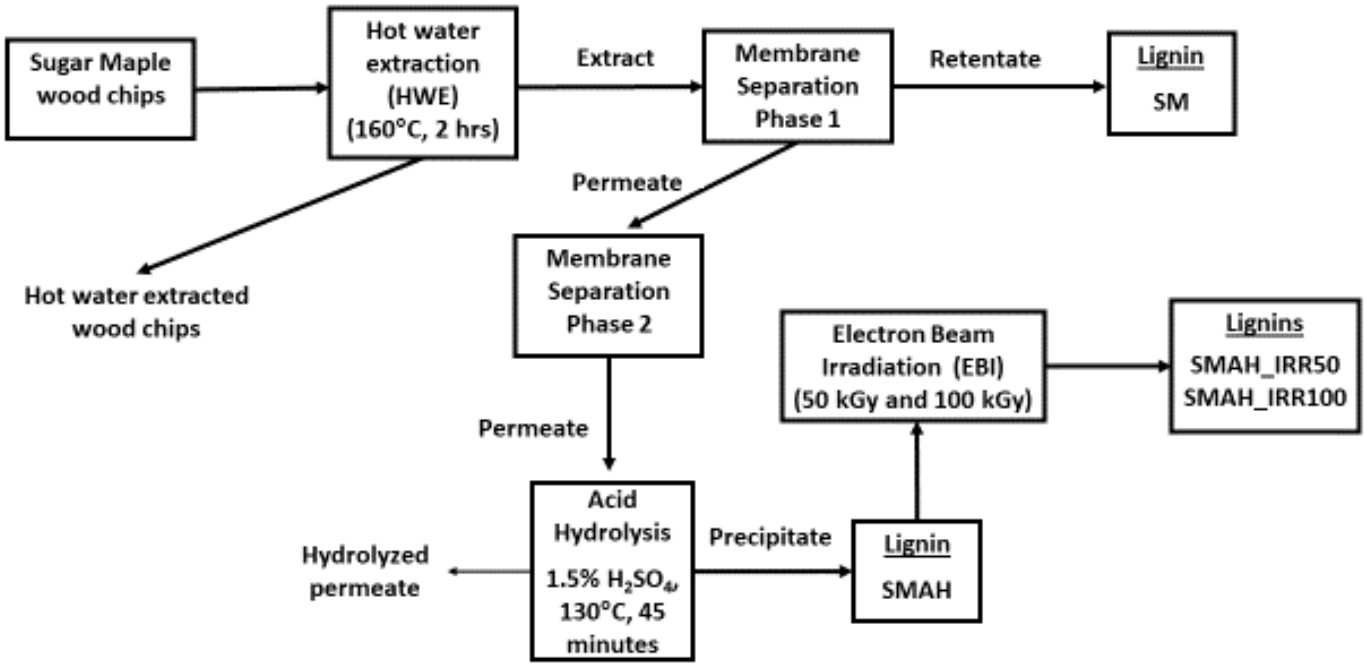

Figure 26: Scheme showing the origin of SM, SMAH SMAH_IRR50 and SMAH_IRR100 lignins. Sugar maple wood chips undergo HWE at 160°C for 2 hours. The extract undergoes membrane separation 1 to produce SM lignins. The permeate from this membrane separation (Phase 1) undergoes membrane separation 2. The permeate from this membrane separation (Phase 2) is subjected to acid hydrolysis (1.5% H_2SO_4, 130°C and 45 minutes). The precipitate collected is SMAH lignin. SMAH lignin was subjected to two levels of EBI – 50 and 100 kGy producing SMAH_IRR50 and SMAH_IRR100.

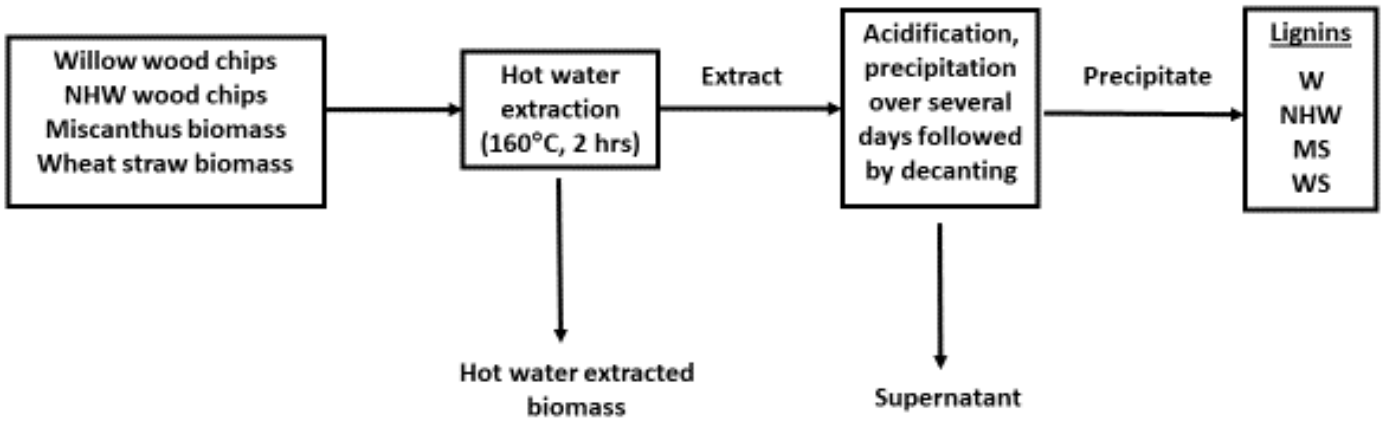

Figure 27: Scheme showing the origin of W, NHW, MS and WS lignins. The respective biomass undergoes HWE at 160°C for 2 hours. The extract is subjected to acidification, precipitation and the supernatant decanted. The precipitate is collected to give W, NHW, MS or WS lignins.

4.1 Materials

Furfural (99%, CAS 98-01-1) was bought from Sigma-Aldrich (St. Louis, MO). Glass fibers filters (Type A/C) for mechanical testing were bought from Pall Corporation (New York City, NY). PF (novolac type) was obtained from Advanced Polymers International (Syracuse, NY). For comparison purposes, two technical lignins were obtained. Kraft lignin (KL) (alkali, CAS 8068-05-1) was obtained from Sigma Aldrich and a biorefinery lignin (PL) was obtained from Pure Lignin Environmental Technologies (Kelowna, BC). The biorefinery lignin has been isolated from dilute acid hydrolysis of sugar maple shavings. For this work, the PL lignin was washed with pH 2 aqueous solution to remove inorganic material, as recommended by the supplier. Friction paper was obtained from Borgwarner Inc (Auburn Hills, MI). Two types of kraft paper (linerboard) – softwood and hardwood - were obtained from International Paper.

4.2 Methods (Experimental):

4.2.1 Lignin Isolation and Characterization

The acid insoluble lignin content of all lignin samples are determined by the Tappi Method T 222 om-02, Acid-insoluble lignin in wood and pulp [150]. Acid soluble lignin content is determined by measuring UV absorbance at 205 nm [151]. The biorefinery lignin samples that are investigated in this work were obtained from hydrolysates produced in hot water extraction of Sugar maple (*Acer saccharum*) (SM; wood chips, industrial size, SUNY-ESF Pilot Plant), Willow (*Salix sp.* (W); mixed commercial varieties, SUNY ESF Tully station), mixture of northern hardwoods (NHW) (Aspen, Red Oak and Maple), Miscanthus (*Miscanthus* sp. Family: *Poaceae)* (MS; harvested from Bono, AK, January 2015) and Wheat straw (WS; harvested from Central NY, Summer 2015). MS and WS were provided at ¾ screen size by

MESA Inc. Auburn, NY. SM, W and NHW chips were of ¾" in length, provided by the SUNY-ESF Pilot plant.

The studied lignins were obtained from the following procedure conducted at our Pilot Plant previously. Biomass is subjected to hot-water extraction (160 °C, 2 h). Hot-water extraction was carried out in a Struthers-Wells 65 ft^3 stainless lined batch digester. During hot-water extraction, mostly xylans and some inorganics and lignin are dissolved in the extract [2]. The procedure of isolation differed slightly from this step onward for different species.

For sugar maple (SM), the extract then undergoes ultrafitration via a membrane which is a Hilco HM634-01 with a pore size of 0.01 µm ceramic filter. The retentate is recovered, the pH dropped to 2 and centrifuged to obtain the SM fraction. The permeate further undergoes nano-filtration. The permeate of the nano-filtration process is acid hydrolyzed with concentrated sulfuric acid (1.5% by mass of extract) at 130 °C for 45 min. The precipitate (SMAH) formed is recovered with dissolution in acetone-water (1:1) mixture and steam stripped to remove the solvents. The scheme is shown in Figure 26.

For willow (W), northern hardwoods (NHW), miscanthus (MS), and wheat straw (WS), the extract was collected and the pH dropped to 2. The lignin was allowed to precipitate for a week at room temperature. The supernatant was decanted and the lignin was air dried. The scheme is shown in Figure 27.

Carbohydrates were analyzed from acid-hydrolysate resulting from Klason lignin determination at the United States Department of Agriculture - Forest Products Lab (USDA-FPL) (Madison, WI) [152].

4.2.2 Ash

The method for ash content is according to Tappi method T 211-om-02, Ash in wood, pulp, paper and paperboard: combustion at 900°C, Test Method. 2 g of moisture free sample was

weighed and ignited in a muffle furnace at 900°C. The resulting sample is used to calculate the ash content.

4.2.3 Molecular Weight Distribution

The molecular weight distribution was determined using size exclusion chromatography (SEC). The columns used were Waters Styragel HR 0.5, HR 3 and HR 4E. The solvent used was THF, concentration of the sample was 1 mg/mL and the flow rate was 0.8 ml/min. The dissolved samples were then filtered through 45μm polyvinylidene fluoride (PVDF) filters. The detection method used was UV spectrophotometry with absorption at 280nm. Polystyrene standards (molecular weight range from 1,500-2,500,000Da) were used for calibration, obtained from Waters (Milford, MA), and a 3rd order polynomial equation was used for quantification and the data was normalized. The samples were acetylated prior to SEC.

4.2.4 Nuclear Magnetic Spectroscopy (NMR)

All 2D heteronuclear single quantum correlation nuclear magnetic resonance spectroscopy (HSQC NMR) experiments were acquired at 30°C on a Bruker AVANCE III 600 spectrometer (600MHz 1H frequency, Bruker Biospin Corporation, Billerica, MA, USA) equipped with a 5 mm triple resonance *z*-gradient probe. Data was processed in Topspin v. 3.2 from Bruker Biospin. SM was dissolved in deuterated dimethyl sulfoxide (DMSO-d_6) and SMAH, W, NHW, MS, WS, SMAH_IRR50 and SMAH_IRR100 were dissolved in deuterated acetone (acetone-d_6) prior to NMR analysis. All samples were acetylated prior to NMR analysis. S/G ratio was determined using HSQC data. Correlations for $S_{2,6}$ and G_2 selected and the G_2 correlations were doubled. [129].

4.2.5 Acetylation

Acetylation was carried out by subjecting the materials to a pyridine: acetic anhydride (1:1) mixture for 24 hrs. at room temperature. The reaction was stopped by dropping the sample in ice-water and filtered via 15mL gooch crucibles [153]. The maximum weight gain due to acetylation was observed to be 20%.

4.2.6 Free Phenolic Hydroxyl Group Content (PhOH)

Free phenolic hydroxyl content of all lignin samples was determined by the periodate method [154]. Cool (below 4°C) 7 ml of distilled water was added to 50mg of lignin samples and 50mg of sodium periodate, and left in the refrigerator for 72 hours. The mixture was shaken occasionally. The supernatant was then filtered through glass fiber filters. 1ml of the clear supernatant and 100µl of internal standard, deuterium oxide (D_2O) were added to a NMR tubes, for ^1H NMR analysis.

The periodate oxidation method of PhOH analysis involves the production of one mole of methanol from each PhOH via demethylation of an adjacent methoxy group [101]. The methanol content was quantified by ^1H NMR. The methanol peak was quantified relative to a known molarity of water in the sample. PhOH results are presented as mmol of PhOH per gram of lignin. PhOH results are averages of two replicates; standard deviation is shown when possible.

However, it is to be noted that this method is useful for lignins that have a methoxy group adjacent (*ortho*- positon) to the free phenolic hydroxyl group [154]. MS and WS being grasses, also have H-lignin. H-lignin does not have methoxy groups on the aromatic ring and therefore the phenolic groups on H lignin are not measured. Therefore, the PhOH content of MS and WS lignins reported in this study are underestimates.

4.2.7 Kappa number

Kappa number of softwood and hardwood paper was determined by the Tappi standard T 236 Kappa number of pulp **[155]**. Lignin level was calculated based on the conversion factor provided in the T 236 shown in Equation (1)

Lignin level (%) = Kappa number X 0.13 (1)

4.2.8 Thermogravimetric Analysis (TGA)

Thermogravimetric analysis (TGA) of untreated lignins and lignin based resin blends was performed using TA instruments Q500. The TGA was run under nitrogen atmosphere and heated up to 700°C at a rate of 10°C/min.

4.2.9 Differential Scanning Calorimetry (DSC)

Differential scanning calorimetry of untreated lignins and lignin based resin blends was performed using TA instruments Q200. The DSC was run under nitrogen atmosphere with a heat/cool/heat cycle. The temperature range was 0 - 200°C and the heating and cooling rate was 10°C/min.

4.2.10 Electron beam irradiation (EBI)

The effect of EBI was studied on the SMAH biorefinery lignin. The SMAH lignin was subjected to irradiation levels of 50 kGy and 100 kGy. The samples were irradiated at IBA Industrial Inc., Edgewood NY using a 3 MeV 90 kW dynamatron electron beam.

Based on preliminary results, it was observed that lower molecular weight lignin was a better candidate for resin production. Therefore, EBI was performed on lignin to decrease the molecular weight of lignin.

4.2.11 Preparation of lignin based resins

Resin blends are made in a slightly modified manner in accordance with Johansson's method where 15%–34% sulfite liquor was reacted at pH = 0.3–0.6 with sulfuric or hydrochloric acid at temperatures of 90–160°C. The resultant products were applied to wood chips, formed into sheets and cured at temperatures of 150–180°C and pressures of 0.8 and 2MPa [156].

In this study, a design of experiment was performed and the matrices are shown in Table 4 and Table *7*. Duplicates of 25g (over-dried) of lignin from the biorefinery, isolated from hot water extraction of different species, are subjected to acid hydrolysis at pH = 1 (30% formic acid), pH = 0.65 or 0.3. The reaction is carried out at 90°C for 1 h with 0%, 5%, 8%, 16%, 50%, 100% or 200% furfural, on lignin content. (Table 4 and

Table *5*). To obtain pH = 0.3 and 0.65, concentrated hydrochloric acid is added to 30% formic acid until desired pH is reached. After the reaction is complete, the product is allowed to cool to room temperature and the pH is adjusted to 2 using 2M NaOH solution. The resin product is then filtered via a Büchner funnel and washed with distilled water several times to remove any water soluble materials and unreacted furfural and then air-dried. The prepared resin blends and PF resin are then dissolved in acetone at 20% consistency for mechanical testing.

The data was collected in two phases. The first phase involved experiments on SMAH lignin only. The furfural content was varied from 0-16% and the pH values tested were 0.3, 0.65 and 1.

Table 4: Lignin-based resin blends studied in these experiments with their furfural content and reaction pH condition – design of experiment matric. The lignin sample used in these experiments: SMAH (the fraction separated from sugar maple hot-water extract after acid hydrolysis). Kraft lignin (KL) was used as a control.

Sample ID	**Furfural content (%)**	**Reaction pH condition**
SMAH F16_1	16	1
SMAH F8_1	8	1
SMAH F5_1	5	1
SMAH F0_1	0	1
SMAH F5_065	5	0.65
SMAH F0_065	0	0.65
SMAH F5_03	5	0.3
SMAH F0_03	0	0.3
KL F5_1	5	1
KL F0_0.65	0	0.65

The second phase was done using miscanthus lignin (MS) and SMAH lignin (the fraction separated from sugar maple hot-water extract after acid hydrolysis). The specific conditions are shown in

Table *5*.

Table 5: Lignin-based resin blends studied in these experiments with their furfural content and reaction pH condition. The lignin sample used in these experiments: miscanthus (MS).

Sample ID	Furfural content (%)	Reaction pH condition
MS F200_1	200	1
MS F100_1	100	1
MS F50_1	50	1
MS F0_065	0	0.65
SMAH_F0_065	0	0.65

The third phase was to include lignins from other species and the specific conditions are shown in Table 6.

Table 6: Lignin-based resin blends studied in these experiments with their furfural content and reaction pH condition. The lignin samples used in these experiments: willow (W), Northern hardwoods (NHW), wheat straw (WS) and PL.

Sample ID	Furfural content (%)	Reaction pH condition
W_F50_1	50	1
NHW_F50_1	50	1
WS_F50_1	50	1
PL_F50_1	50	1
SMAH_IRR100_F0_065	0	0.65
W_F0_065	0	0.65
NHW_F0_065	0	0.65
WS_F0_065	0	0.65
PL_F0_065	0	0.65

4.2.12 Mechanical testing on glass fiber filters

The method for testing tensile strength is according to [8] and Tappi method T 494-om-01 [157] with slight modifications. Glass filter fibers are cut into 4″ × 1″ strips, oven dried at 105 °C and weighed. The strips are then immersed in the prepared resin blends and the PF commercial resin for 5 min, removed and left to dry overnight. The dried strips are then pressed in an electric hydraulic press at different curing temperatures and pressures. The blends obtained from the first phase (Table 4) were cured at the temperatures and pressures shown in Table 7. The blends obtained from phases 2 and 3 (Table 5 and Table 6) were cured at 180°C and 1.9 MPa.

The pressed glass fibers are oven dried at 105 °C and weighed once again to determine the amount of resin absorbed by the glass fiber. The glass fiber strips are conditioned at 23 °C and 50% humidity. The strips are then tested in MTS 1/S Sintech tensile equipment for tensile properties. The inert glass fibers do not swell in water and any change can be associated with the resin and not the fiber substrate itself. The tensile strength per gram of the resin is calculated with Equation (2).

$$Tensile\ strength\ per\ gram\ (N/m\ g) = \frac{Tensile\ strength\ of\ reinforced\ fiber\ (N/m) - Tensile\ strength\ of\ the\ blank\ fiber\ (N/m)}{Mass\ of\ adhesive\ absorbed\ by\ the\ glass\ fiber\ (g)} \quad (2)$$

Tensile strength (N/m) is defined as the maximum stress experienced by the material prior to catastrophic failure. The Young's modulus (GPa) or elastic modulus (used interchangeably throughout this text) is the slope of the linear portion of the stress-strain curve. A representative stress-strain curve is shown in Figure 28.

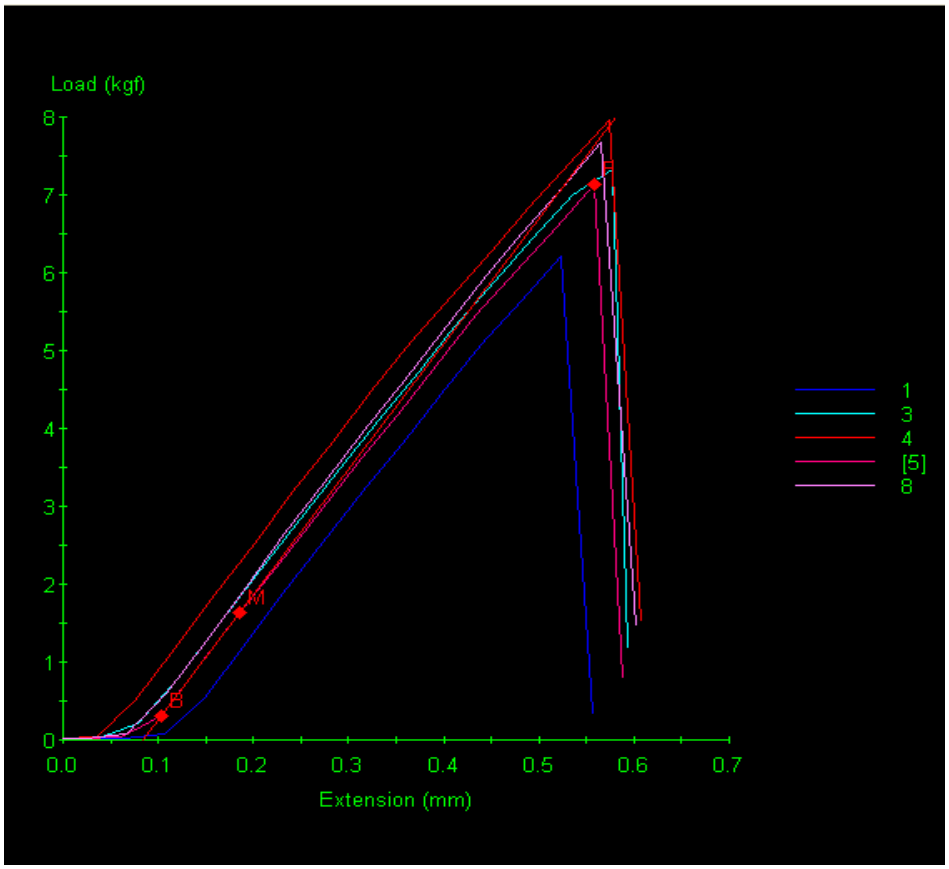

Figure 28: Representative stress-strain curves of PF and lignin-based resins.
(1) SMAH_IRR100_F0_065; (3) KL_F0_065; (4) PF; (5) SMAH_F0_065; (8) MS_F50_1.

Table 7: The pH and curing conditions at which the experiments were carried out with 5% furfural and 0% furfural – design of experiment matrix. Additional blends with 8% and 16% furfural prepared at pH = 1 were pressed at 1.9 MPa and 180 °C. The tensile strength per gram of the resin is calculated using Equation (2).

Curing conditions		**Pressure (MPa)**	
		1.9	**3.8**
Temperature (°C)	**180**	pH = 1	pH = 1
		pH = 0.3	pH = 0.3
		pH = 0.65	-
	150	pH = 1	-
		pH = 0.3	

4.2.13 Mechanical testing on friction paper

Mechanical testing of resin blends on friction paper was performed according to methods provided by Borgwarner Inc. Two types of tests - heat aged tensile retention and hot oil exposure were performed on the PF, MS F50_1 and SMAH_F0_065 and SMAH_IRR100_F0_065 resins. The heat aged tensile retention was performed by exposing resin reinforced samples to 22 hours in a 150°C oven and the tensile loss was measured. The hot oil exposure test was performed by subjecting resin reinforced friction paper samples to 22 hours in hot transmission oil (automatic transmission fluid, ATF) at 110°C and tensile loss was measured. The tensile strength per gram of the resin is calculated using Equation (2).

4.2.14 Mechanical testing on kraft paper

Novolac, MS F50_1 and W F50_1 were used to reinforce two types of kraft papers – softwood and hardwood. The samples were tested in accordance with according to [8] and Tappi method T 494-om-01 [157] with slight modifications as stated in Section 4.2.12. The tensile strength per gram of the resin is calculated using Equation (2).

CHAPTER V: RESULTS AND DISCUSSION

5.1 Characterization of Crude Lignins

Crude biorefinery and technical lignins (SM, W, NHW, SMAH, SMAH_IRR50, SMAH_IRR100, MS, WS, KL and PL) were characterized for their chemical composition – total lignin content (acid soluble and insoluble), and ash content (Table 8), carbohydrate composition in regard to monosaccharide constituents (Table 9), Lignin samples were also characterized for their free phenolic hydroxyl content (PhOH) and S/G ratio (Table 10), molecular weight distribution (

Figure *29*), thermal degradation behavior (Figure 31 and Figure 32), and glass transition temperature (Tg) (Table 12). A thorough characterization was performed in attempts to elucidate the factors which govern reactivity of studied lignins in trials to use them as phenol-formaldehyde alternatives.

5.1.1 Chemical Composition of Crude Lignins

The total lignin content varied from 79-95% of the crude lignins (Table 8). The purity of biorefinery lignins is higher than that of technical KL and PL lignins. W, NHW, MS and WS have higher acid soluble lignin (4.5%, 4.7%, 4.9% and 3.4%, respectively) compared to the SM fraction (1.9%). This may be because of the different recovery method in regard to use of membrane separation vs. precipitation. Unlike SM, the hot water extracts of these species were allowed to precipitate over several days after acidification, the supernatant was decanted and the precipitated lignin was left to air dry. This may have retained some low molecular weight compounds, resulting in higher readings of acid soluble lignin (results of UV-spectral analysis at 205nm).

A closer look is taken at the comparison between SM and SMAH as they are both products of the same starting materials (Figure 26). The acid insoluble lignin content of SM and SMAH lignins is approximately the same, whereas the acid-soluble lignin content of SMAH is higher compared to SM, which again might reflect different recovery methods. SM is the retentate of the ultrafiltration process where low molecular weight fractions were filtrated out. In contrast, SMAH was recovered as the precipitate from the digester after acid hydrolysis of the permeate from the ultrafiltration process (see Materials and Methods Section). The low molecular weight compounds may have been retained in SMAH resulting in higher readings of acid soluble lignin than in SM (results of UV-spectral analysis at 205nm).

EBI treatment appears to improve the purity (total lignin content) of SMAH lignin by ~4%, independent of the irradiation intensity (50 or 100kGy). The acid-insoluble lignin content of SMAH_IRR50 and SMAH_IRR100 is ~91% whereas the acid-soluble lignin content is 3.4% and 2.6%, respectively. It is possible that constituents detected in the acid soluble solution of SMAH may have condensed with Klason lignin. Due to radical formation during irradiation, polymerization of lignin and carbohydrates may have occurred, increasing the Klason lignin content (Klason lignin is measured via gravimetric method - see Materials and Methods). However, it is unclear whether this polymerization occurred during irradiation or acid hydrolysis when performing the Klason method.

The ash content for all lignin samples is relatively low. The low ash content in lignin recovered from hot water extraction is expected as the water soluble supernatant/filtrate is separated from the lignin portion during recovery. NHW has the highest ash content of 2.26% which is not expected but might be a result of higher levels of bark/mineral impurities in the mixture of hardwood feedstock for hot water extraction, used in these experiments. As stated in the materials and methods section, NHW lignin is recovered form hot water extraction of wood accumulated over a period of several years at the SUNY-ESF pilot plant. The raw material may

have accumulated impurities during this idle period. W lignin contains the lowest amount of ash (0.2%), followed by KL (0.4%). This value for KL is unexpectedly low as literature reports KL ash content to be as high as 25% [14,158].

Table 8: Lignin content and ash content of biorefinery and technical lignins based on oven-dried mass (SM, SMAH, NHW, W, MS, WS, KL and PL)

Lignin sample ID	**Lignin (%)**			**Ash @ 900°C (%)**
	AISL	**ASL**	**Total**	
SM	86.4	1.9	88.3±1.48	0.29±0.07
W	80.2	4.5	84.7±0.8	0.20±0.02
NHW	78.2	4.7	82.9±0.21	2.26±0.03
SMAH	85.8	4.9	90.7±0.35	0.31±0.2
SMAH_IRR50	91.2	3.4	94.6±1.72	0.29±0.1
SMAH_IRR100	91.4	2.6	94.0±0.76	0.19±0.09
MS	74.7	4.7	79.4±0.37	1.47±0.03
WS	77.0	3.7	81.0±0.95	1.78±0.05
PL	71.2	6.2	77.4±0.47	1.10±0.04
KL	51.6	19.9	71.5±2.36	0.40±0.01

It appears lignin recovered from hot water extraction contains lignin that is associated to carbohydrates, probably in the form of lignin carbohydrate complex (LCC). LCCs are soluble in water to some extent [159]. The carbohydrate composition of the lignins in Table 9 shows that the most abundant carbohydrate is xylan based. This is expected as angiosperms are xylan-rich and the preferred raw material for hot water extraction. [38,160]. MS and WS contain the highest amount of xylan as shown in Table 9. The bonds between lignin and carbohydrates can

be varied – benzyl ester, benzyl ether or phenyl glycosidic (Figure 13). Both benzyl ester and phenyl glycosidic bonds are acid stable whereas benzyl ether is not. The pH of the hot water extract ranges from 3.5-4 depending on the species. These mild acid conditions may retain some of the lignin-carbohydrate linkages resulting in an impure lignin.

Table 9: Carbohydrate composition of biorefinery and technical lignins: SM, SMAH, MS, WS, KL and PL (based on oven-dried mass)

Lignin sample ID	Carbohydrates[1] (%)					
	Arabinan	**Galactan**	**Glucan**	**Xylan**	**Mannan**	**Total**
W	ND	ND	1.19	1.19	0.60	2.99
SMAH	0.06	0.11	0.22	0.45	ND	0.84
SMAH_IRR50	ND	ND	ND	0.6	ND	0.6
SMAH_IRR100	ND	ND	ND	0.56	ND	0.56
MS	0.48	ND	0.96	3.85	ND	5.29
WS	0.66	ND	1.99	3.32	ND	5.98
PL	1.1	ND	0.37	0.55	0.31	1.22
KL	ND	ND	0.75	ND	ND	0.75

[1]Results from Forest Products Lab. Method according to [152]
ND: not detected

Free phenolic hydroxyl groups are characteristic of native lignin and range from 10-15 PhOH per 100 C_6C_3 units (0.5-0.75mmol/g lignin) for hardwoods, 15-30 PhOH per 100 C_6C_3 (0.84-1.7mmol/g lignin) for softwoods [29], and 1.46-3.4mmol/g lignin for graminae [153,161,162]. The specific values are shown in Table 10. The PhOH groups are also produced when cleavage of aryl ether bonds occurs during chemical processing of lignins [29]. Therefore, lignins with higher PhOH content can be more reactive during further chemical processing of lignin,

performed for valorization. The PhOH content of crude lignins are shown in Table 10 and range from 0.84 to 2.23mmol/g lignin. Lignin recovered from hot water extraction has shown to have higher PhOH content than native lignin due to acid-catalyzed cleavage of aryl ether bonds [98,163]. This is specifically seen in the cases of SM, W, and NHW; the values are higher than in native lignin of hardwoods. This may indicate that lignin from hot water extraction is of lower molecular weight than native lignin. Molecular weight distribution of crude lignins will be discussed in detail later in the document.

Table 10: Free phenolic hydroxyl groups (PhOH) content and S/G ratios of biorefinery lignins. Reference values of PhOH and S/G ratios are also provided.

Lignin sample ID	**S/G ratio (HSQC)**	**S/G ratio (literature)**	**PhOH (mmol/g lignin) (Periodate)**	**PhOH (mmol/g lignin) (literature)**
SM	-	2.66[1]	1.95±0.06	0.4[9]
W	1.25	1.70[2]	1.97±0.02	-
NHW	0.52	0.78-2.12[3]	2.23±0.01	0.5-0.75[10]
SMAH	3.23	-	1.58±0.1	-
SMAH-IRR50	2.49	-	1.30±0.02	-
SMAH-IRR100	-	-	1.08±0.09	-
MS	2.86	0.70[4]	1.96[7]	1.53[11]
WS	1.90	0.50[5]	1.19±0.01	1.46[12]
PL	NA	2.76[6]	0.84±0.01[8]	-
KL		-	1.10±0.01[8]	

[1] [25]
[2] [164]
[3] Milled wood lignin, [165,166]
[4] Milled wood lignin, [167]
[5] Milled wood lignin, [58]
[6] non-acetylated, [168]
[7] [95]
[8] [169]
[9] Milled wood lignin, [25]
[10] Milled wood lignin, [29]
[11] Milled wood lignin, [170]
[12] Milled wood lignin, [161]

The differences between SMAH and its irradiated counterparts (SMAH_IRR50 and SMAH_IRR100) appear to be noteworthy. SMAH lignin has a PhOH content of 1.58mmol/g lignin and SMAH_IRR50 and SMAH_IRR100 have PhOH contents of 1.30 and 1.08mmol/g lignin, respectively. It can be seen that increasing the intensity of irradiation decreases PhOH content. EBI causes radical formation which can lead to polymerization of lignin at the PhOH position resulting in a decrease of free phenolic hydroxyl groups. Therefore, it can be expected that the molecular weight of SMAH IRR50 and SMAH IRR100 is higher than SMAH, discussed later.

Table 10 also shows the S/G ratios of the crude lignins, determined by the quantitative 2D HSQC analysis method [25,129]. The literature S/G values are also provided in Table 10. The S/G values for SM lignin [25] and PL lignin [168] were reported earlier. The literature values of W, MS, WS and NHW are that of milled wood lignin, reported in Table 10 [164–167]. The lignins recovered from hot water extraction have a relatively higher S/G ratio compared to native lignins. This indicates that, in the case of hardwood, lignin containing higher amounts of S units (lignin from fibers) is more readily soluble during hot water extraction, than lignin that is more G-enriched (lignin from vessels).

It is worth mentioning that even though the quantitative 2D HSQC method for S/G ratio determination is reported in literature [28,58,98], it is important to note that these values can be error prone. Error can arise from potential overlap of $S_{2,6}$ and G_2 correlations which makes selecting the area for integration tricky and subjective. However, S/G ratio is an important metric for understanding the possible reaction mechanism that may occur during resin productions. It has been proposed that crosslinking of lignin during resin production in acid conditions takes place at the $S_{2,6}$ or $G_{2,6}$ positions (Figure 23). Therefore the quantification of S and G units can be indicative of the reactivity of the lignin. A reference method such as

nitrobenzene oxidation or pyrolysis must be performed to confirm these values for future studies.

Low S/G ratio entails more G units which could lead to condensation at the G_5 position in addition to the $S_{2,6}$ or $G_{2,6}$ position, resulting in a highly crosslinked polymer. A high S/G ratio (more S units) would only crosslink at the $S_{2,6}$ or $G_{2,6}$, a less extensively crosslinked polymer. An extensively crosslinked polymer may possess good mechanical properties suitable for resin applications as is the case for PF resin. Lignin rich in G lignin has been proposed as better raw material for resin production.

5.1.2 Molecular Weight Distribution of Biorefinery Lignins

A specific molecular weight of lignin cannot be determined due to the non-uniformity of chain lengths seen in lignin. Therefore, average molecular weights are defined. Two common averages used are, number average molecular weight (Mn) and weight average molecular weight (Mw) as shown in Equation (3) and (4). Molecular weight distribution is defined by the polydispersity (PD), Equation (5) [171].

$$Mn = \frac{\sum NiMi}{Ni} \quad (3)$$

$$Mw = \frac{\sum NiMi^2}{NiMi} \quad (4)$$

$$PD = \frac{Mw}{Mn} \quad (5)$$

Here the index number, i, represents the number of different molecular weights present in the lignin sample and Ni is the total number of moles with the molar mass of Mi.[171–174].

Figure *29* shows the molecular weight distribution of the six biorefinery lignin samples; SM, SMAH, W, NHW, MS and WS. Figure 30 compares the molecular weight distributions of SMAH_IRR50 and SMAH_IRR100 with SMAH. The Mn, Mw and the PD of all lignin samples are shown in (Table 11). All lignin samples (Figure 29 and Figure 30) demonstrate at least a bimodal distribution.

Table 11: Number average molecular weight (Mn), weight average molecular weight (Mw) and polydispersity (PD) of biorefinery lignins

	SM	W	NHW	SMAH	SMAH IRR 50	SMAH IRR 100	MS	WS
Mn	1825	2186	1924	1748	3421	3241	2124	2850
Mw	3058	5962	4745	1861	8772	8377	4672	12114
PD	1.68	2.73	2.47	1.06	2.56	2.58	2.2	4.25

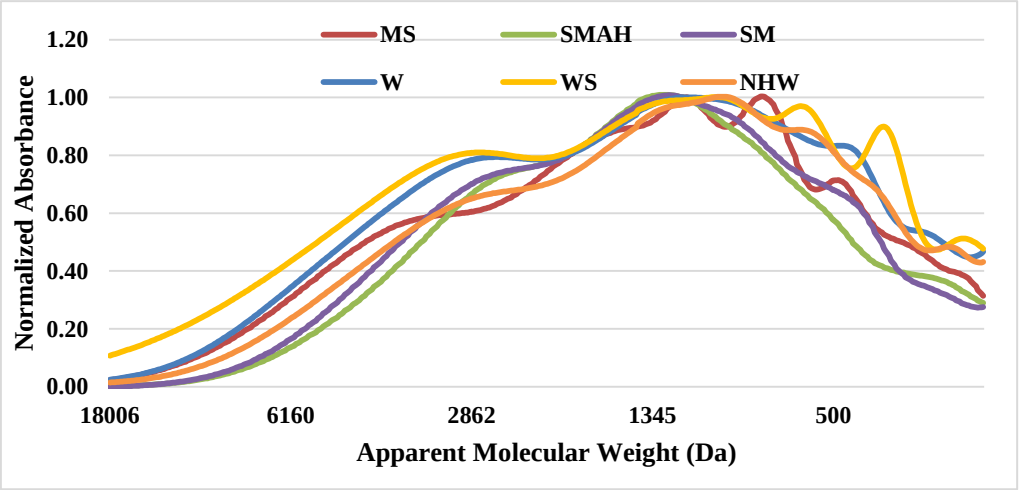

Figure 29: Normalized molecular weight distribution of lignin samples isolated from different species from the SUNY-ESF biorefinery: sugar maple before acid hydrolysis (SM), sugar maple after acid hydrolysis (SMAH) hot-water extract, willow (W), miscanthus (MS) and wheat straw (WS)

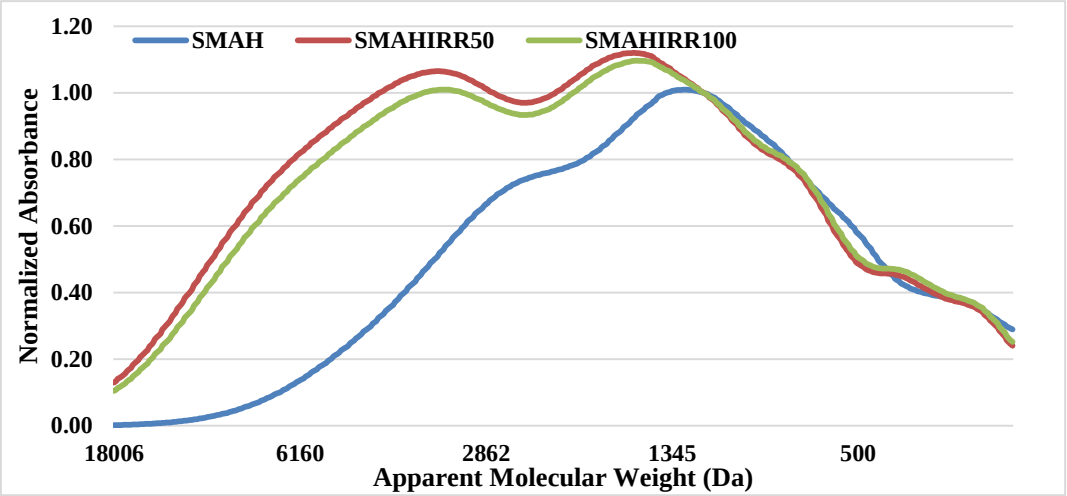

Figure 30: Normalized molecular weight distribution of lignin samples isolated from different species from the SUNY-ESF biorefinery: sugar maple after acid hydrolysis (SMAH), SMAH electron beam irradiated at, 50 kGy (SMAH_IRR50) and 100 kGy) SMAH_IRR100).

In regard to molecular weight, lignin can be a very diverse material depending on the species, chemical processing and isolation methods. Native lignin is generally of higher molecular weight. The Mn values can range from 2,000-8,000Da, Mw can range from 5,000-23,000Da and PD can be between 1.6-3.7 approximately [174]. Technical lignin, such as, softwood kraft lignin has been reported to have Mn, Mw and PD values from 545-1,700Da, 1,099-8,000Da, and 2-8, respectively [14,175,176]. Crude lignins in this study are of lower molecular weight (Table 11) than their native counterparts but are in the range of kraft lignin reported in literature. It has been suggested that a lignin of low molecular weight is preferable for resin applications, especially phenol-formaldehyde based applications, as it is more reactive [5]. The PD of crude lignins is also on the lower side which makes it an attractive candidate for high value applications, as it is more homogenous.

Some significant differences are seen in non-irradiated lignins (SM, SMAH, W, WS, MS and NHW). The molecular weight distribution curves of W, WS, MS, NHW exhibit multiple low molecular weight shoulders, as compared to SM and SMAH (Figure 29). This is reflected in the PD values as well - W, WS, WS and NHW have higher PD than SM and SMAH. This

may be the result of different isolation procedures. SM and SMAH were obtained from membrane separation whereas W, WS, MS and NHW were isolated from precipitating the lignin over several days and decanting the supernatant. The decanting procedure is not as efficient as membrane separation and may retain some low molecular weight compounds that the filtration step removes. Therefore the lignins from the filtration method (SM and SMAH) are much more uniform (PD of 1.68 and 1.06, respectively).

A closer look is taken at the comparison between SM and SMAH. The molecular weight of SMAH is expected to be lower than SM due to membrane separation and acid hydrolysis procedures. Cleavage of aryl ether bonds, mainly β-O-4 bonds in lignin, is expected in acidic conditions. This cleavage may result in a much more uniform lignin. However, lignin undergoes competing polymerization and depolymerization reactions in acid conditions [24,177,178]. Cleavage occurs at the β-O-4 position and condensation occurs at the G_5 position. The simultaneous reaction in opposite direction may result in a more uniform lignin.

The effect of electron bean irradiation on molecular weight is also noteworthy. There is a significant increase in molecular weight and polydispersity of lignin after irradiation for both SMAH_IRR50 and SMAH_IRR100 (Figure 30 and Table 11), compared to SMAH. EBI can either cause condensation reactions via coupling of radicals or cleavage [81,179,180]. Studies on lignin model compounds have shown cross-coupling of lignin cause by the removal of a hydrogen atom on the hydroxyl or methyl groups. [181,182]. The increase in molecular weight corroborates with the PhOH values discussed earlier (Table 10). The irradiated lignins have lower PhOH indicating that polymerization is taking place at the OH position.

5.1.4 Thermal Behavior of Biorefinery Lignins

The biorefinery lignins recovered from HWE were also characterized for their thermal decomposition behavior via thermogravimetric analysis (TGA) and derivative (D) TGA and the data is presented in Figure 31. These lignins demonstrate decomposition over a wide range of temperatures but the maximum weight loss occurs at around 360°C for all lignins except KL (318°C). All lignins show a shoulder at approximately 235°C except for W. It is to be noted that willow biomass was not debarked prior to HWE. Therefore, the lignin recovered from this raw material may contain some hemicellulose-like compounds (peak at 192°C) from bark, such as pectins, which are most likely absent in other lignin samples.

Thermal degradation behavior of lignin occurs in three stages. Stage one occurs in the range of 30–120°C and is attributed to the evaporation of water. Stage two occurs at around 180–250°C and signifies degradation of the carbohydrates in the lignin samples. As seen from Figure 31, the peak representing hemicellulose degradation is a shoulder indicating a smaller amount of hemicelluloses in the lignins. The carbohydrates are converted to volatile gases such as CO, CO_2, and CH_4. The third and final stage of degradation occurs in the range of 300-450°C. Degradation in this region involves the breakdown of inter-unit linkages. This releases monomeric phenols in the vapor phase. Therefore, volatile compounds derived from lignin including phenolics, alcohols, aldehyde acids and gaseous products are removed in this stage. Any degradation observed above 500°C occurs due to decomposition of some aromatic rings. The residual mass after degradation for all samples lies in the range of 40-50% due to highly condensed structure of lignin [15,183,184].

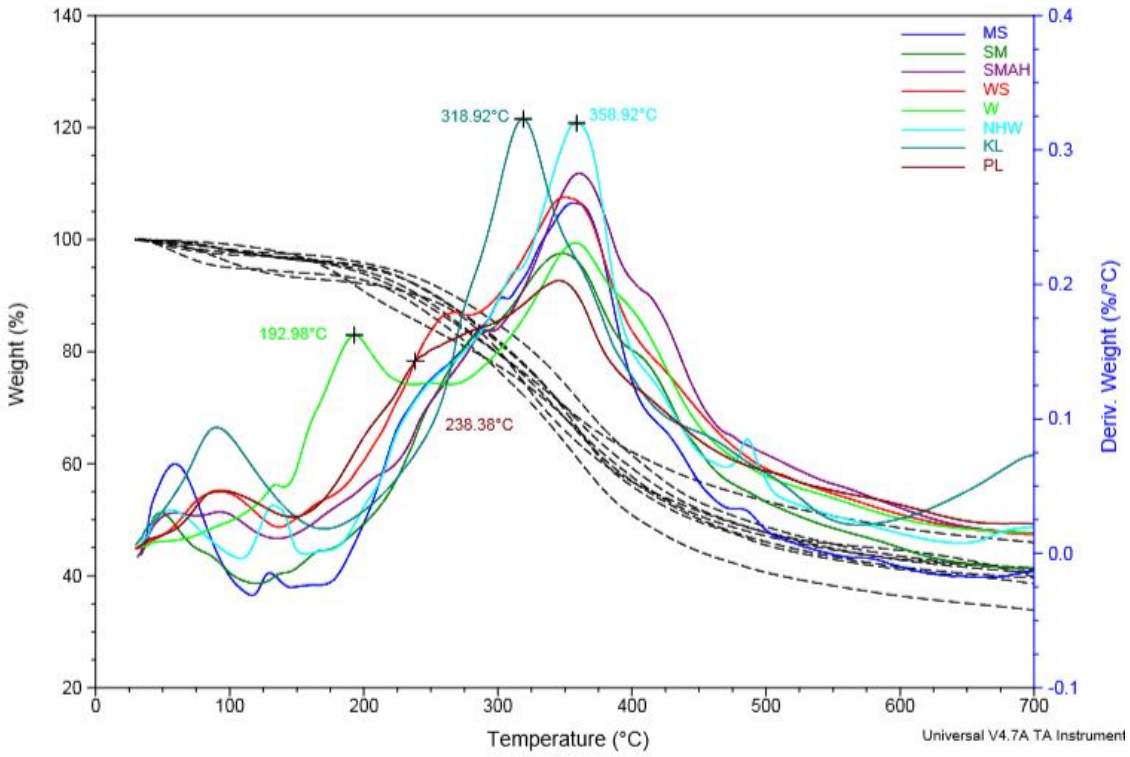

Figure 31: TGA of biorefinery and technical lignins: SM, SMAH, W, NHW, MS, WS, KL, PL

Figure 32 shows the thermal decomposition of SMAH and its corresponding irradiated fractions of 50 and 100 kGy (SMAH_IRR50 and SMAH_IRR100, respectively. The residual char of SMAH and SMAH_IRR100 is approximately 40%. On the contrary the residual char yield for SMAH_IRR50 is 60%.

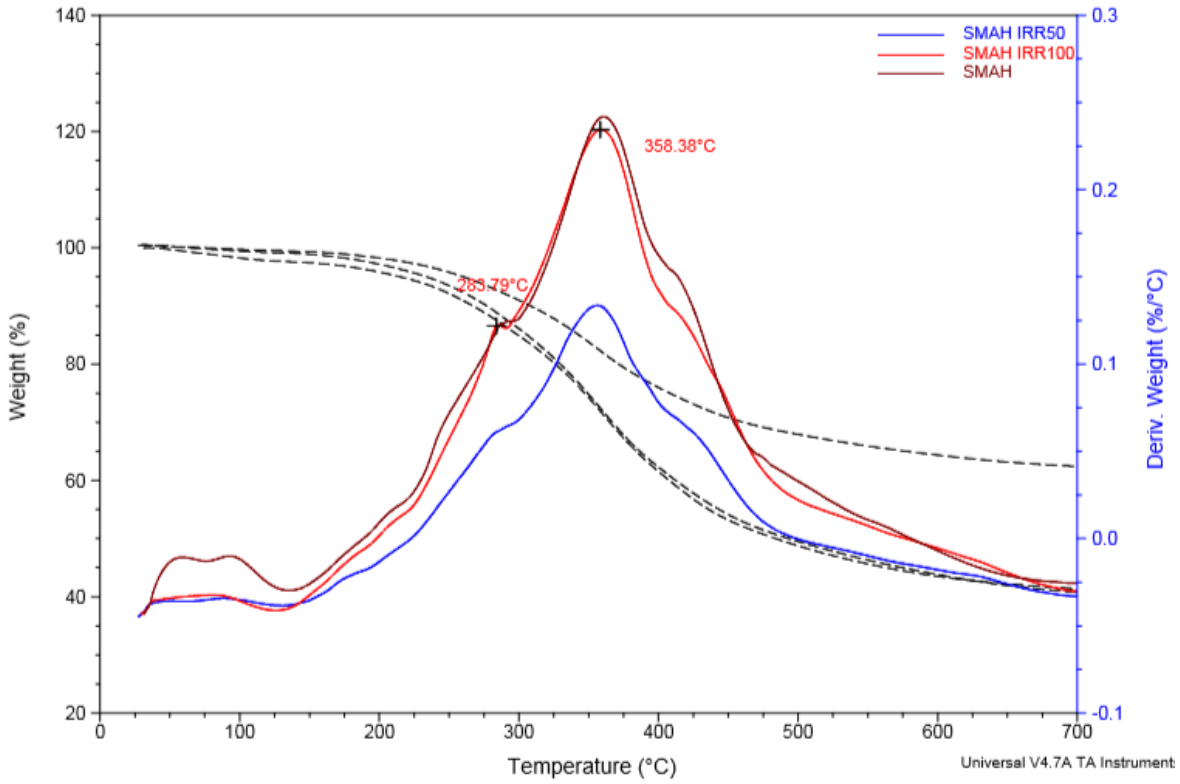

Figure 32: TGA of SMAH lignin and its corresponding irradiated fractions of 50 and 100 kGy (SMAH IRR50 and SMAH IRR100)

Table 12: Glass transition temperature of biorefinery and technical lignins (SM, W, MHW, SMAH, SMAH_IRR50, SMAH_IRR100, MS, WS, KL and PL). [1] *[185]*

Lignin sample ID	**Tg (˚C)**
SM	143
W	159
NHW	132
SMAH	161
SMAH_IRR50	160
SMAH_IRR100	160
MS	123
WS	143
PL	ND
KL	172
Softwood kraft lignin[1]	138-174
Hardwood kraft lignin[1]	110-130
Organosolv lignin[1]	91-97
Steam explosion lignin[1]	113-139

The biorefinery lignins were also studied for their glass transition temperature (Tg) and the results are shown in Table 12. The Tg of the samples ranges from 123°C to 172°C. Tg is the temperature at which localized segments of a polymer chain demonstrate mobility. Below the Tg, polymers will demonstrate more brittle behavior whereas above Tg, more flexible behavior. The variability of Tg can be attributed to the different non-phenolic content in the lignins (Table 8). These contaminants may act as plasticizers or antiplasticizers which may decrease or increase Tg [186]. Plasticizers decrease Tg of a polymer, as they create more free volume for the chains to move [187]. The general trend observed, is that higher xylan content results in lower Tg. MS and WS have higher xylan content (5.29% and 5.98% respectively, Table 8) and both exhibit lower Tg (123°C and 143°C, respectively, Table 12). Furthermore, SMAH, which has the lowest xylan content (0.45%, Table 8), among the non-irradiated biorefinery lignins, has the highest Tg of 161°C. EBI does not appear to have an effect on Tg. The Tg of SMAH_IRR50 and SMAH_IRR100 is the same as that of SMAH, even though lignin purity does slightly improve and xylan content is reduced (Table 8 and Table 9). It is important to note that xylan has a Tg of its own at around 180°C. However the Tg of xylan is difficult to detect due to thermal degradation at higher temperatures [188,189].

5.2 Lignin based resins

The preparation of lignin based resins occurred in several stages, mainly based on availability of the type of lignin. Initial scouting studies (Section 5.2.1) were performed on SMAH lignin alone. The effect of pH (0.3, 0.65 and 1), furfural (0%, 5%, 8%, 16%, 50%), curing temperature (180°C and 150°C), and curing pressure (1.9MPa and 3.8MPa) on the tensile properties of resin reinforced glass fibers was determined. All results were compared to PF reinforced glass fibers as the control. Based on the results obtained from the initial scouting studies, curing conditioned were kept constant for all future studies (180°C and 1.9MPa).

MS lignin was selected for preparation of resins in the second stage where even higher amounts of furfural were added to the lignin for resin preparation. The conditions that were chosen were 0% furfural at pH 0.65 and 50%, 100% and 200% furfural (% based on lignin) at pH 1 (Section 5.2.2).

This was then followed by adding other lignin species – W, NHW, WS, SMAH_IRR50, SMAH_IRR100, KL and PL (5.2.3). The conditions at which resins were prepared were 0% furfural, pH 0.65 (F0_065) and 50% furfural, pH 1 (F50_1). All results were compared to PF resins.

The effect of two curing agents (HMTA and furfural) on the formulations was also studied to determine if a curing agent was required as is the case for PF based novolac-type resins (Section 5.2.4).

Based on the results obtained on the glass fiber substrate, three other substrates were chosen – friction paper, and softwood and hardwood kraft papers (Section 5.2.5). The purpose was to determine if the lignin based resins could be used as binders in industrial applications such as, friction paper in brake parts or in composite materials such as Richlite™. Richlite™ is a

composite material that is made by immersing several layers of kraft paper in PF based novolac resin and cured at high temperature and pressure, producing a solid stable sheet of material. The applications of Richlite™ include countertops, musical instruments, and furniture. The resins were also tested on wood veneers for an adhesive application.

Wood veneer testing: 3-ply wood veneer, according to ASTM standard D 906 [190], was performed on select lignin based resins (MS_F50_1 and SMAH_F0_065). The resins were applied to the plies and then cured at 180°C and 1.9MPa. No data was obtained as there was no catastrophic failure observed – wood fiber did not fracture. This implies that the resin did not bond with the wood fiber or penetrate into the wood surface. The curing times ranged from 15-60 minutes. The curing temperatures ranged from 180-220°C. The curing pressures ranged from 1.9-3.8MPa.

5.2.1 Initial Scouting Studies

As stated above the effect of pH (0.3, 0.65 and 1), *ex situ* furfural (5%, 8% and 16%), curing temperature (180°C and 150°C), and curing pressure (1.9MPa and 3.8MPa) were studied on the mechanical properties of lignin. The resin was prepared by the method detailed in Section 4.2.11 and dissolved in acetone: water (6:4). Glass fiber filters were immersed in this solution, cured and then tested for mechanical properties.

It was concluded from these results that the optimum curing conditions were 180°C and 1.9MPa. No additional furfural was required below pH 1 to produce good mechanical properties in the resins and the formulation SMAH_F0_065 demonstrates the best tensile strength (90% that of PF). At pH 1, addition of furfural is required and the resin with 16% furfural (SMAH_F16_1) demonstrates comparable properties to PF. The results that are presented in this section have also been published previously [90].

Effect of Curing Pressure and Temperature on Mechanical Properties of Resin Reinforced Glass Fibers

The curing study of two pressures (1.9MPa and 3.8MPa) and two temperatures (180°C and 150°C) was conducted on formulations prepared with 5% and 0% furfural in pH = 0.3 and 1. The tensile testing was done on resin reinforced glass fibers. Figure 33 shows the effect of curing temperature on the mechanical properties of the resin blends prepared at pH = 0.3 and 1 with 5% furfural (F5_03 and F5_1) and with constant curing pressure of 1.9MPa. Figure 34 shows the effect of curing pressure on the same blends (F5_03 and F5_1) with a constant curing temperature of 180°C. The purpose of curing is to further promote the resin-resin and the resin-substrate (glass fiber) cross-linking process. Tensile strength per gram (N/m·g) was determined using Equation (2).

$$Tensile\ strength\ per\ gram\ (N/m\ g) = \frac{Tensile\ strength\ of\ reinforced\ fiber\ (N/m) - Tensile\ strength\ of\ the\ blank\ fiber\ (N/m)}{Mass\ of\ adhesive\ absorbed\ by\ the\ glass\ fiber\ (g)} \quad (2)$$

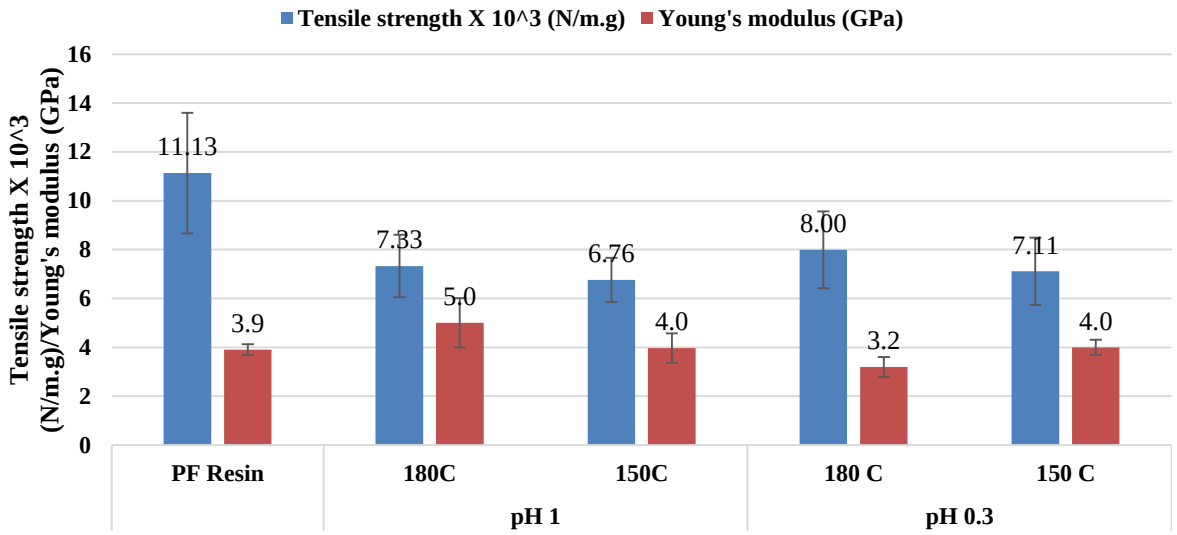

Figure 33: Effect of curing temperature (150°C and 180°C) on tensile properties of resin blends with 5% furfural at curing pressure of 1.9MPa and reaction pH = 0.3 and 1. All samples are compared to PF resin which was cured at 180°C and 1.9MPa. Tensile strength per gram (N/m·g) was determined using Equation (2).

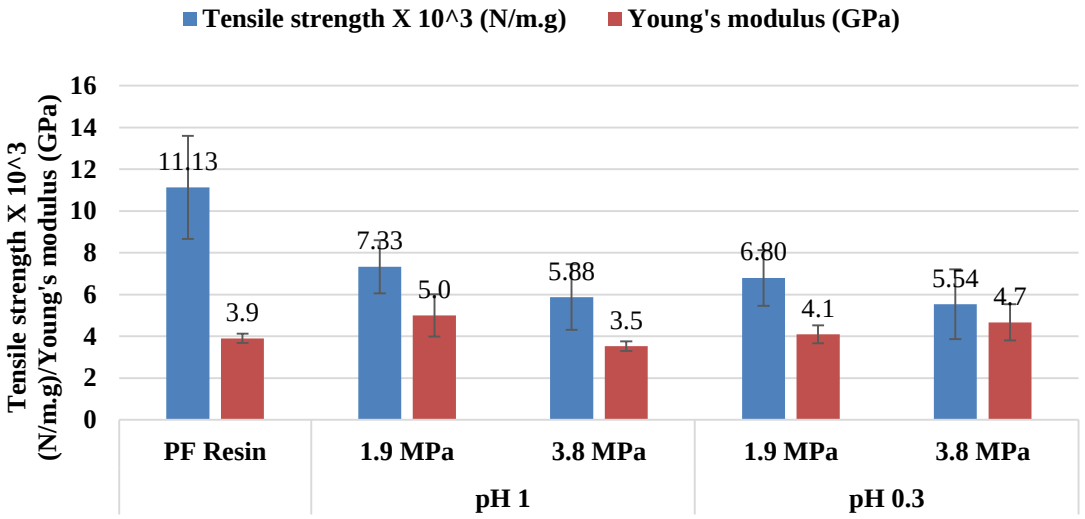

Figure 34: Effect of curing pressure (1.9MPa and 3.8MPa) on tensile properties of resin blends with 5% furfural at curing temperature of 180°C and reaction pH = 0.3 and 1. All samples are compared to PF resin which was cured at 180°C and 1.9MPa. Tensile strength per gram (N/m·g) was determined using Equation (2).

For both F5_1 and F5_03, decreasing the curing temperature from 180°C to 150°C compromised the tensile strength of the resins by 8% and 11%, respectively. This suggests that at the lower temperature, the rate of the curing process is slower, causing fewer cross links and thus causing a decrease in the tensile strength.

At both studied pH conditions, increasing the curing pressure from 1.9MPa to 3.8MPa decreased the tensile strength by 20%. Samples pressed at the higher pressure (3.8MPa) were brittle, compromising the tensile strength and causing catastrophic failure to occur earlier than for the samples pressed at the lower pressure (1.9MPa). At the higher pressure, several resin-resin and resin-substrate crosslinks may have formed. Highly cross-linked polymers experience restricted motion and thus reduced elasticity. This can also be observed via the elastic modulus as samples with higher tensile strength have a lower elastic modulus and vice versa (Figure 34). It was observed that resin blends cured under the conditions 180°C and 1.9MPa performed better, than resin blends cured under other conditions. Therefore, the curing conditions of 180°C and 1.9MPa were kept constant for all future studies.

Effect of pH on Mechanical Properties of Resin Reinforced Glass Fiber Filters

The resin blends with and without furfural were formulated at three pH conditions, 0.3, 0.65 and 1, and their effect on the tensile strength and elastic modulus was determined and compared to PF resin (Figure 35). The curing conditions were kept constant at 180°C and 1.9MPa for all pH conditions based on the findings from earlier studies (Figure 34 and Figure 35).

The formulation produced in pH = 0.65 with 0% furfural (F0_065) resulted in the highest strength of 10,053N/m·g which is about 90% of the PF resin (11,133N/m·g). At pH conditions of 0.3 and 0.65, adding 5% furfural *ex situ* (F5_03 and F5_065) compromised the tensile properties; therefore, experiments with higher amounts of furfural were not conducted at pH < 1. With 5% or 0% furfural, blends prepared at pH = 0.65 produced the best mechanical properties, followed by blends prepared at pH = 0.3 and then pH = 1 (pH 0.65 > pH 0.3 > pH 1). However, it is important to note that blends prepared at pH = 1 with 8% and 16% furfural also exhibited good mechanical properties (Figure 35). This can be attributed to the high concentrations of furfural present in the blends which promotes the cross-linking process.

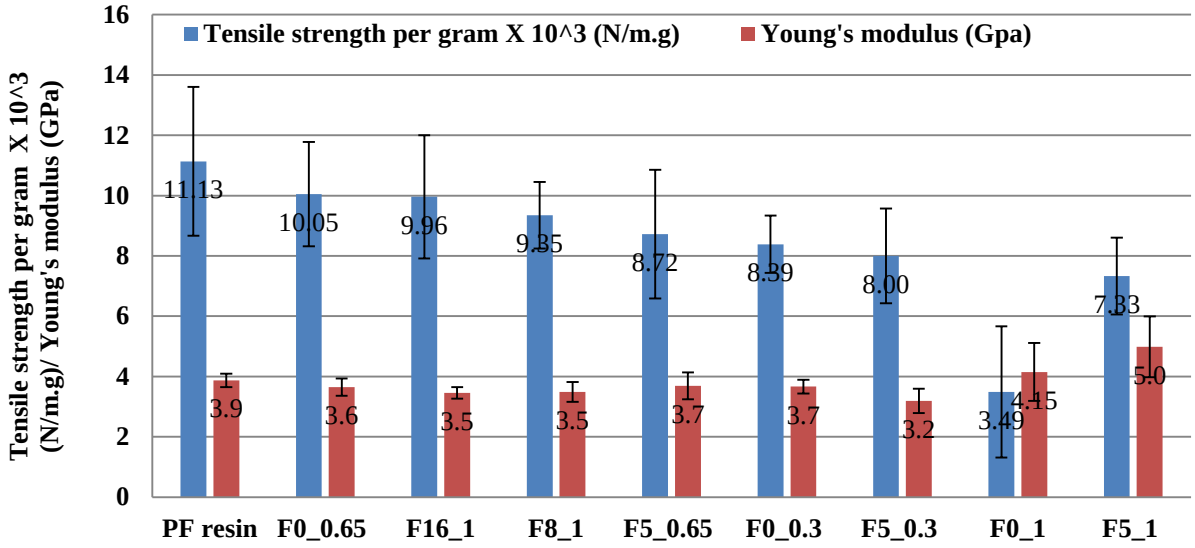

Figure 35: Effect of pH on tensile properties (tensile strength and elastic modulus) resin blends at curing temperature and pressure of 180°C and 1.9MPa. Tensile strength per gram (N/m·g) was determined using Equation (2).

At pH = 1, adding 5% (F5_1) furfural increased the tensile strength per gram by 110% compared to F0_1. The formulation with 8% furfural (F8_1) further improved the tensile strength by 167% and adding 16% furfural (F16_1) improved the strength by 185% compared to F0_1. At pH = 1, the reaction rate is slower and, therefore, additional furfural is required for the polymerization reaction, and these blends may contain lignin-furfural bonds in addition to lignin-lignin linkages.

The samples with 0% furfural produced at pH = 0.65 (F0_065) demonstrate a ~20% improved strength compared to those produced at pH = 0.3 (F0_03). The samples with 5% added furfural (F5_065), demonstrate ~9% increase in strength compared to the sample formulated at pH = 0.3 (F5_03).

Generally, at conditions pH below 1, the reaction rate seems to be high enough for cross-linking reactions to take place via lignin-lignin bonding and/or with the *in situ* furfural that maybe generated from xylose conversion (Figure 23). It appears that the bonds formed *in situ* consume the reactive sites, and the additional furfural does not contribute toward improving tensile properties.

Along with tensile strength, a good elastic modulus is also desired to resist stress at the bond line. The PF resin has an elastic modulus of 3.9GPa, which is higher than the best resin blend (F0_065) by only 8%. In general, samples exhibiting lower tensile strength exhibit higher elastic modulus (Figure 35). It can be concluded that the lignin-based resin blends exhibit elastic moduli that lie in the desired range.

5.2.2 Effect of Higher Furfural Contents

Furfural contents of 0%, 50%, 100% and 200% on lignin, were chosen to be studied in the next step. The species that was selected was MS lignin and the resins that were produced were MS_F0_065, MS_F50 1, MS_F100_1 and MS_F200_1. 50% furfural was also added to SMAH lignin to produce SMAH_F50_1 resin. SMAH_F0_065 resin was used as a reference from earlier studies. The mechanical properties resins made from MS lignin and SMAH lignin are shown in Figure 36. The results showed that adding higher amounts of furfural is beneficial for MS lignin but not SMAH lignin. The results of this section also have been previously published **[95]**.

As seen in Figure 36, MS_F50_1 demonstrates highest strength (20% and 9.5% higher than MS_F0_1 and SMAH_F0_0.65, respectively). However, increasing the furfural content to 100% (MS_100_1) showed lower strength when compared to MS_F50_1 and SMAH_F0_1 (6% and 2.9% lower, respectively).

Adding more furfural to SMAH did not have the same effect (Figure 36). At 50% furfural on SMAH lignin (SMAH_F50_1), the strength decreased by 40% when compared to the reference (SMAH_F0_065). Experiments of 100% furfural on SMAH lignin were not performed as it was hypothesized that the strength will further decrease.

Lignin undergoes competing polymerization and depolymerization reactions under acidic conditions [177,178,191–193]. It has been seen from our studies on SMAH that extensive cross-linking compromised tensile strength of the resin (Figure 35).

Results previously published suggested that SMAH lignin is more condensed and has undergone cleaving of aryl ether β-O-4 bonds due to the acid hydrolysis step performed during isolation, when compared to the SM fraction of sugar maple [90]. Adding 50% furfural to the already condensed SMAH lignin further promotes cross-linking, reducing elasticity of the polymer and decreasing strength (SMAH_F50_1). Adding 50% furfural to MS promotes cross-linking but simultaneously cleaves ether linkages (lignin-lignin and/or lignin-ferulate) under acidic conditions causing depolymerization. This may result in a polymer that has higher tensile strength (MS_F50_1). However, adding 100% furfural could promote extensive cross-linking resulting in decreased strength because of reduced elasticity (MS_F100_1).

It was also observed that the Young's modulus for the formulations varied from 3GPa to 4.1GPa. The different furfural contents did not affect the Young's modulus as much as tensile strength (Figure 36).

These experiments demonstrated that in regard to the tensile strength of resulting formulations adding furfural is more beneficial to lignin recovered from hot-water extract of miscanthus (MS) than to lignin recovered from acid hydrolysate of hot water extract of sugar maple (SMAH).

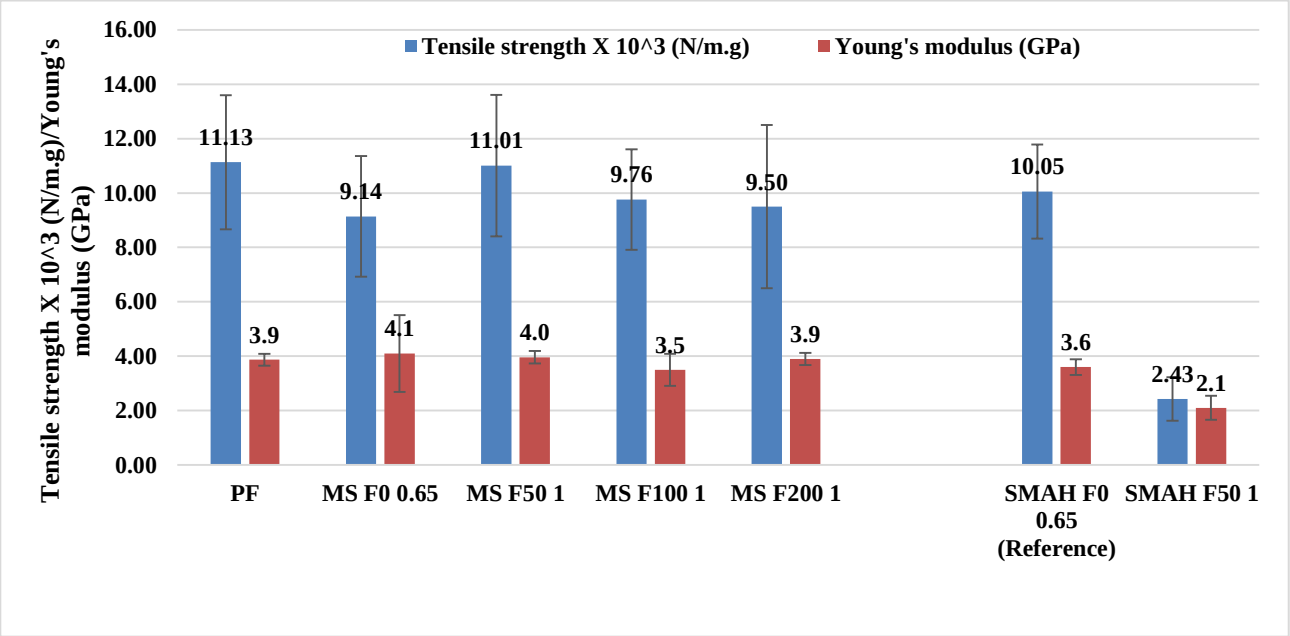

Figure 36: Mechanical properties (tensile strength and Young's modulus) of resin blends prepared from MS lignin at 0% furfural at pH 0.65 (MS F0 0.65) and 50%, 100% and 200% furfural at pH 1 (MS_F50_1, MS_F100_1, and MS_200_1). The results are compared to SMAH_F0_0.65 and SMAH_F50_1. All resins were cured at of 180°C and 1.9MPa. Tensile strength per gram (N/m·g) was determined using Equation (2).

5.2.3 Evaluation of Mechanical Properties of Biorefinery Lignins and their Resin Blends

It was observed from the results obtained from studies on SMAH and MS lignin that resins prepared from these lignins behave differently, in terms of their mechanical properties. Therefore resins prepared from lignins of other species (W, NHW, WS, SMAH_IRR50 SMAH_IRR100, PL and KL) were tested for their mechanical properties on glass fiber filters. First, biorefinery and technical crude lignins (untreated) were tested for mechanical properties to obtain a baseline (Figure 37), which had not been performed in earlier experiments. This was followed by resin production at two conditions: 0% furfural, pH 0.65 (F0_065, Figure 38) and 50% furfural, pH 1 (F50_1, Figure 39). These conditions were chosen based on the data

obtained from studies on SMAH and MS. SMAH performs the best at F0_065 (Figure 35) and MS performs the best at F50_1 (Figure 36). Curing conditions were 180°C and 1.9MPa. The lignin based resins were also characterized for molecular weight distribution to determine if crosslinking was taking place during the reaction.

It appears that only certain lignins show improvement in tensile strength when exposed to resin production conditions of F0_065 and F50_1, and the trends are not consistent across the two different conditions. There was little or no change in the Young's modulus of the resins compared to their crude counterparts. Furthermore, resins prepared from MS (MS_F0_065 and MS_F50_1) and SMAH (SMAH_F0_065) lignins were still the better performing resins compared to other resins. In addition, high molecular weight of resins did not correspond to better mechanical properties. This section also attempts to look at the mechanical properties of the resins in the context of the inherent properties of crude lignin, such as the PhOH-group content, S/G ratio, and molecular weight. A Pearson correlation analysis was also performed to determine the relationships between the crude lignin characteristics and mechanical properties of resins. However, no significant correlations were found to explain these differences. Nevertheless, an attempt has been made to explain the results on a case by case basis.

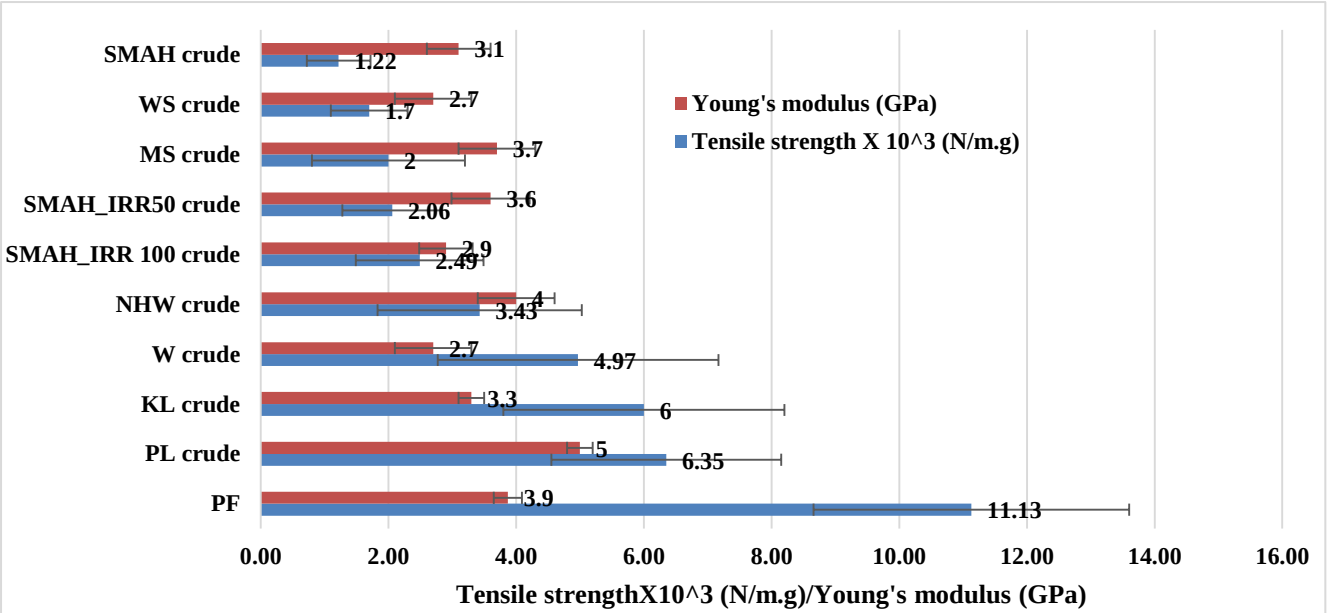

Figure 37: Mechanical properties of crude lignin fractions (SMAH, W, NHW, MS, WS, PL, KL, SMAH IRR 50 and SMAH IRR 100). All resins were cured at of 180°C and 1.9MPa. Tensile strength per gram (N/m·g) was determined using Equation (2).

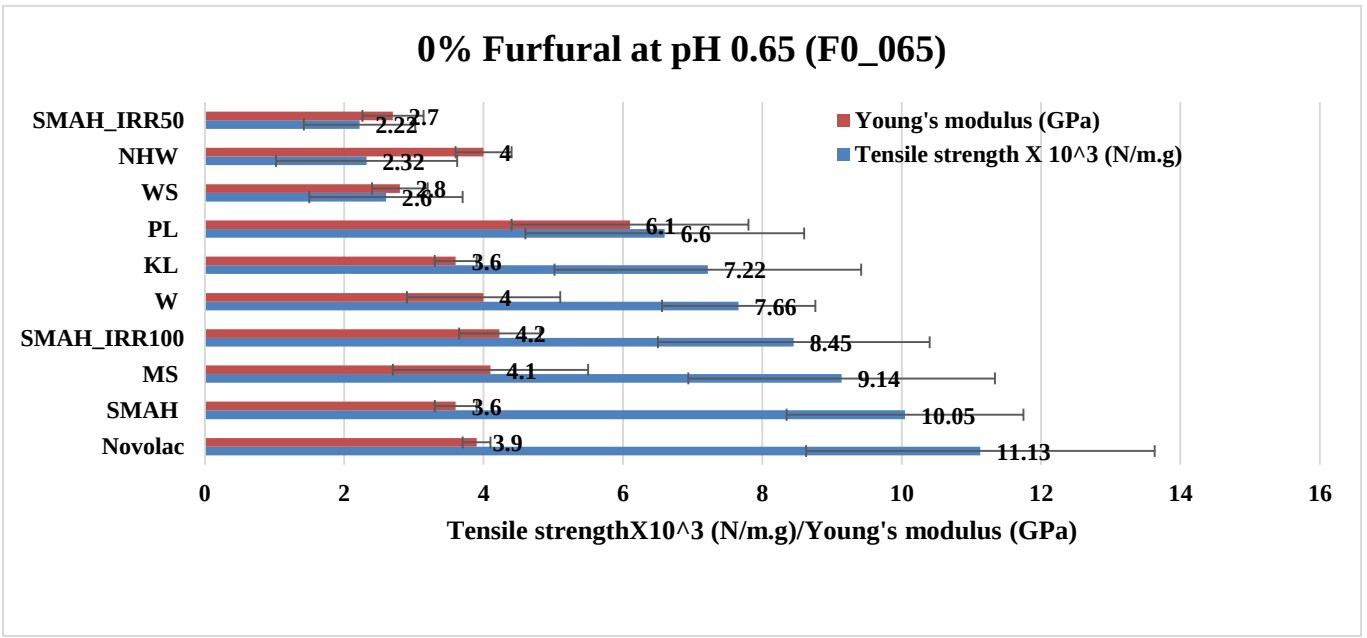

Figure 38: Mechanical properties (tensile strength and elastic modulus) of resin blends at curing temperature and pressure of 180°C and 1.9MPa. All blends were prepared at pH 0.65 with 0% furfural. Tensile strength per gram (N/m·g) was determined using Equation (2).

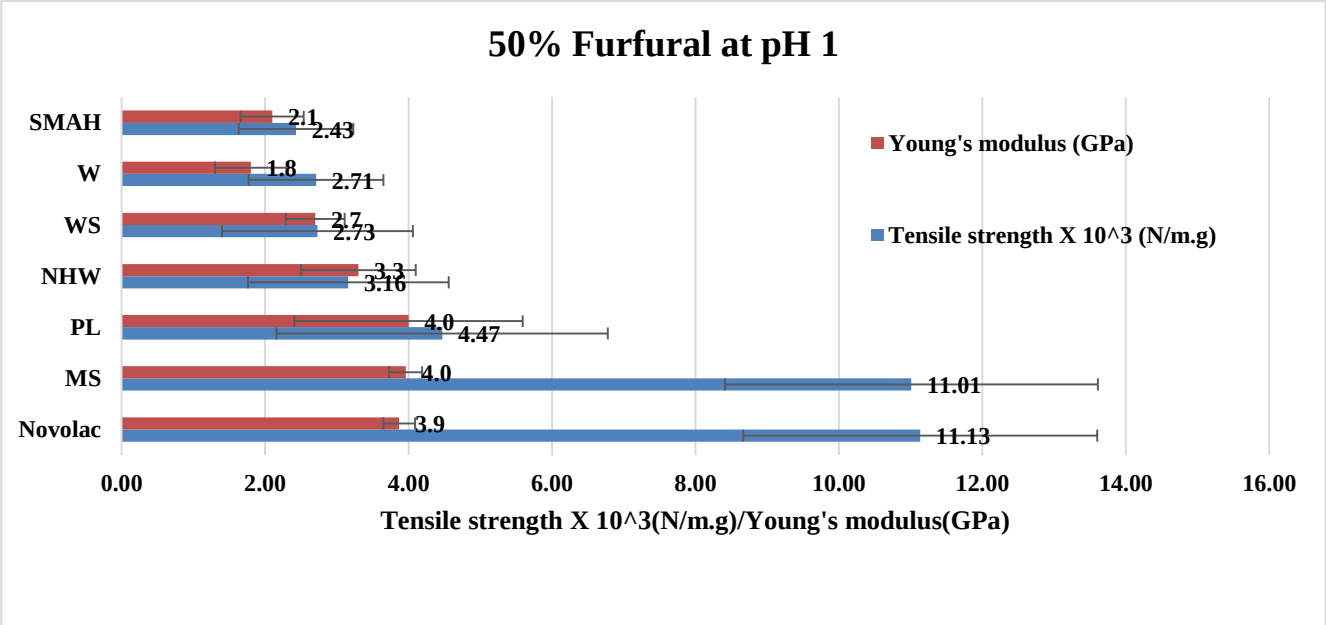

Figure 39: Mechanical properties (tensile strength and elastic modulus) of resin blends at curing temperature and pressure of 180°C and 1.9MPa. All blends were prepared at pH 1 with 50% furfural. Tensile strength per gram (N/m·g) was determined using Equation (2).

Figure 37 shows the mechanical properties of crude lignins compared to PF. In general, it can be concluded that the crude lignins have poor mechanical properties as can be expected, compared to their resin counterparts. The best performing crude lignin was PL achieving 42% of the strength that of PF. The Young's modulus of PL was 28% higher than PF. It should be noted that in these reference experiments, lignins produced from hot-water extracts performed less satisfactorily than both technical lignins, KL crude and PL crude. SMAH lignin was the least effective and the tensile strength and Young's modulus were 90% and 21% lower than PF, respectively.

At pH 0.65 and 0% furfural (Figure 38), blends prepared from SMAH demonstrate the best strength (90% of PF) followed by MS (83% of PF), W (70% of PF), KL (66% of PF), PL (60% of PF), WS (24% of PF) and NHW (21% of PF).

At pH 1 and 50% furfural (Figure 39), the highest strength is exhibited by MS (98% of PF). All other resin formulations appear to be weak in comparison to PF. In fact, SMAH_F50_1,

W_F50_1 and PL_F50_1 demonstrate a drop in strength by 76%, 64% and 32%, respectively, from their F0_065 resin counterparts. Other than MS_F50_1 (20% gain in tensile strength compared to F0_065 counterpart) NHW_F50_1 and WS_F50_1 show an increase in strength of 36% and 5%, respectively.

It appears that MS and SMAH lignins are comparatively better raw materials for resin production than other lignin types. SMAH lignin demonstrates best strength in the F0_065 condition (Figure 38) whereas MS lignin performs well in both conditions (F0_065 and F50_1, Figure 38 and Figure 39, respectively). Both SMAH and MS lignins have higher S/G ratios (3.23 and 2.86, respectively, Table 10) and a high PhOH content (1.58 mmol/g and 1.96 mmol/g, respectively, Table 10), compared to other lignins studied. The S/G ratios imply a dominant presence of S units in comparison to G units in both lignins (76% S units in SMAH and 74% S units in MS). Resin preparation is performed in acid conditions where it is expected that lignin-lignin condensation will occur at the G_5 position. A lower amount of G lignin implies that this polymerization reaction is hindered. High PhOH content implies fewer β-O-4 bonds as has been suggested previously [192,194,195] and these bonds are expected to cleave in acid conditions. The cleavage reaction may also be slowed due to fewer β-O-4 linkages. However, polymerization can also take place at the C2 and C6 position, in both S and G units, as proposed by Figure 22, which is the only reaction that dominates during the preparation and curing phases. This may produce a resin that is more elastic and mobile which results in good mechanical properties.

W lignin has a relatively high PhOH content of 1.97mmol/g and an S/G ratio of 1.25 (55% S units). It is expected that the polymerization reactions (G_5 condensation and polymerization at S2 and/or S6) will dominate due to the relatively low presence of β-O-4 bonds. An increase in strength by 54% is seen in W_F0_065 from its crude counterpart. Addition of furfural

extensively crosslinks the polymer compromising strength by 45% for the W_F50_1 resin (Figure 39).

NHW lignin, compared to lignins studied, is characterized by the highest PhOH content (2.23mmol/g, Table 10) and the lowest S/G ratio (0.52, 66% G units). Abundance of G units may lead to extensive crosslinking of the polymer during the reaction phase, leading to a resin that is highly inelastic, compromising its tensile strength. Addition of furfural does not seem to benefit the NHW_F50_1 resin as no significant change in tensile strength was observed compared to Figure 39.

In contrast, PL has the lowest PhOH content (0.84mmol/g) and a high S/G ratio (2.76, 73% S units, Table 10), compared to other lignins studied. This case is demonstrating effects of low presence of PhOH groups and abundance of S units; in accordance with these two, a relatively high content of β-O-4 is expected. Therefore, the resin prepared from PL may not be crosslinked enough to demonstrate good mechanical properties. This is in corroboration with results of PL_F0_065, where the increase in strength from its crude counterpart (PL crude) is approximately 4%. This change may be considered insignificant as it is within the standard deviation of the PL crude strength (Figure 37 and Figure 38). However, for PL_F50_1, the resin strength drops by 30%.

WS lignin has comparatively low PhOH content (1.19mmol/g) and high S/G ratio (1.90, 66% S units). Both WS_F0_065 and WS_F50_1 resins demonstrates poor mechanical properties – no significant difference in tensile strength is observed at both conditions from its crude counterpart (Figure 37, Figure 38 and Figure 39). It is possible that neither the depolymerization nor the polymerization reactions dominate resulting in weak formulations in both conditions (F0_065 and F50_1). KL_F0_065 does not show a significant improvement from its crude counterpart. KL_F50_1 was not prepared as resin prepared at 5% furfural did not show any improvement. KL has been isolated from softwoods and therefore contains G

lignin. Extensive crosslinking in acid conditions and/or lowered reactivity due to the presence of sulfur-containing entities [29,48] may lead to poor mechanical properties. It is important to note that KL crude lignin does demonstrate better tensile strength compared to the biorefinery crude lignins (W, NHW, SMAH, SMAH_IRR50, SMAH_IRR100, MS and WS, Figure 37). The conditions used in this study for resin production are not suitable for kraft lignin and do not improve its mechanical properties.

Studies in literature have reported kraft lignin to be a better raw material for LPF resins compared to other lignins, such as lignosulfonates, soda, and organosolv (ethanol) lignins. This was concluded based on abundance of G units and PhOH groups [14,15,196], low molecular weight and low Tg [197]. PhOH and G units are potential active sites for polymerization. Low molecular lignin is also more reactive and a low Tg suggests easier plasticization. It is important to note that the PhOH content of KL was as high as 6.52mmol/g lignin, in studies performed by Ibrahim et al (2013) [197]. Comparatively, KL used in the experiments of this work has PhOH of 1.10mmol/g (Table 10). It is also possible that the curing conditions (180°C and 1.8MPa, 5 minutes) may not have been suitable for KL. It has been reported that softwood kraft lignin undergoes a dramatic increase in molecular weight when heated to temperatures 20°C above its Tg for 20 minutes. Lignin also becomes insoluble in solvents (THF, DMSO, acetone) when heating time is increased to 30 minutes due to the formation of 3D crosslinked structures [100,198]. The Tg reported for KL used in this work is 172°C (Table 12). The resins made from KL may not have had sufficient energy to undergo translational motion for curing to occur resulting in poor mechanical properties. Furthermore, it is possible that the curing time was not sufficient for resins that demonstrated poor mechanical properties. Longer curing time has been one of the drawbacks of LPF resins reported in literature [199].

It appears that a lignin with high PhOH content and high S/G ratio is the most suitable raw material for production of resin with comparable mechanical properties to that of PF. The high

PhOH indicates low β-O-4 bonds, therefore slowing the depolymerization reaction. A high S/G ratio indicates lower amount of G units and accordingly less frequent the lignin-lignin condensation at the G_5 position. As a result, the polymerization reaction at the S2 and/or S6 position dominates leading to a resin that is similar in strength characteristics to PF. The benefit of high S/G ratio was in contrast with reports in literature [14,15] which suggested higher G content is more beneficial – for both novolac-type (acid conditions) and resole-type (alkaline conditions) applications. MS has the lowest Tg (123°C, Table 12) and demonstrates the highest tensile strength among the lignins. However, SMAH also demonstrates good mechanical properties however it has one of the highest Tg (161°C, Table 12).

5.2.3.1 Molecular Weight Distribution of Resin Blends

Molecular weight data (Mn, Mw and PD) of resin blends prepared at 0% furfural at pH 0.65 (F0_065) and 50% furfural and pH 1 (F50_1) are shown in Table 13 and Table 14, respectively. The tables also contain data of crude lignins (previously reported in Table 11) for reference purposes. The molecular weight distributions of the resin blends are shown in Figure 40 and Figure 41, respectively.

It is clear from the data that polymerization and depolymerization reactions were occurring during the resin preparation step. All resin blends except for MS_F50_1 demonstrate an increase in molecular weight compared to their crude counterparts. MS_F50_1 shows a decrease in molecular weight and polydispersity when compared to MS lignin. However, it is not clear as to why this phenomenon occurs.

For the resins studied at the F0_065 conditions, the change in PD for the resins is noteworthy. SMAH_F0_065 and MS_F0_065 show an increase in PD whereas the others demonstrate a decrease in PD from their crude lignin counterparts. SMAH_F0_065 and MS_F0_065

demonstrated higher tensile strength (Figure 37) than other resin blends at these conditions (0% furfural, pH 0.65).

It was apparent from the data that molecular weight of the resin was not indicative of its mechanical properties – as suggested by the Pearson correlation statistical analysis discussed later. This was unexpected as molecular weight distribution from the initial scouting studies (resins prepared from SMAH lignin only) previously published [90] suggested otherwise. Those results also demonstrated that all resins were of higher molecular weight than the crude lignin (SMAH). However, a trend was observed where the higher molecular weight resins corresponded to lower tensile strength. It was suggested that highly crosslinked polymers lack mobility which results in compromised tensile strength. It appears that this trend did not apply to resins across different lignin species.

Table 13: Number average molecular weight (Mn), weight average molecular weight (Mw) and polydispersity (PD) of crude biorefinery lignins and their resins prepared at 0% furfural and pH 0.65.

	W	W_F0_065	NHW	NHW_F0_065	SMAH	SMAH_F0_065	MS	MS_F0_065	WS	WS_F0_065
Mn	2186	3829	1924	2532	1748	3506	2124	2783	2850	3454
Mw	5962	9785	4745	5585	1861	8288	4672	6706	12114	11929
PD	2.73	2.56	2.47	2.21	1.06	2.37	2.2	2.41	4.25	3.45

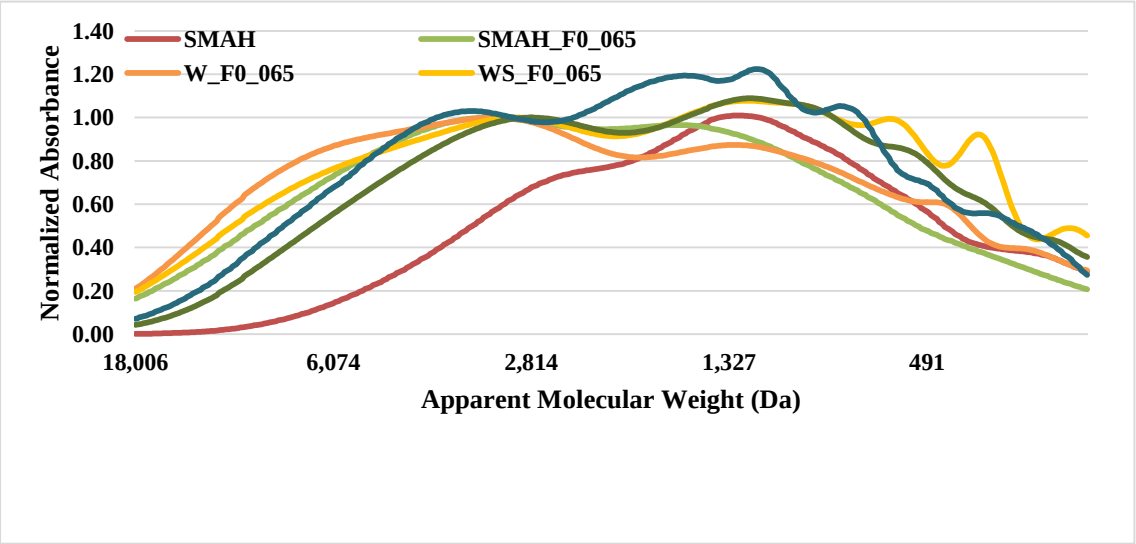

Figure 40: Normalized molecular weight distribution of resins blends prepared at 0% furfural and pH 0.65. Normalized molecular weight distribution of SMAH crude lignin from Figure 29 lignin is used as a reference.

Table 14 Number average molecular weight (Mn), weight average molecular weight (Mw) and polydispersity (PD) of crude biorefinery lignins and their resins prepared at 50% furfural and pH 1.

	W	W_ F50_1	NHW	NHW_ F50_1	MS	MS_ F50_1	WS	WS_ F50_1
Mn	2186	2590	1924	2224	2124	1691	2850	3813
Mw	5962	9077	4745	4580	4672	2700	12114	13945
PD	2.73	3.50	2.47	2.06	2.2	1.61	4.25	3.66

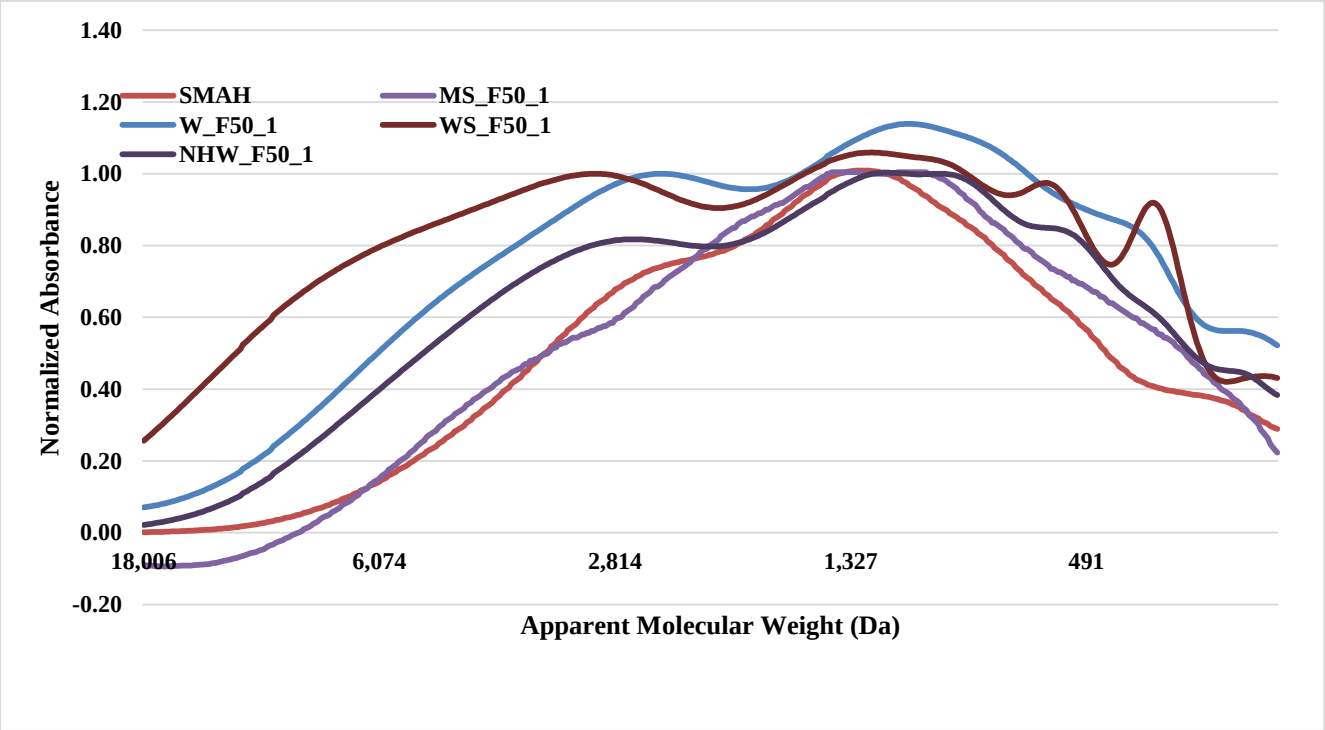

Figure 41 Normalized molecular weight distribution of resins blends prepared at 50% furfural and pH 1. Normalized molecular weight distribution of SMAH crude lignin from Figure 29 is used as a reference.

5.2.3.2 Data analysis

A Pearson correlation was performed on the data that was collected to determine trends between the inherent properties of the lignins studied and the improvement in tensile strength obtained at 0% furfural, pH 0.65 and 50% furfural, pH 1. The lignin samples that were chosen were W, SMAH, SMAH_IRR50, SMAH_IRR100, MS, WS and NHW. PL and KL were not selected as some of the data for these samples is yet to be determined. These lignins were recovered from different processes, mild acid pretreatment (PL) and kraft pulping (KL). Furthermore, KL is produced from softwood species.

The factors that were studied to determine correlations were: Klason lignin, acid soluble lignin, total lignin content and ash content (Table 8), xylan content (Table 9), the PhOH-group content, and S/G ratio (Table 10), number average molecular weight (Mn), weight average molecular weight (Mw), and polydispersity (PD) (Table 11), tensile strength and Young's modulus of crude lignins (Figure 37), improvement in strength of resin and crude lignin at conditions of F0_065 and F50_1. A p-value was then calculated to determine the significance of the correlation. If the p-value is below 0.05, the correlation is considered significant. No correlations were significant (p-value<0.05) for improvement in tensile properties or any other variable. However, the inherent properties (Klason lignin, acid soluble lignin, total lignin content, ash content, xylan content PhOH, S/G ratio, Mn, Mw and PD, and tensile strength and Young's modulus) of crude lignins did show some significant correlations, which was to be expected. The complete data table, Pearson correlations and corresponding p-values are displayed in Appendix A, Table 16 and Table 17, respectively.

Improvement in tensile strength at F0_065 and F50_1 was calculated by Equations (6) and (7), respectively.

Table 18 in Appendix A includes the calculated values.

$$Improvement\ in\ tensile\ strength\ at\ F0\ (\%) = \frac{Tensile\ strength\ at\ F0 - Tensile\ strength\ of\ crude\ lignin}{Tensile\ strength\ of\ crude\ lignin} X100 \quad (6)$$

$$Improvement\ in\ tensile\ strength\ at\ F50\ (\%) = \frac{Tensile\ strength\ at\ F50 - Tensile\ strength\ of\ crude\ lignin}{Tensile\ strength\ of\ crude\ lignin} X100 \quad (7)$$

5.2.4 Effect of Curing Agents on Mechanical Properties of Resin Reinforced Glass Fibers

Two curing agents – HMTA, which is the most commonly used curing agent for PF novolac type-resins [9,12,200], and furfural were investigated for their effect on mechanical properties of resin reinforced glass fibers. 10% of furfural or HMTA was dissolved into the resin prior to curing (180°C and 1.9MPa). The effect of the curing agents on the mechanical properties was tested on the strongest (MS_F50_1) and the weakest formulation (W_F50_1) selected from previous studies. The purpose of these experiments was to determine if curing agents could improve the strength of the lignin based resins to be competitive with PF resins. It was found that neither HMTA nor furfural is beneficial for the resins tested (MS_F50_1 and W_F50_1). The results are shown in Figure 42. All formulations were compared to PF resin.

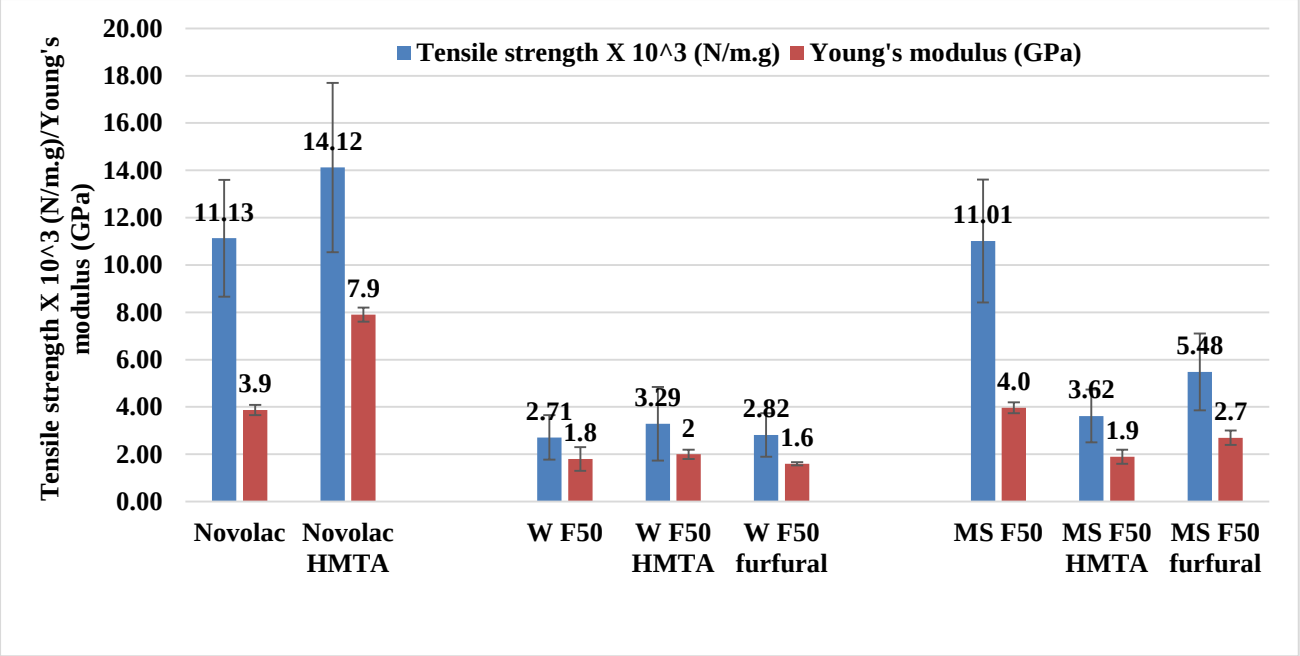

Figure 42: Effect of curing agents (HMTA and furfural) on the mechanical properties of MS F50 and W F50 reinforced glass fibers. All resins were cured at 180°C and 1.9MPa. Tensile strength per gram (N/m·g) was determined using Equation (2).

As expected, using HMTA with PF improved the tensile strength (~25%) and the Young's modulus (100%).

A 21% increase in tensile strength and an 11% increase in Young's modulus are seen in the case of W_F50_1, however it cannot be concluded as a significant improvement. Accordingly, HMTA has little or no effect in the case of W_F50_1.

A significant decrease of 67% in tensile strength and 50% in Young's modulus is observed in the case of MS_F50_1. The decrease in mechanical properties can be attributed to extensive crosslinking that may have occurred during the curing process in the presence of HMTA.

Similar conclusions can be drawn in the case of furfural. No significant improvement is observed in the mechanical properties of W_F50_1. A decrease in both tensile strength and Young's modulus (50% and 33%, respectively) is observed for MS_F50_1.

It is possible that the higher S/G ratio of MS lignin (2.86, Table 10) may play a role in the different effects observed, with the addition of the two curing agents. W lignin (S/G ratio = 1.25, Table 10) may already be extensively crosslinked (44% G units) during the preparation

of the resin in acid conditions, compromising its strength. Therefore, adding a curing agent has little or no effect as observed with both furfural and HMTA in the case of W_F50_1. On the other hand, MS lignin has 26% G units, and may not be as extensively crosslinked post preparation phase. Therefore, the addition of HMTA or furfural further crosslinks the MS_F50_1 resin during the curing process, compromising its tensile properties.

Nevertheless, adding HMTA or furfural did not benefit any of the lignin based resins in improving their mechanical properties.

5.2.5 Reinforcement applications

Lignin based resins were tested for their viability as wood adhesives (resole-type) and in binder (novola-type) applications. No data was obtained from adhesive testing. 3-ply wood testing was performed on select resins according to ASTM standard - D 906 [190]. Adhesion was observed initially, after curing however, shear testing of the samples did not yield catastrophic failure – the wood fibers did not fracture. This implies that the resins did not penetrate into the wood and there was no interaction between the resin and the wood fibers. It may be that the molecular weight of the lignin is too high and prevents the resin from penetration.

In the glass fiber tests, the lignin based resins act as a reinforcing agent and improve the strength of the glass fiber filters. Therefore, applications where PF is used as a reinforcing agent or a binder (novolac-type) were sought. Two such applications are tested here – friction paper and the composite material Richlite™.

PF is used as a binder in friction materials for brake parts [13]. Richlite™ is a composite material which is made from immersing several layers of kraft paper in PF and curing it at high temperature and pressure, producing a solid stable sheet of material. This study only tests one layer of the kraft paper (softwood and hardwood) to determine compatibility and strength properties and thus is a preliminary investigation.

It is of importance to note that glass fibers are inert and there is no interaction between the resin and the glass fibers. Therefore, any improvement in mechanical properties of resin enforced glass fibers can be attributed to the resin alone. It can be expected that the trends observed in the glass fiber tests will transfer onto the three substrates – softwood and hardwood kraft paper and friction paper. However, the lignocellulosic constituents in friction and kraft papers (hardwood and softwood), will interact with the resins (PF and lignin based). Thus, the tensile strength numbers that are reported in the following sections (Figure 44 - Figure 48) are those of the resin and any contribution that is made because of the interaction between resin and

paper (friction and kraft) fibers – magnitude of the strength numbers is comparatively higher. A detailed description of how tensile strength is calculated is presented in the Materials and Methods section.

5.2.5.1 Reinforcement of friction paper

Two tests were performed on the friction paper as the substrate- the heat aged test and the hot oil exposure test (detailed in the Material and Methods section). The heat aged test measured the tensile strength loss after the resin reinforced friction paper samples were exposed to heat only (150℃, 22 hours). The hot oil exposure test measured the tensile strength loss after the resin reinforced friction paper samples were exposed to automatic transmission fluid and heat (110℃, 22 hours).

However, prior to reinforcing the friction paper with resins and measuring their mechanical properties, thermal degradation behavior of resin blends was studied via TGA. The purpose of these experiments was to determine the thermal stability of the resins in comparison to PF resin. PF is well-known for its excellent thermal stability [113] which makes it an ideal candidate for applications that experience harsh thermal conditions. Results from the TGA provide insight into the potential of lignin based resins in applications that require high thermal stability such as friction paper applications.

Results from TGA showed that all lignin based resin blends except MS_F50_1, demonstrate similar thermal degradation behavior to that of PF, as seen in Figure 43. The degradation occurs over a range of 200-500°C. The maximum weight loss for lignin based resins is seen at 366°C. The PF shows a maximum weight loss at 349°C. Figure 44 also contains the corresponding crude lignin thermal degradation behavior, previously seen in Figure 31 and Figure 32. MS_F50_1 however shows a maximum weight loss at 298°C. In addition, two peaks – at 150°C

and at 195°C – which are absent in other samples (crude lignin and resins) are also seen. The molecular weight analysis of MS_F50_1 showed a drop in Mn and Mw, compared to its crude counterpart. Also, the peak in the range of 100-200°C may correspond to furfural degradation. However this is yet to be confirmed

Based on the results obtained from TGA of lignin based resins (Figure 43) and mechanical properties from previous experiments (Figure 38 and Figure 39), select resins were tested on friction paper.

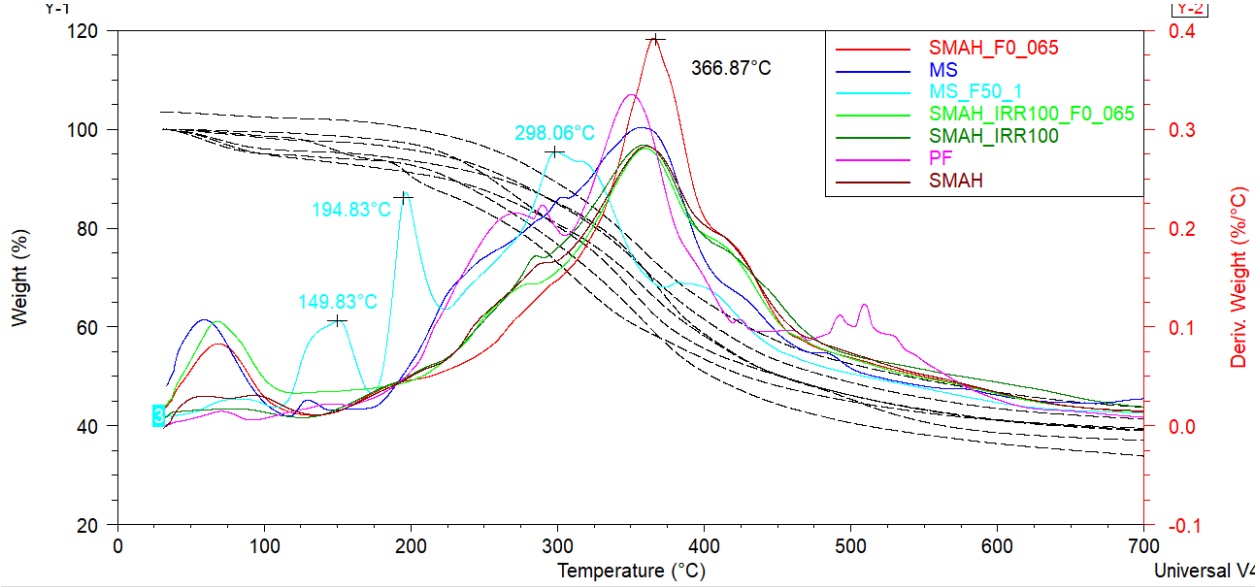

Figure 43: Thermal degradation behavior of select crude lignins (MS, SMAH and SMAH_IRR100), corresponding resins (MS_F50_1 and SMAH_IRR100_F0_065) and PF. All resins tested are prior to curing.

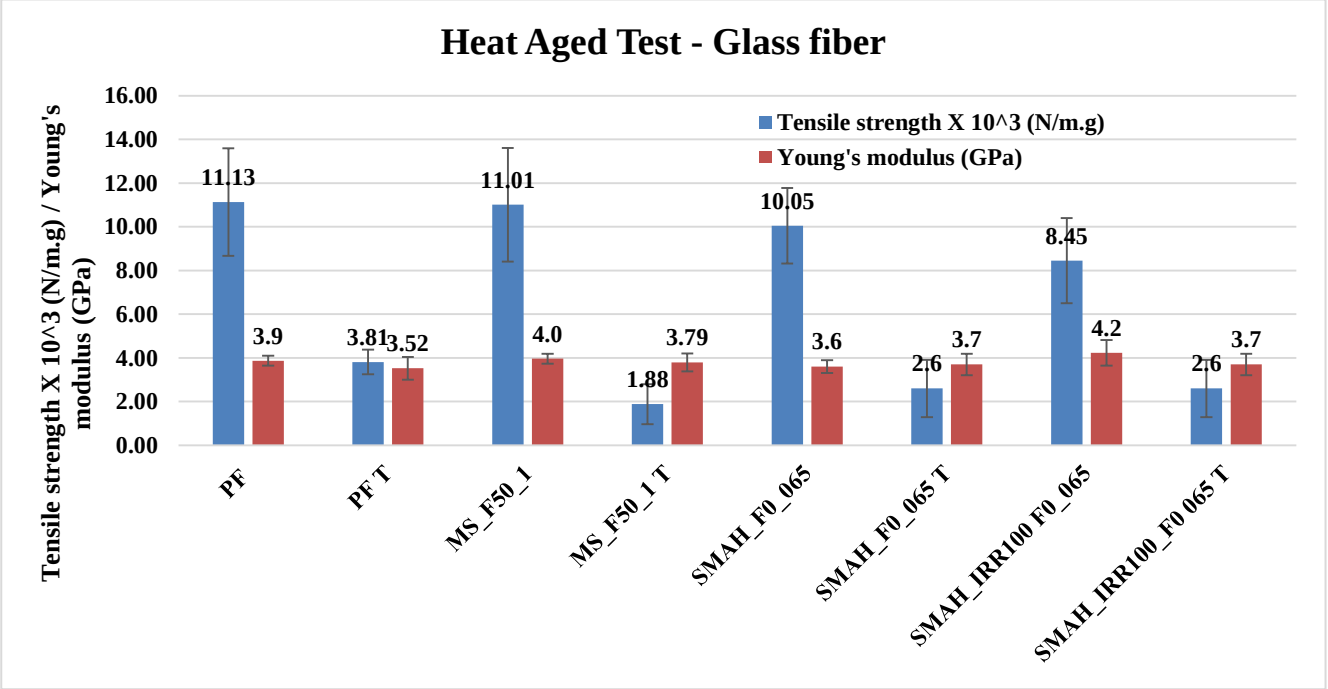

Figure 44: Effect of heat aging on the mechanical properties of PF, MS_F50_1, SMAH_F0_1, and SMAH_IRR100_F0_1 reinforced glass fibers. All resins were cured at 180°C and 1.9MPa. Tensile strength per gram (N/m·g) was determined using Equation (2). PF T, MS_F50_1 T, SMAH_F0_065 T and SMAH_IRR100_F0 065 T represent the mechanical properties of the respective resins after being exposed to 150°C for 22 hours.

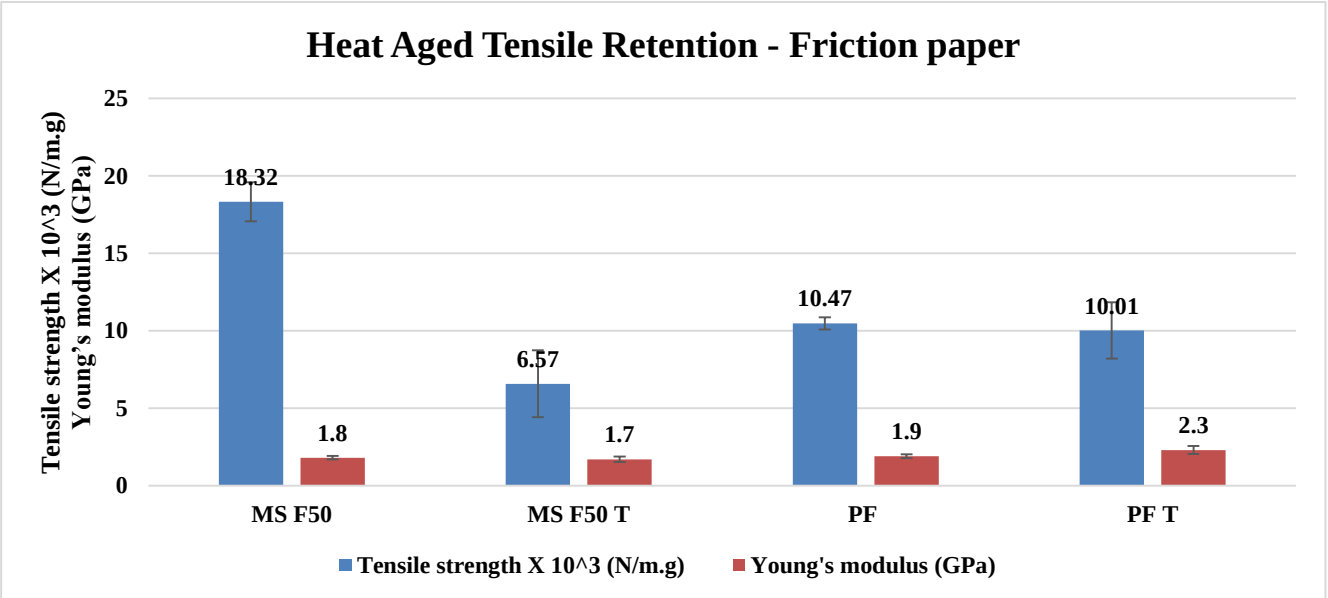

Figure 45: Effect of heat aging on the mechanical properties of PF and MS_F50_1 reinforced friction paper. All resins were cured at 180°C and 1.9MPa. Tensile strength per gram (N/m·g) was determined using Equation (2).MS F50 T and PF T represent the mechanical properties of the resins after being exposed to 150°C for 22 hours.

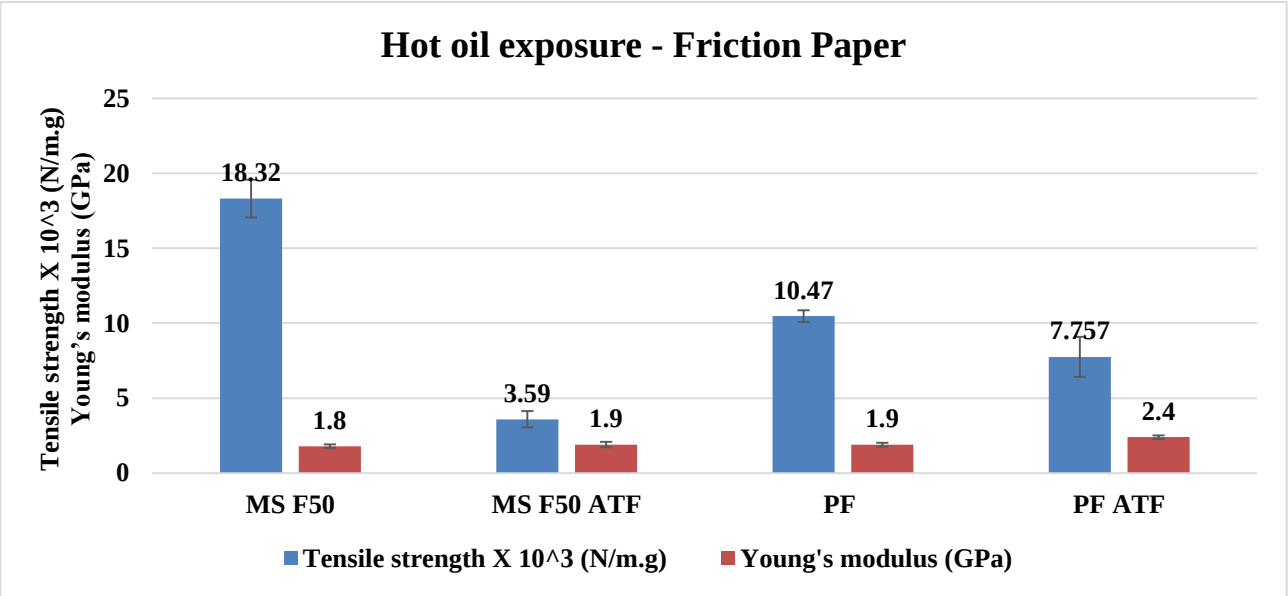

Figure 46: Effect of hot oil exposure on the mechanical properties of PF and MS_F50_1 reinforced friction paper. All resins were cured at 180°C and 1.9MPa. Tensile strength per gram (N/m·g) was determined using Equation (2). MS F50 ATF and PF ATF are representative of the resins exposed to automatic transmission fluid (ATF) and 110°C for 22 hours.

The friction paper tests were performed in two phases. In phase 1, selected resins (MS_F50_1, SMAH_F0_1, and SMAH_IRR100_F0_1) were first reinforced on glass fibers (Figure 44) and subjected to the heat aged. All resins were compared to PF. The three resins selected showcased the highest strengths, after PF (Figure 36), thus were most likely to show thermal stability. Based on results obtained from phase 1, MS_F50_1 was chosen to be tested on friction paper (Figure 45 and Figure 46).

The heat aged test performed on glass fibers (Figure 44) shows that PF is more stable than the lignin based resins. This can be attributed to the type of bonds that are formed during the reaction and the curing process. PF mostly consists of C-C bonds whereas lignin based resins mostly form C-O-C bonds. C-C bonds are much more stable under harsh thermal and chemical conditions. When the lignin based resins are exposed to harsh thermal and chemical conditions, the C-O-C bonds cleave which compromises the strength of the resin.

As can be seen from Figure 44 all the resins tested lose strength when exposed to heat over a longer period of time (22 hrs). The loss of tensile strength is highest for MS_F50_1 (83%),

followed by SMAH_F0_065 (74%), SMAH_IRR100_F0_065 (69%) and then PF (66%). The loss in Young's modulus is less prominent. The largest drop in modulus is seen in the case of SMAH_IRR100_F0_065 (13%), followed by PF (9%), MS_F50_1 (4%) and then SMAH_F0_065 (3%).

Among the lignin based resins, MS_F50_1 has shown to be the least thermally stable and the SMAH_IRR100_F0_065 resin to the most thermally stable. The loss of strength and modulus for the latter are also similar in magnitude to PF.

The PhOH values of lignins studied are shown in Table 10. SMAH_IRR100 has the lowest free phenolic hydroxyl groups (1.08mmol/g), followed by SMAH (1.58) and the MS (1.96). It is possible that when resins are produced from these lignins, SMAH_IRR100 forms fewer C-O-C bonds, as there are a limited number of reactive PhOH sites available. Accordingly this lignin contains more C-C bonds compared to MS and SMAH lignins. This provides the resin prepared from SMAH_IRR100 (SMAH_IRR100_F0_065) more thermal stability than the resins prepared from MS (MS_F50_1) or SMAH (SMAH_F0_065). In fact, the loss of tensile strength due to exposure to heat (110°C and 22 hours) seems to follow the trend of PhOH – the higher PhOH value, the greater the loss in strength. This is unexpected as higher PhOH content would imply fewer of β-O-4 bonds – which are more susceptible to thermal and chemical conditions than C-C bonds.

No data was obtained for the hot oil test on the glass fiber filters as the samples either broke in the clamp or experienced excessive slippage. The automatic transmission fluid was especially detrimental to the resins when reinforced with glass fibers.

Figure 45 and Figure 46 show the mechanical properties of friction paper reinforced with PF and MS_F50_1 resins after they were subjected to the heat aged and hot exposure tests, respectively. Both resins are more stable when exposed to heat only. Exposure to a combination of heat and ATF, further degrade the resins.

The loss of strength during the heat aged test is as follows: PF demonstrates a loss of 4% where as MS_F50_1 shoes a loss of 26%. Both resins (PF and MS_F50_1) show a gain in Young's modulus of 21% and 6%, respectively.

During the hot oil exposure tests, loss of 64% and 80% in tensile strength is seen in PF an MS_F50_1 are seen respectively. A gain in Young's modulus of 26% for PF and 6% for MS_F50_1 is also seen.

5.2.5.2 Reinforcement of kraft paper

Table *15* shows the kappa numbers for both hardwood and softwood kraft papers. Softwood kraft paper has a higher kappa number (87.10) with a corresponding lignin level of 11.32% than its hardwood counterpart (kappa number = 41.76, lignin level 5.43%). Lignin level was calculated by using the kappa number-Klason lignin content conversion factor of 0.13 as per the Tappi standard [155]. It can be expected that higher lignin content in the kraft paper will lead to more interaction between the fiber and the lignin based resin. Furthermore, paper produced from softwoods, has longer fibers thus providing more sites for bonding.

The lignin based formulations chosen for these studies are MS_F50_1 and W_F50_1. MS_F50_1 demonstrates the best strength characteristics and W_F50_1 is the weakest formulation, compared to all other lignin based resins, on glass fiber filters (Figure 39). All results are compared to PF resin. The factors that being studied are: resin type (PF, MS_F50_1 and W_F50_1), kraft paper type (softwood and hardwood) and effect of HMTA (0% and 10%). Overall, the highest strength is observed in the case of softwood paper reinforced with W_F50_1, without the use of HMTA as a curing agent (Figure 47). The lowest strength is seen in the case of hardwood paper reinforced with W_F50_1, with 10% HMTA (Figure 47). For softwood paper, the highest strength is achieved using W_F50_1, without HMTA and for hardwood, the highest strength is achieved by MS_F50_1 with 10% HMTA.

With HMTA, both PF and W_F50_1 perform better on softwood kraft paper. Conversely, MS_F50_1 performs better on the hardwood paper. Without HMTA, W_F50_1 still performs better on softwood but PF and MS_F50 perform better on hardwood. Therefore, resin selection is very much dependent on paper type and HMTA to obtain good mechanical properties.

For both softwood and hardwood kraft papers without HMTA, W_F50_1 exhibited the highest strength, followed by PF and then MS_F50_1. However, this trend is not observed when HMTA is added to all three resins. In case of softwood paper (Figure 47), adding HMTA improves the strength of PF and MS_F50_1 significantly (134% and 122%, respectively). The significant increase is expected in the case of PF. However, strength is compromised for W_F50_1 (loss of 84%).

In the case of hardwood paper (Figure 48), adding HMTA does not seem to benefit PF and W_F50_1. The strength decreases by 6% and 88%, respectively. However, HMTA seems to be beneficial for MS_F50_1, where an increase of 227% in tensile strength is seen.

Therefore, HMTA is least beneficial to W_F50_1, regardless of paper type as tensile strength decreases in both hardwood and softwood paper types. On the other hand, HMTA proves to be beneficial to MS_F50_1 in the both the softwood and hardwood paper cases, where an increase of tensile strength is seen. Furthermore, HMTA is beneficial to PF in the softwood paper case only.

The S/G ratios of MS and W lignins are 2.86 and 1.25, respectively (Table 10). This implies that W lignin has approximately 44% G units whereas MS lignin only has 24% G units. HMTA will act as a crosslinker for both MS and W lignins. However, a higher G lignin content may lead to self-condensation of lignin. Highly crosslinked polymers have lower mobility which can compromise tensile strength, as can be seen in the case of W_F50_1, where adding HMTA does not benefit the resin in both the softwood and the hardwood case (Figure 47 and Figure 48). Due to the high S/G ratio of MS (2.86, Table 10), carbon-carbon condensation at the G_5

position is lowered. Therefore, the extent of crosslinking that occurs with the addition of HMTA to MS_F50_1 seems to be more favorable for its tensile properties in both the hardwood and softwood case (Figure 47 and Figure 48). It can be concluded that HMTA is more beneficial for the MS_F50_1 resin than W_F50_1 resin.

Table 15: Kappa number of softwood and hardwood kraft paper used for reinforcement applications

Kraft paper type	Kappa number	Lignin Level (%)
Softwood (SW)	87.10	11.32
Hardwood (HW)	41.76	5.43

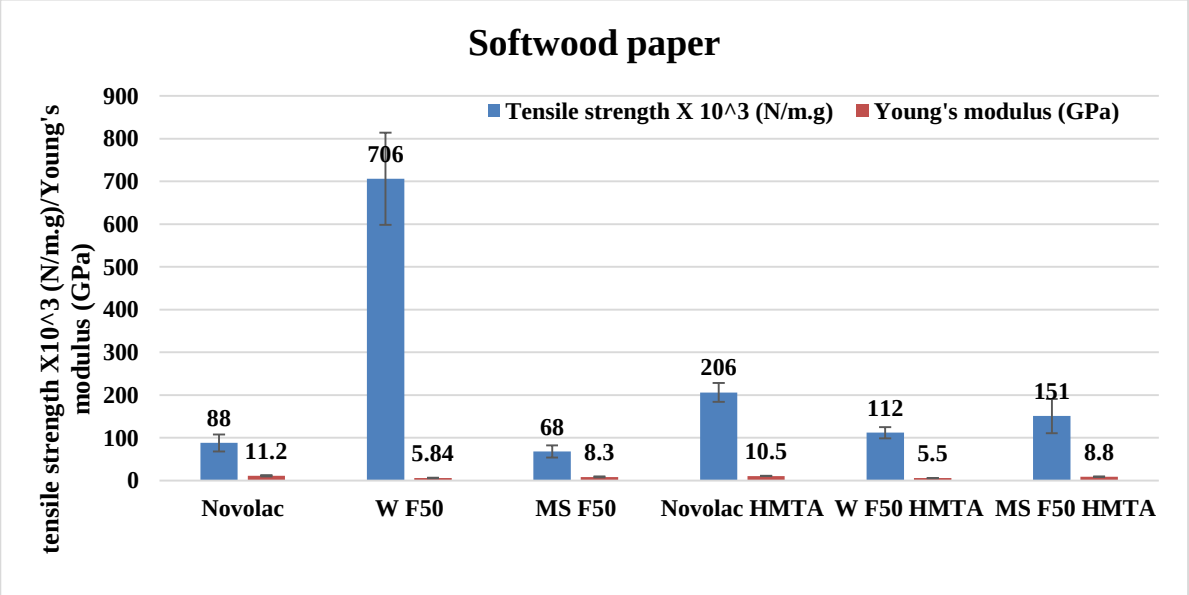

Figure 47: Effect of HMTA on the mechanical properties of MS F50 and W F50 reinforced softwood kraft paper. All resins were cured at 180 °C and 1.9 MPa. Tensile strength per gram (N/m·g) was determined using Equation (2).

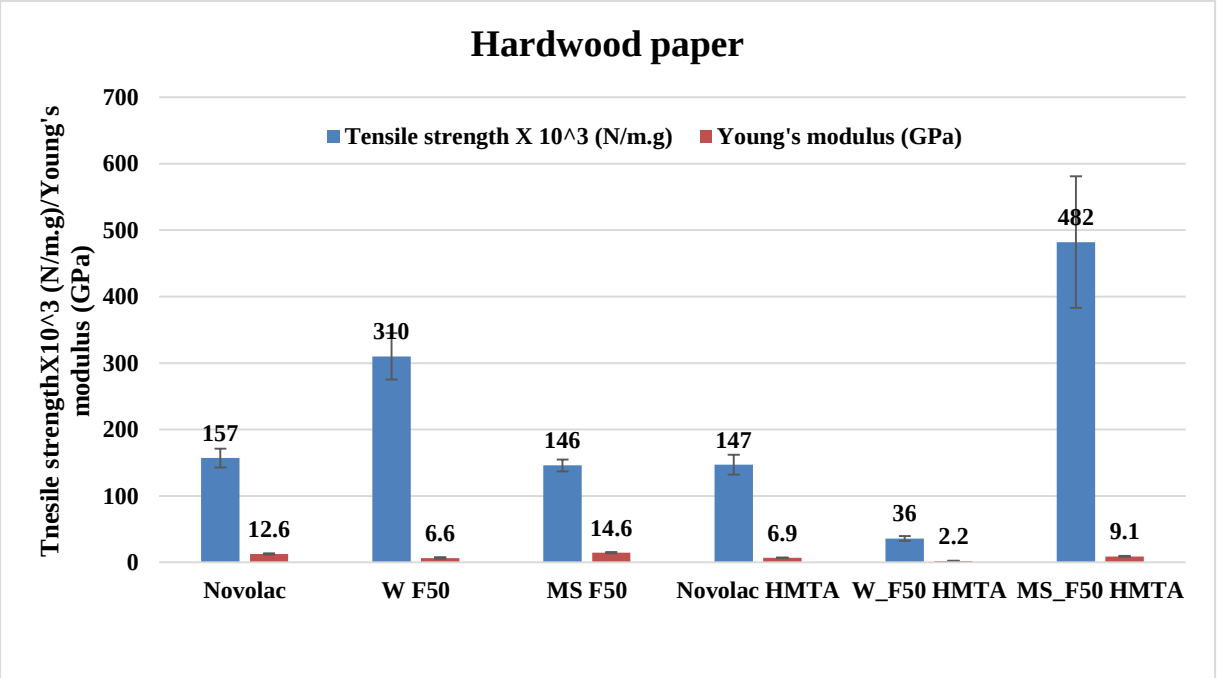

Figure 48: Effect of HMTA on the mechanical properties of MS F50 and W F50 reinforced hardwood kraft paper. All resins were cured at 180°C and 1.9MPa. Tensile strength per gram (N/m·g) was determined using Equation (2).

The trends regarding Young's modulus are slightly more consistent. In case of softwood, adding HMTA decreases the modulus for PF and W_F50_1 by 6% but improves by 6% for MS_F50_1. In case of hardwoods, the modulus decreases for PF, MS_F50_1 and W_F50_1 by 45%, 66% and 22%, respectively. Addition of HMTA has a more prominent effect on the elasticity of the resins in the case of hardwood than softwood kraft paper.

For both softwood and hardwood kraft papers, without HMTA, PF has the highest modulus, followed by MS_F50_1 and then W_F50. This trend is maintained with the addition of HMTA. In the case for hardwood kraft paper without HMTA, this trend is also maintained, however, adding HMTA results in MS_F50_1 exhibiting the highest modulus followed by PF and then W_F50_1.

Overall, lignin based resins are more elastic compared to PF as they have lower Young's modulus. Furthermore MS_F50_1 is more brittle compared to W_F50_1. The addition of

HMTA to MS_F50_1 on hardwood makes it even more brittle along with significantly increasing its tensile strength (62%, Figure 48).

Paper type and addition of HMTA, seem to affect the tensile properties of the resins tested (PF, MS_F50_1 and W_F50_1), differently. Furthermore, the trends observed on glass fibers do not transfer onto kraft papers. Other resins should be tested on both softwood and hardwood papers to draw more robust conclusions. Studies on penetration of the resin via contact angle measurements, further analysis of the paper types may shed light onto why certain combinations of factors (resin type, HMTA and paper type) result in better mechanical properties than others. One factor that may influence the results is the roughness of the surface of the paper. More rough surfaces contain deeper external voids which are connected to larger capillaries with large internal cavities [201].

CHAPTER VI: CONCLUSIONS

This work attempted to utilize biorefinery lignin recovered from HWE of different angiosperm species (SM, W, MS and WS) to produce formaldehyde-free resins for resin applications. Furfural is investigated as a crosslinking agent for lignin and the effect of reaction pH, furfural content, curing conditions (180°C and 1.9MPa) and curing agents (HMTA and furfural) on the mechanical properties of the resins is determined. Mechanical properties are first tested on glass fiber filters and then select formulations are tested on friction paper and softwood and hardwood kraft papers. From the results obtained, the following general observations and conclusions have been drawn:

1. The crude biorefinery lignins recovered from hot water extraction hydrolyzates (SM, W, NHW, MS, WS, SMAH_IRR50 and SMAH_IRR100) are relatively purer than the technical lignins (PL and KL) studied. However, crude lignins contain carbohydrates which are predominantly xylan based and have low ash content. Crude lignins are diverse in their characteristics as besides their origin, hot water extraction has vastly different effects on their properties. This is evident by the varying carbohydrate content, S/G ratios, PhOH content, Tg and molecular weight distributions that were observed. However, all biorefinery crude lignins except NHW have larger amount of S-units compared to their MWL counterparts. This indicates that lignin enriched in S-units is predominantly dissolved during HWE and lignin dissolved during HWE originates most likely from fibers rather than vessels, in the case of hardwoods.
2. Recovery methods after HWE were shown to influence the molecular weight distribution of the lignins, in this study. Lignins that were separated with acidification of the extract, precipitation of the lignin and decanting, were polydisperse with low molecular weight shoulders seen in the molecular weight distribution. In contrast, the

lignins that were separated using ultrafiltration were more homogenous and demonstrated a lower polydispersity.

3. All lignin based resins, except MS_F50_1, demonstrate an increase in molecular weight compared to their crude lignin counterparts and it can be concluded that condensation of lignin does occur during resin production. However, higher molecular weight did not correspond to higher tensile strength or vice versa.
4. Glass fiber filters: Results on glass fiber filters showed that additional furfural was required at pH 1, however, not below pH 1, to produce resins with comparable properties to that of PF. Among the curing conditions investigated, optimum curing temperature and pressure were 180°C and 1.9MPa.
5. Glass fiber filters: The two lignins that produce superior mechanical properties are MS and SMAH lignins. Resins prepared from MS demonstrate relatively good mechanical properties in all conditions (F0_065, F50_1, F100_1 and F200_1). SMAH demonstrates good mechanical properties at F0_065, F8_1 and F16_1.
6. Both MS and SMAH have high S/G ratio and PhOH content and it appears that lignin with high S/G ratio and PhOH content may be more suitable for resin applications, however, further study is required.
7. Wood veneers: Based on studies performed on wood veneers, it was concluded that lignin based resins produced in this work are not suitable for resole-type wood adhesive applications. 3-ply wood veneer testing did not fracture the wood fibers.
8. Novolac type- fiber reinforcement applications were investigated with select formulations, based on glass fiber tests. The resins successfully reinforced kraft papers (softwood and hardwood) and friction paper and showed comparable properties to PF.
9. The trends of mechanical properties observed on the glass fiber filters, did not corroborate with those observed on the kraft (hardwood and softwood) and friction

papers, in particular in regard to the effect of curing agents (HMTA and furfural) which varied based on the fiber and resin type. The interaction between the lignocellulosic constituents in these papers and lignin based resin requires further investigation.

10. Friction paper: Lignin from HWE is not thermally stable over longer periods of time and may be more suitable for applications in ambient conditions as evident from the reinforcement of friction paper. PF did not demonstrate a significant loss of tensile strength when exposed to higher temperatures over longer period of time.
11. Hardwood kraft papers: Among the resins tested, W_F50_1 showcased better mechanical properties than PF resin, whereas MS_F50_1 was comparable to PF.
12. Softwood kraft paper: MS_F50_1 with HMTA and W_F50_1, were two formulations that demonstrated better mechanical properties than PF.
13. A wide variety of techniques was employed but did not provide adequate understanding. Current techniques may not be sufficient to elucidate the lignin reactions, new techniques may need to be developed.

CHAPTER VII: RECOMMENDATIONS FOR FUTURE WORK

1. The recovery method appears to influence the molecular weight distribution of lignin. For a more uniform lignin, membrane separation is recommended over precipitation and decanting. A more homogenous lignin may be advantageous for resin production, as well as other lignin based value-added products such as hydrogels, thermoplastics carbon fiber and activated carbon.
2. The mechanisms of lignin reactions during resin production were not explored in depth in this research. A model compound study may provide insight into better understanding the cleavage and condensation reactions occurring during resin production.
3. Characterization of the resin itself for different properties, including the content of PhOH groups and S/G ratio may provide answers to the possible reactions taking place. Furthermore, characterization and evaluation of the cured resin will be beneficial in understating the right applications for the lignin based resin. It is recommended the resin be cured at 120°C for 2 hours and then analyzed via analytical techniques such as NMR or FTIR.
4. Other experimental parameters such as oxalic acid as a catalyst, other crosslinking agents such as glyoxal – a non-toxic aldehyde, range of reaction times, temperatures and longer curing times may produce resins with superior properties and need to be investigated.
5. The method used is in this study was the “catch all” pathway, where no modification or purification of lignin was performed prior to resin production. Modification of lignin via hydroxymethylation, phenolation or demethylation may improve reactivity of the lignin and produce resins with better mechanical properties.

6. For resole-type application such as adhesives, alkaline conditions are recommended for resin preparation.
7. Results on friction paper were performed without the curing agent HMTA, a study with HMTA may improve the properties of the resin.
8. The resin shows good compatibility with both softwood and hardwood paper. A study of the interactions between the paper fiber and resin via SEM may provide insight into the distribution of lignin along the fiber. It is recommended that gold nanoparticles be mixed with the resin, followed by fiber reinforcement and curing, and prepare samples for SEM studies. Determination of surface properties of the paper, absorption studies, and contact angle studies on glass fibers, kraft papers and friction paper can also be performed to elucidate fiber-resin interaction.
9. The purpose of kraft paper testing was to determine the applicability of the lignin based resins in products such as Richlite™. Richlite™ is a composite material that is composed of several layers of kraft paper reinforced with PF resin and cured. An experimental study on using lignin based resin for this application can be performed and properties compared.

REFERENCES

1. Ye, P.; Cheng, L.; Ma, H.; Bujanovic, B.; Goundalkar, M. J.; Amidon, T. E. Biorefinery with Water. In *The Role of Green Chemistry in Biomass Processing and Conversion*; Xie, H., Gathergood, N., Eds.; John Wiley & Sons, Inc., 2012; pp. 135–180 ISBN 978-1-118-44940-0.
2. Amidon, T.; Wood, C. Biorefinery: Conversion of Woody Biomass to Chemicals, Energy and Materials. *J. Biobased Mater. Bioenergy* **2008**, *2*, 100–120, doi:10.1166/jbmb.2008.302.
3. *Wood Adhesives*; Pizzi, A., Mittal, K. L., Eds.; CRC Press: Leiden, Netherlands; Boston, 2011; ISBN 978-90-04-19093-1.
4. *Kent and Riegel's Handbook of Industrial Chemistry and Biotechnology*; Kent, J. A., Ed.; 11th ed.; Springer: New York, 2007; ISBN 978-0-387-27842-1.
5. Pizzi, A. *Advanced Wood Adhesives Technology*; CRC Press: New York, 1994; ISBN 978-0-8247-9266-4.
6. Jin, Y.; Cheng, X.; Zheng, Z. Preparation and characterization of phenol–formaldehyde adhesives modified with enzymatic hydrolysis lignin. *Bioresour. Technol.* **2010**, *101*, 2046–2048, doi:10.1016/j.biortech.2009.09.085.
7. Zhang, W.; Ma, Y.; Wang, C.; Li, S.; Zhang, M.; Chu, F. Preparation and properties of lignin–phenol–formaldehyde resins based on different biorefinery residues of agricultural biomass. *Ind. Crops Prod.* **2013**, *43*, 326–333, doi:10.1016/j.indcrop.2012.07.037.
8. Çetin, N.S; Özmen, N. Studies on Lignin-Based Adhesives for Particleboard Panels. *Turk. J. Agric. For.* **2003**, *27*, 183–189.
9. Wolfgang, H.; Jürgen, L. Phenolic Resins. In *Ullmann's Encyclopedia of Industrial Chemistry*; John Wiley & Sons, Inc: Somerset, NJ, 2011.
10. Gardziella, A.; Pilato, L. .; Knop, A. *Phenolic Resins: Chemistry, Applications, Standardization, Safety and Ecology*; 2nd ed.; Springer, 2000;
11. Hoyong Chung, N. R. W. Chemistry of lignin-based materials. *Green Mater.* **2012**, *1*, 137– 160.
12. De Medeiros Eliton S.; Agnelli José A. M.; Joseph Kuruvilla; De Carvalho Laura H.; Mattoso Luiz H. C. Curing behavior of a novolac-type phenolic resin analyzed by differential scanning calorimetry. *J. Appl. Polym. Sci.* **2003**, *90*, 1678–1682, doi:10.1002/app.12838.
13. Kuroe Motoki; Tsunoda Tomoki; Kawano Yusuke; Takahashi Akio Application of lignin-modified phenolic resins to brake friction material. *J. Appl. Polym. Sci.* **2012**, *129*, 310–315, doi:10.1002/app.38703.
14. Mansouri, N.-E. E.; Salvadó, J. Structural characterization of technical lignins for the production of adhesives: Application to lignosulfonate, kraft, soda-anthraquinone, organosolv and ethanol process lignins. *Ind. Crops Prod.* **2006**, *24*, 8–16, doi:10.1016/j.indcrop.2005.10.002.
15. Tejado, A.; Peña, C.; Labidi, J.; Echeverria, J. M.; Mondragon, I. Physico-chemical characterization of lignins from different sources for use in phenol–formaldehyde resin synthesis. *Bioresour. Technol.* **2007**, *98*, 1655–1663, doi:10.1016/j.biortech.2006.05.042.
16. Alonso, M. V.; Oliet, M.; Domínguez, J. C.; Rojo, E.; Rodríguez, F. Thermal degradation of lignin–phenol–formaldehyde and phenol–formaldehyde resol resins. *J. Therm. Anal. Calorim.* **2011**, *105*, 349–356, doi:10.1007/s10973-011-1405-0.

17. Agirrezabal-Telleria, I.; Gandarias, I.; Arias, P. Production of furfural from pentosan-rich biomass: Analysis of process parameters during simultaneous furfural stripping. *Bioresour. Technol.* **2013**, *143*, 258–264.
18. Dias, A. S.; Pillinger, M.; Valente, A. A. Dehydration of xylose into furfural over micro-mesoporous sulfonic acid catalysts. *J. Catal.* **2005**, *229*, 414–423, doi:10.1016/j.jcat.2004.11.016.
19. Dias, A. S.; Lima, S.; Pillinger, M.; Valente, A. A. Acidic cesium salts of 12-tungstophosphoric acid as catalysts for the dehydration of xylose into furfural. *Carbohydr. Res.* **2006**, *341*, 2946–2953, doi:10.1016/j.carres.2006.10.013.
20. Fusaro, M. B.; Chagnault, V.; Postel, D. Reactivity of d-fructose and d-xylose in acidic media in homogeneous phases. *Carbohydr. Res.* **2015**, *409*, 9–19, doi:10.1016/j.carres.2015.03.012.
21. Hu, L.; Zhao, G.; Hao, W.; Tang, X.; Sun, Y.; Lin, L.; Liu, S. Catalytic conversion of biomass-derived carbohydrates into fuels and chemicals via furanic aldehydes. *RSC Adv.* **2012**, *2*, 11184–11206, doi:10.1039/C2RA21811A.
22. Binder, J. B.; Blank, J. J.; Cefali, A. V.; Raines, R. T. Synthesis of Furfural from Xylose and Xylan. *ChemSusChem* **2010**, *3*, 1268–1272, doi:10.1002/cssc.201000181.
23. Sakostschikoff, A. P.; Iwanowa, W. T.; Kurennowa, A. M. Determination of Pentosans in Vegetable Materials Containing Tannins. *Ind. Eng. Chem. Anal. Ed.* **1934**, *6*, 205–208, doi:10.1021/ac50089a019.
24. Li, J.; Gellerstedt, G. Improved lignin properties and reactivity by modifications in the autohydrolysis process of aspen wood. *Ind. Crops Prod.* **2008**, *27*, 175–181.
25. Goundalkar, M. Investigating the effect of hot-water extraction on phenolic constituents of selected hardwoods, State University of New York, College of Environmental Science and Forestry: Syracuse, NY, 2014.
26. Chua, M. G. S.; Wayman, M. Characterization of autohydrolysis aspen (P.tremuloides) lignins. Part 3. Infrared and ultraviolet studies of extracted autohydrolysis lignin. *Can. J. Chem.* **1979a**, *57*, 2603–2611.
27. Zuckerstätter, G.; Weber, H.; Patt, R.; Sixta, S. Effect of autohydrolysis of Eucalyptus globulus wood on lignin structure. Part 1: Comparison of different lignin fractions formed during water prehydrolysis. *Holzforschung* **2008**, *62*, 645–652.
28. Stewart, D. Lignin as a base material for materials applications: Chemistry, application and economics. *Ind. Crops Prod.* **2008**, *27*, 202–207, doi:10.1016/j.indcrop.2007.07.008.
29. Sjostrom, E. *Wood Chemistry, Second Edition: Fundamentals and Applications*; 2 edition.; Academic Press, 1993; ISBN 978-1-4933-0194-2.
30. Saha, B. C. Hemicellulose bioconversion. *J. Ind. Microbiol. Biotechnol.* **2003**, *30*, 279–291, doi:10.1007/s10295-003-0049-x.
31. Brosse, N.; Dufour, A.; Meng, X.; Sun, Q.; Ragauskas, A. Miscanthus: a fast-growing crop for biofuels and chemicals production. *Biofuels Bioprod. Biorefining* **2012**, *6*, 580–598, doi:10.1002/bbb.1353.
32. Stolarski, M. J.; Szczukowski, S.; Tworkowski, J.; Klasa, A. Yield, energy parameters and chemical composition of short-rotation willow biomass. *Ind. Crops Prod.* **2013**, *46*, 60–65, doi:10.1016/j.indcrop.2013.01.012.
33. Moon, R. J.; Martini, A.; Nairn, J.; Simonsen, J.; Youngblood, J. Cellulose nanomaterials review: structure, properties and nanocomposites. *Chem. Soc. Rev.* **2011**, *40*, 3941–3994, doi:10.1039/C0CS00108B.
34. Horn, S. J.; Vaaje-Kolstad, G.; Westereng, B.; Eijsink, V. Novel enzymes for the degradation of cellulose. *Biotechnol. Biofuels* **2012**, *5*, 45, doi:10.1186/1754-6834-5-45.

35. Mittal, A.; Katahira, R.; Himmel, M. E.; Johnson, D. K. Effects of alkaline or liquid-ammonia treatment on crystalline cellulose: changes in crystalline structure and effects on enzymatic digestibility. *Biotechnol. Biofuels* **2011**, *4*, 41, doi:10.1186/1754-6834-4-41.
36. Zhao, X.; Zhang, L.; Liu, D. Biomass recalcitrance. Part I: the chemical compositions and physical structures affecting the enzymatic hydrolysis of lignocellulose. *Biofuels Bioprod. Biorefining* **2012**, *6*, 465–482, doi:10.1002/bbb.1331.
37. Ebringerová, A.; Hromádková, Z.; Heinze, T. Hemicellulose. In *Polysaccharides I*; Heinze, T., Ed.; Advances in Polymer Science; Springer Berlin Heidelberg, 2005; pp. 1–67 ISBN 978-3-540-26112-4.
38. Timell, T. E. Recent progress in the chemistry of wood hemicelluloses. *Wood Sci. Technol.* **1967**, *1*, 45–70, doi:10.1007/BF00592255.
39. Teleman, A. Hemicelluloses and Pectins. In *M. Ek, G. Gellerstedt, & G Henriksson, Pulp and Paper Chemistry and Technology: Wood Chemistry and Wood Biotechnology*; De Gruyter: Stockholm, Sweden, 2009; pp. 101–120.
40. Xu, F. Structure, Ultrastructure, and Chemical Composition. In *Cereal Straw as a Resource for Sustainable Biomaterials and Biofuels*; 2010; pp. 9–47 ISBN 978-0-444-53234-3.
41. Peng, F.; Peng, P.; Xu, F.; Sun, R.-C. Fractional purification and bioconversion of hemicelluloses. *Biotechnol. Adv.* **2012**, *30*, 879–903, doi:10.1016/j.biotechadv.2012.01.018.
42. de O Buanafina, M. M. Feruloylation in grasses: current and future perspectives. *Mol. Plant* **2009**, *2*, 861–872, doi:10.1093/mp/ssp067.
43. Patil, R. A. *Cleavage of Acetyl Groups for Acetic Acid Production in Kraft Pulp Mills*; University of Maine, 2012;
44. Hu, F.; Ragauskas, A. Pretreatment and Lignocellulosic Chemistry. *BioEnergy Res.* **2012**, *5*, 1043–1066, doi:10.1007/s12155-012-9208-0.
45. Sjöström, E.; Alen, R. *Analytical Methods in Wood Chemistry, Pulping, and Papermaking*; Springer Science & Business Media, 2013; ISBN 978-3-662-03898-7.
46. Ralph, J.; Brunow, G.; Boerjan, W. Lignins. In *eLS*; John Wiley & Sons, Ltd, 2007 ISBN 978-0-470-01590-2.
47. Boerjan, W.; Ralph, J.; Baucher, M. Lignin Biosynthesis. *Annu. Rev. Plant Biol.* **2003**, *54*, 519–546, doi:10.1146/annurev.arplant.54.031902.134938.
48. KV Sarkanen; CH Ludwig Lignins: Occurrence, formation, structure and reactions, K. V. Sarkanen and C. H. Ludwig, Eds., John Wiley & Sons, Inc., New York, 1971. 916 pp. $35.00. *J. Polym. Sci. [B]* **1972**, *10*, 228–230, doi:10.1002/pol.1972.110100315.
49. Vanholme, R.; Demedts, B.; Morreel, K.; Ralph, J.; Boerjan, W. Lignin Biosynthesis and Structure. *Plant Physiol.* **2010**, *153*, 895–905, doi:10.1104/pp.110.155119.
50. Rippert, P.; Puyaubert, J.; Grisollet, D.; Derrier, L.; Matringe, M. Tyrosine and phenylalanine are synthesized within the plastids in Arabidopsis. *Plant Physiol.* **2009**, *149*, 1251–1260, doi:10.1104/pp.108.130070.
51. Higuchi, P. T. Lignin biochemistry: Biosynthesis and biodegradation. *Wood Sci. Technol.* **1990**, *24*, 23–63, doi:10.1007/BF00225306.
52. Ehlting, J.; Mattheus, N.; Aeschliman, D. S.; Li, E.; Hamberger, B.; Cullis, I. F.; Zhuang, J.; Kaneda, M.; Mansfield, S. D.; Samuels, L.; Ritland, K.; Ellis, B. E.; Bohlmann, J.; Douglas, C. J. Global transcript profiling of primary stems from Arabidopsis thaliana identifies candidate genes for missing links in lignin biosynthesis and transcriptional regulators of fiber differentiation. *Plant J. Cell Mol. Biol.* **2005**, *42*, 618–640, doi:10.1111/j.1365-313X.2005.02403.x.

53. Kaneda, M.; Rensing, K. H.; Wong, J. C. T.; Banno, B.; Mansfield, S. D.; Samuels, A. L. Tracking Monolignols during Wood Development in Lodgepole Pine. *Plant Physiol.* **2008**, *147*, 1750–1760, doi:10.1104/pp.108.121533.
54. Dorrestijn, E.; Laarhoven, L. J. J.; Arends, I. W. C. E.; Mulder, P. The occurrence and reactivity of phenoxyl linkages in lignin and low rank coal. *J. Anal. Appl. Pyrolysis* **2000**, *54*, 153–192, doi:10.1016/S0165-2370(99)00082-0.
55. Zhou, X.; Broadbelt, L. J.; Vinu, R. Chapter Two - Mechanistic Understanding of Thermochemical Conversion of Polymers and Lignocellulosic Biomass. In *Advances in Chemical Engineering*; Van Geem, K. M., Ed.; Thermochemical Process Engineering; Academic Press, 2016; Vol. 49, pp. 95–198.
56. Adler, E. Lignin chemistry—past, present and future. *Wood Sci. Technol.* **1977**, *11*, 169–218, doi:10.1007/BF00365615.
57. Henriksson, G. 6. Lignin. In *Wood Chemistry and Wood Biotechnology*; De Gruyter: Berlin, Boston, 2009 ISBN 978-3-11-021340-9.
58. del Río, J. C.; Rencoret, J.; Prinsen, P.; Martínez, Á. T.; Ralph, J.; Gutiérrez, A. Structural Characterization of Wheat Straw Lignin as Revealed by Analytical Pyrolysis, 2D-NMR, and Reductive Cleavage Methods. *J. Agric. Food Chem.* **2012**, *60*, 5922–5935, doi:10.1021/jf301002n.
59. Gösta Brunow; Kilpeläinen, I.; Sipilä, J.; Rummakko, P. Oxidative coupling of phenols and the biosynthesis of lignin. **1998**, 131–147.
60. Akiyama, T.; Matsumoto, Y.; Okuyama, T.; Meshitsuka, G. Ratio of erythro and threo forms of beta-O-4 structures in tension wood lignin. *Phytochemistry* **2003**, *64*, 1157–1162.
61. Karhunen, P.; Rummakko, P.; Sipilä, J.; Brunow, G.; Kilpeläinen, I. The formation of dibenzodioxocin structures by oxidative coupling. A model reaction for lignin biosynthesis. *Tetrahedron Lett.* **1995**, *36*, 4501–4504, doi:10.1016/0040-4039(95)00769-9.
62. Lawoko, M.; Henriksson, G.; Gellerstedt, G. Structural Differences between the Lignin−Carbohydrate Complexes Present in Wood and in Chemical Pulps. *Biomacromolecules* **2005**, *6*, 3467–3473, doi:10.1021/bm058014q.
63. Toledano, A.; García, A.; Mondragon, I.; Labidi, J. Lignin separation and fractionation by ultrafiltration. *Sep. Purif. Technol.* **2010**, *71*, 38–43, doi:10.1016/j.seppur.2009.10.024.
64. Wen, J.-L.; Sun, S.-L.; Xue, B.-L.; Sun, R.-C. Recent Advances in Characterization of Lignin Polymer by Solution-State Nuclear Magnetic Resonance (NMR) Methodology. *Materials* **2013**, *6*, 359–391, doi:10.3390/ma6010359.
65. Bjorkman, A. Lignin and Lignin-Carbohydrate Complexes. *Ind. Eng. Chem.* **1957**, *49*, 1395–1398, doi:10.1021/ie50573a040.
66. Alvira, P.; Tomás-Pejó, E.; Ballesteros, M.; Negro, M. J. Pretreatment technologies for an efficient bioethanol production process based on enzymatic hydrolysis: A review. *Bioresour. Technol.* **2010**, *101*, 4851–4861, doi:10.1016/j.biortech.2009.11.093.
67. Hendriks, A. T. W. M.; Zeeman, G. Pretreatments to enhance the digestibility of lignocellulosic biomass. *Bioresour. Technol.* **2009**, *100*, 10–18, doi:10.1016/j.biortech.2008.05.027.
68. Mosier, N.; Wyman, C.; Dale, B.; Elander, R.; Lee, Y. Y.; Holtzapple, M.; Ladisch, M. Features of promising technologies for pretreatment of lignocellulosic biomass. *Bioresour. Technol.* **2005**, *96*, 673–686, doi:10.1016/j.biortech.2004.06.025.
69. Garrote, G.; Dominguez, H.; Parajo, J. C. Hydrothermal processing of lignocellulosic materials. *Eur. J. Wood Wood Prod.* **1999**, *57*, 191–202.

70. Carvalheiro, F.; Duarte, L. C.; Gírio, F. M. Hemicellulose biorefineries: a review on biomass pretreatments. *JSIR Vol6711 Novemb. 2008* **2008**.
71. Taherzadeh, M. J.; Karimi, K. Pretreatment of Lignocellulosic Wastes to Improve Ethanol and Biogas Production: A Review. *Int. J. Mol. Sci.* **2008**, *9*, 1621–1651, doi:10.3390/ijms9091621.
72. Amidon, T. E.; Bujanovic, B.; Liu, S.; Howard, J. R. Commercializing Biorefinery Technology: A Case for the Multi-Product Pathway to a Viable Biorefinery. *Forests* **2011**, *2*, 929–947, doi:10.3390/f2040929.
73. Sun, Y.; Cheng, J. Hydrolysis of lignocellulosic materials for ethanol production: a review. *Bioresour. Technol.* **2002**, *83*, 1–11, doi:10.1016/S0960-8524(01)00212-7.
74. Gong, C.; Goundalkar, M. J.; Bujanovic, B. M.; Amidon, T. E. Evaluation of Different Sulfur-Free Delignification Methods for Hot-Water Extracted Hardwood. *J. Wood Chem. Technol.* **2012**, *32*, 93–104, doi:10.1080/02773813.2011.607534.
75. Hammel, K. E. Fungal Degradation of Lignin. **1997**, 13.
76. Cheng, K.; Barber, V. A.; Driscoll, M. S.; Winter, W. T.; Stipanovic, A. J. Reducing Woody Biomass Recalcitrance by Electron Beams, Biodelignification and Hot-Water Extraction. *J. Bioprocess Eng. Biorefinery* **2013**, *2*, 143–152, doi:10.1166/jbeb.2013.1048.
77. Sundar, S.; Bergey, N. S.; Salamanca-Cardona, L.; Stipanovic, A.; Driscoll, M. Electron beam pretreatment of switchgrass to enhance enzymatic hydrolysis to produce sugars for biofuels. *Carbohydr. Polym.* **2014**, *100*, 195–201, doi:10.1016/j.carbpol.2013.04.103.
78. Bak, J. S.; Ko, J. K.; Han, Y. H.; Lee, B. C.; Choi, I.-G.; Kim, K. H. Improved enzymatic hydrolysis yield of rice straw using electron beam irradiation pretreatment. *Bioresour. Technol.* **2009**, *100*, 1285–1290, doi:10.1016/j.biortech.2008.09.010.
79. Khan, A. W.; Labrie, J.-P.; McKeown, J. Effect of electron-beam irradiation pretreatment on the enzymatic hydrolysis of softwood. *Biotechnol. Bioeng.* **1986**, *28*, 1449–1453, doi:10.1002/bit.260280921.
80. Argyropoulos Dimitris S.; Sun Yujun Photochemically Induced Solid-State Degradation, Condensation, and Rearrangement Reactions in Lignin Model Compounds and Milled Wood Lignin. *Photochem. Photobiol.* **2008**, *64*, 510–517, doi:10.1111/j.1751-1097.1996.tb03098.x.
81. Lanzalunga, O.; Bietti, M. Photo- and radiation chemical induced degradation of lignin model compounds. *J. Photochem. Photobiol. B* **2000**, *56*, 85–108, doi:10.1016/S1011-1344(00)00054-3.
82. Chuaqui, C. A.; Rajagopal, S.; Kovács, A.; Stepanik, T.; Merritt, J.; György, I.; Whitehouse, R.; Ewing, D. Radiation-induced effects in lignin model compounds: a pulse and steady-state radiolysis study. *Tetrahedron* **1993**, *49*, 9689–9698, doi:10.1016/S0040-4020(01)80172-1.
83. Driscoll, M. S.; Stipanovic, A. J.; Cheng, K.; Barber, V. A.; Manning, M.; Smith, J. L.; Sundar, S. Ionizing radiation and a wood-based biorefinery. *Radiat. Phys. Chem.* **2014**, *94*, 217–220, doi:10.1016/j.radphyschem.2013.05.045.
84. Casebier, R. L.; Hamilton, J. K.; Hergert, H. L. Chemistry and mechanism of water prehydrolysis on southern pine wood. *Tappi Tech Pulp Pap Indus* **1969**.
85. Conner, A. H. Kinetic Modeling of Hardwood Prehydrolysis. Part I. Xylan Removal by Water Prehydrolysis. *Wood Fiber Sci.* **2007**, *16*, 268–277.
86. Mittal, A. Kitetics of hemicellulose extraction during autohydrolysis of sugar maple wood. PhD, State University of New York College of Environmental Science and Forestry: Syracuse, New York, 2006.
87. Amidon, T. E.; Liu, S. Water-based woody biorefinery. *Biotechnol. Adv.* **2009**, *27*, 542–550, doi:10.1016/j.biotechadv.2009.04.012.

88. Amidon, T.; Bujanovic, B.; Liu, S.; Hasan, A.; Howard, J. R. Niche position and opportunities for woody biomass conversion. *RSC Green Chem.* **2013**, 151–179.
89. Corbett, D. B.; Kohan, N.; Machado, G.; Jing, C.; Nagardeolekar, A.; Bujanovic, B. M. Chemical Composition of Apricot Pit Shells and Effect of Hot-Water Extraction. *Energies* **2015**, *8*, 9640–9654, doi:10.3390/en8099640.
90. Dongre, P.; Driscoll, M.; Amidon, T.; Bujanovic, B. Lignin-Furfural Based Adhesives. *Energies* **2015**, *8*, 7897–7914, doi:10.3390/en8087897.
91. Gong, C.; Bujanovic, B. M. Impact of Hot-Water Extraction on Acetone-Water Oxygen Delignification of Paulownia Spp. and Lignin Recovery. *Energies* **2014**, *7*, 857–873.
92. Liu, T.; Lin, L.; Sun, Z.; Hu, R.; Liu, S. Bioethanol fermentation by recombinant E. coli FBR5 and its robust mutant FBHW using hot-water wood extract hydrolyzate as substrate. *Biotechnol. Adv.* **2010**, *28*, 602–608, doi:10.1016/j.biotechadv.2010.05.008.
93. Lu, H.; Hu, R.; Ward, A.; Amidon, T. E.; Liang, B.; Liu, S. Hot-water extraction and its effect on soda pulping of aspen woodchips. *Biomass Bioenergy* **2012**, *39*, 5–13, doi:10.1016/j.biombioe.2011.01.054.
94. Mante, O. D.; Amidon, T. E.; Stipanovic, A.; Babu, S. P. Integration of biomass pretreatment with fast pyrolysis: An evaluation of electron beam (EB) irradiation and hot-water extraction (HWE). *J. Anal. Appl. Pyrolysis* **2014**, *110*, 44–54, doi:10.1016/j.jaap.2014.08.004.
95. Wang, K.-T.; Jing, C.; Wood, C.; Nagardeolekar, A.; Kohan, N.; Dongre, P.; Amidon, T. E.; Bujanovic, B. M. Toward Complete Utilization of Miscanthus in a Hot-Water Extraction-Based Biorefinery. *Energies* **2017**, *11*, 39, doi:10.3390/en11010039.
96. Wyman, C. E.; Dale, B. E.; Elander, R. T.; Holtzapple, M.; Ladisch, M. R.; Lee, Y. Y. Coordinated development of leading biomass pretreatment technologies. *Bioresour. Technol.* **2005**, *96*, 1959–1966, doi:10.1016/j.biortech.2005.01.010.
97. Uygut, M. A.; Corbet, D.; Wood, C.; Zelie, M.; Bujanovic, B. Potential for Enhancement of Enzymatic Hydrolysis of Sugar Maple (Acer saccharum). In; 2015.
98. Goundalkar, M. J.; Corbett, D. B.; Bujanovic, B. M. Comparative Analysis of Milled Wood Lignins (MWLs) Isolated from Sugar Maple (SM) and Hot-Water Extracted Sugar Maple (ESM). *Energies* **2014**, *7*, 1363–1375, doi:10.3390/en7031363.
99. Kubo, S.; Kadla, J. F. Poly (ethylene oxide)/organosolv lignin blends: Relationship between thermal properties, chemical structure, and blend behavior. *Macromolecules* **2004**, *37*, doi:10.1021/ma0490552.
100. Kubo, S.; Kadla, J. F. Lignin-based Carbon Fibers: Effect of Synthetic Polymer Blending on Fiber Properties. *J. Polym. Environ.* **2005**, *13*, 97–105, doi:10.1007/s10924-005-2941-0.
101. Dence, C. W. The Determination of Lignin. In *Methods in Lignin Chemistry*; Lin, D. S. Y., Dence, P. E. D. C. W., Eds.; Springer Series in Wood Science; Springer Berlin Heidelberg, 1992; pp. 33–61 ISBN 978-3-642-74067-1.
102. Hatfield, R.; Fukushima, R. S. Can Lignin Be Accurately Measured? *Crop Sci.* **2005**, *45*, 832–839, doi:10.2135/cropsci2004.0238.
103. Gong, C.; Goundalkar, M. J.; Bujanovic, B. M.; Amidon, T. E. Delignification studies on hot-water extracted wood. *ResearchGate* **2010**, *2*, 1316–1347.
104. Saxena, I. M.; Brown, R. M. Cellulose biosynthesis: current views and evolving concepts. *Ann. Bot.* **2005**, *96*, 9–21, doi:10.1093/aob/mci155.
105. Johnson, D. B.; Moore, W. E.; Zank, L. C. The spectrophotometric determination of lignin in small wood samples Available online: https://eurekamag.com/research/014/272/014272813.php (accessed on Apr 16, 2018).
106. Björkman, A. Studies on finely divided wood. Part 5. The effect of milling. *Sven Papperstidn* **1957**, *60*, 329–335.

107. Mansouri, N. E.; Pizzi, A.; Salvadó, J. Lignin-based wood panel adhesives without formaldehyde. *Holz Als Roh- Werkst.* **2006**, *65*, 65–70, doi:10.1007/s00107-006-0130-z.
108. Liou, T.-H. Development of mesoporous structure and high adsorption capacity of biomass-based activated carbon by phosphoric acid and zinc chloride activation. *Chem. Eng. J.* **2010**, *158*, 129–142, doi:10.1016/j.cej.2009.12.016.
109. Montané, D.; Torné-Fernández, V.; Fierro, V. Activated carbons from lignin: kinetic modeling of the pyrolysis of kraft lignin activated with phosphoric acid. *Chem. Eng. J.* **2005**, *106*, 1–12, doi:10.1016/j.cej.2004.11.001.
110. Olivares, M.; Guzmán, J. A.; Natho, A.; Saavedra, A. Kraft lignin utilization in adhesives. *Wood Sci. Technol.* **1988**, *22*, 157–165, doi:10.1007/BF00355851.
111. Pan, H. Synthesis of polymers from organic solvent liquefied biomass: A review. *Renew. Sustain. Energy Rev.* **2011**, *15*, 3454–3463, doi:10.1016/j.rser.2011.05.002.
112. Zhang, Y. Production and Applications of Formaldehyde-Free Phenolic Resins Using 5-Hydroxymethylfurfural Derived from Glucose In-Situ, 2014.
113. Pizzi, A. P. Phenolic Resin Adhesives. **2003**, doi:10.1201/9780203912225.ch26.
114. Duong, L. D.; Luong, N. D.; Binh, N. T. T.; Park, I.-K.; Lee, S. H.; Kim, D. S.; Lee, Y. S.; Lee, Y. K.; Kim, B. W.; Kim, K. H.; Yoon, H. K.; Yun, J. H.; Nam, J.-D. Chemical and Rheological Characteristics of Thermally Stable Kraft Lignin Polycondensates Analyzed by Dielectric Properties. *BioResources* **2013**, *8*, 4518–4532, doi:10.15376/biores.8.3.4518-4532.
115. Jeong, H.; Park, J.; Kim, S.; Lee, J.; Ahn, N.; Roh, H. Preparation and characterization of thermoplastic polyurethanes using partially acetylated kraft lignin. *Fibers Polym.* **2013**, *14*, 1082–1093, doi:10.1007/s12221-013-1082-7.
116. Cui, C.; Sadeghifar, H.; Sen, S.; Argyropoulos, D. S. Toward Thermoplastic Lignin Polymers; Part II: Thermal & Polymer Characteristics of Kraft Lignin & Derivatives. *BioResources* **2013**, *8*, 864–886, doi:10.15376/biores.8.1.864-886.
117. Maisonneuve, L.; Lebarbé, T.; Grau, E.; Cramail, H. Structure–properties relationship of fatty acid-based thermoplastics as synthetic polymer mimics. *Polym. Chem.* **2013**, *4*, 5472–5517, doi:10.1039/C3PY00791J.
118. Peters, E. N. Plastics: Thermoplastics, Thermosets, and Elastomers. In *Handbook of Materials Selection*; Wiley-Blackwell, 2007; pp. 335–355 ISBN 978-0-470-17255-1.
119. Handbook of Thermoplastics, Second Edition Available online: https://www.crcpress.com/Handbook-of-Thermoplastics-Second-Edition/Olabisi-Adewale/p/book/9781466577220 (accessed on Apr 15, 2018).
120. Baeurle, S. A.; Hotta, A.; Gusev, A. A. On the glassy state of multiphase and pure polymer materials. *Polymer* **2006**, *47*, 6243–6253, doi:10.1016/j.polymer.2006.05.076.
121. Dante Roberto C.; Santamaria Diego A.; Gil Jesús Martín Crosslinking and thermal stability of thermosets based on novolak and melamine. *J. Appl. Polym. Sci.* **2009**, *114*, 4059–4065, doi:10.1002/app.31114.
122. Ma, Y.; Zhao, X.; Chen, X.; Wang, Z. An approach to improve the application of acid-insoluble lignin from rice hull in phenol–formaldehyde resin. *Colloids Surf. Physicochem. Eng. Asp.* **2011**, *377*, 284–289, doi:10.1016/j.colsurfa.2011.01.006.
123. Tejado A.; Kortaberria G.; Peña C.; Labidi J.; Echeverría J. M.; Mondragon Inaki Lignins for phenol replacement in novolac-type phenolic formulations, part I: Lignophenolic resins synthesis and characterization. *J. Appl. Polym. Sci.* **2007**, *106*, 2313–2319, doi:10.1002/app.26941.
124. Yang Sheng; Zhang Yue; Yuan Tong-Qi; Sun Run-Cang Lignin–phenol–formaldehyde resin adhesives prepared with biorefinery technical lignins. *J. Appl. Polym. Sci.* **2015**, *132*, doi:10.1002/app.42493.

125. Jing, Z.; Lihong, H.; Bingchuan, L.; Caiying, B.; Puyou, J.; Yonghong, Z. Preparation and characterization of novolac phenol–formaldehyde resins with enzymatic hydrolysis lignin. *J. Taiwan Inst. Chem. Eng.* **2015**, *54*, 178–182, doi:10.1016/j.jtice.2015.03.023.
126. Yan, N.; Zhang, B.; Zhao, Y.; Farnood, R. R.; Shi, J. Application of Biobased Phenol Formaldehyde Novolac Resin Derived from Beetle Infested Lodgepole Pine Barks for Thermal Molding of Wood Composites. *Ind. Eng. Chem. Res.* **2017**, *56*, 6369–6377, doi:10.1021/acs.iecr.7b00353.
127. Vázquez, G.; González, J.; Freire, S.; Antorrena, G. Effect of chemical modification of lignin on the gluebond performance of lignin-phenolic resins. *Bioresour. Technol.* **1997**, *60*, 191–198, doi:10.1016/S0960-8524(97)00030-8.
128. Gonçalves, A. R.; Benar, P. Hydroxymethylation and oxidation of organosolv lignins and utilization of the products. *Bioresour. Technol.* **2001**, *79*, 103–111, doi:10.1016/S0960-8524(01)00056-6.
129. Lee, W.-J.; Chang, K.-C.; Tseng, I.-M. Properties of phenol-formaldehyde resins prepared from phenol-liquefied lignin. *J. Appl. Polym. Sci.* **2012**, *124*, 4782–4788, doi:10.1002/app.35539.
130. L. Wooten, A.; Sellers Jr, T.; M. Tahir, P. Reaction of formaldehyde with liginin. **1988**, *38*, 45–46.
131. Cavdar, A. D.; Kalaycioglu, H.; Hiziroglu, S. Some of the properties of oriented strandboard manufactured using kraft lignin phenolic resin. *J. Mater. Process. Technol.* **2008**, *202*, 559–563, doi:10.1016/j.jmatprotec.2007.10.039.
132. Wirpsza, Z. *Polyurethanes: chemistry, technology, and applications*; E. Horwood, 1993; ISBN 978-0-13-683186-0.
133. Sen, S.; Patil, S.; S. Argyropoulos, D. Thermal properties of lignin in copolymers, blends, and composites: a review. *Green Chem.* **2015**, *17*, 4862–4887, doi:10.1039/C5GC01066G.
134. Cox, R. L. *Engineered Tribological Composites: The Art of Friction Material Development*; 2011; ISBN 978-0-7680-3485-1.
135. Chan, D.; Stachowiak, G. W. Review of automotive brake friction materials. *Proc. Inst. Mech. Eng. Part J. Automob. Eng.* **2004**, *218*, 953–966, doi:10.1243/0954407041856773.
136. Gerrit H. van der Klashorst Modification of Lignin at the 2- and 6-Positions of the Phenylpropanoid Nuclei. In *Lignin*; ACS Symposium Series; American Chemical Society, 1989; Vol. 397, pp. 346–360 ISBN 0-8412-1631-2.
137. Lundquist, K. Low-molecular weight lignin hydrolysis products. In *Applied Polymer Symposia*; 1976; Vol. 28, pp. 1393–1407.
138. Lora, J. .; Wayman, M. Delignification of hardwoods by autohydrolysis and extraction. *Tappi J.* **1979**, *61*, 47–50.
139. Robert, D.; Gellerstedt, G.; Bardet, M. Carbon-13 NMR analysis of lignin obtained after sulfonation of stream exploded aspen wood. *Nord. Pulp Pap. Res.* **1986**, *1*, 18–25.
140. Roberts, R.; Muzzy, J. D.; Faasa, G. S. Process of extracting lignin from lignocellulosic material using an aqueous organic solvent and an acid neutralizing agent 1988.
141. Wayman, M.; Lora, J. H. Aspen autohydrolysis. The effects of 2-naphthol and other aromatic compounds. *Tappi J.* **1978**, *61*, 55–57.
142. Samuel, R.; Cao, S.; Das, B. K.; Hu, F.; Pu, Y.; Ragauskas, A. J. Investigation of the fate of poplar lignin during autohydrolysis pretreatment to understand the biomass recalcitrance. *RSC Adv.* **2013**, *3*, 5305, doi:10.1039/c3ra40578h.
143. Bu, L.; Tang, Y.; Gao, Y.; Jian, H.; Jiang, J. Comparative characterization of milled wood lignin from furfural residues and corncob. *Chem. Eng. J.* **2011**, *175*, 176–184, doi:10.1016/j.cej.2011.09.091.

144. Binder, J. B.; Gray, M. J.; White, J. F.; Zhang, Z. C.; Holladay, J. E. Reactions of lignin model compounds in ionic liquids. *Biomass Bioenergy* **2009**, *33*, 1122–1130, doi:10.1016/j.biombioe.2009.03.006.
145. Brownlee, H. J.; Miner, C. S. Industrial Development of Furfural. *Ind. Eng. Chem.* **1948**, *40*, 201–204, doi:10.1021/ie50458a005.
146. Wood, C. D. Novel solvent and catalyst system for production of furfural from biomass-derived xylose. Ph.D., State University of New York College of Environmental Science and Forestry: United States -- New York, 2016.
147. Root, D. F. Kinetics of the acid catalyzed conversion of xylose to furfural, 1956.
148. Antal Jr., M. J.; Leesomboon, T.; Mok, W. S.; Richards, G. N. Mechanism of formation of 2-furaldehyde from d-xylose. *Carbohydr. Res.* **1991**, *217*, 71–85, doi:10.1016/0008-6215(91)84118-X.
149. Yang, W.; Li, P.; Bo, D.; Chang, H. The optimization of formic acid hydrolysis of xylose in furfural production. *Carbohydr. Res.* **2012**, *357*, 53–61, doi:10.1016/j.carres.2012.05.020.
150. *TAPPI T 222 om-02 Acid-insoluble lignin in wood and pulp*; 2002;
151. Schoening, A. G.; Johansson, G. Absorptimetric Determination of Acid-Soluble Lignin in Semichemical Pulps and in Some Woods and Plants. *Sven. Papperstid* **1965**, *68*, 607.
152. Davis, M. W. A Rapid Modified Method for Compositional Carbohydrate Analysis of Lignocellulosics by High pH Anion-Exchange Chromatography with Pulsed Amperometric Detection (HPAEC/PAD). *J. Wood Chem. Technol.* **1998**, *18*, 235–252, doi:10.1080/02773819809349579.
153. Chen, C. L.; Danielle, R. Characterization of lignin by 1H and 13C NMR Spectroscopy. In *Methods in Enzymology*; Academic Press: New York, 1988; Vol. 161B, pp. 137–174.
154. Lai, Y.-Z.; Guo, X.-P. Variation of the phenolic hydroxyl group content in wood lignins. *Wood Sci. Technol.* **1991**, *25*, 467–472, doi:10.1007/BF00225239.
155. TAPPI T 236 Kappa number of pulp 2013.
156. Johansson, I. K. G. Method of producing synthetic resin from waste products 1981.
157. *TAPPI 494om-01 Tensile properties of paper and paperboard (using constant rate of elongation apparatus)*; 2001;
158. Brodin, I. Chemical Properties and Thermal Behaviour of Kraft Lignins. **2009**.
159. Takahashi, N.; Koshijima, T. Ester linkages between lignin and glucuronoxylan in a lignin-carbohydrate complex from beech (<Emphasis Type="Italic">Fagus crenata</Emphasis>) wood. *Wood Sci. Technol.* **1988**, *22*, 231–241, doi:10.1007/BF00386018.
160. Duarte, G. V.; Ramarao, B. V.; Amidon, T. E.; Ferreira, P. T. Effect of Hot Water Extraction on Hardwood Kraft Pulp fibers (Acer saccharum, Sugar Maple). *Ind. Eng. Chem. Res.* **2011**, *50*, 9949–9959, doi:10.1021/ie200639u.
161. Crestini, C.; Argyropoulos, D. S. Structural Analysis of Wheat Straw Lignin by Quantitative 31P and 2D NMR Spectroscopy. The Occurrence of Ester Bonds and α-O-4 Substructures. *J. Agric. Food Chem.* **1997**, *45*, 1212–1219, doi:10.1021/jf960568k.
162. Monteil-Rivera, F.; Phuong, M.; Ye, M.; Halasz, A.; Hawari, J. Isolation and characterization of herbaceous lignins for applications in biomaterials. *Ind. Crops Prod.* **2013**, *41*, 356–364, doi:10.1016/j.indcrop.2012.04.049.
163. Narron, R. H.; Kim, H.; Chang, H.; Jameel, H.; Park, S. Biomass pretreatments capable of enabling lignin valorization in a biorefinery process. *Curr. Opin. Biotechnol.* **2016**, *38*, 39–46, doi:10.1016/j.copbio.2015.12.018.
164. Agarwal, U. P.; Ralph, S. A.; Padmakshan, D.; Liu, S.; Karlen, S. D.; Foster, C.; Ralph, J. Estimation of S/G ratio in woods using 1064 nm FT-Raman spectroscopy. *Proc. 18th*

ISWFPC Int. Symp. Wood Fiber Pulping Chem. Held Vienna Sept 9 -11 2015 2015 Pp 333-336 **2015**, 333–336.
165. Obst, J. R. (US D. of A.; Landucci, L. L. Quantitative (13)C-NMR of lignins - Methoxyl: Aryl ratio. *Holzforsch. Ger. FR* **1986**.
166. Santos, R. B.; Capanema, E. A.; Balakshin, M. Y.; Chang, H.; Jameel, H. Lignin Structural Variation in Hardwood Species. *J. Agric. Food Chem.* **2012**, *60*, 4923–4930, doi:10.1021/jf301276a.
167. Villaverde, J. J.; Li, J.; Ek, M.; Ligero, P.; de Vega, A. Native Lignin Structure of Miscanthus x giganteus and Its Changes during Acetic and Formic Acid Fractionation. *J. Agric. Food Chem.* **2009**, *57*, 6262–6270, doi:10.1021/jf900483t.
168. Corbett, D.; Mante, O.; Bujanovic, B. Toward valorization of lignin: Characterization and fast pyrolysis of lignin recovered from hot-water extracts of electron-beam irradiated sugar maple. *Tappi J.* **2017**, *16*, 213–226.
169. Corbett, D. Recovery of lignin from hot water extracts of sugar maple: Valorization by catalytic fast pyrolysis. M.S., State University of New York College of Environmental Science and Forestry: United States -- New York, 2016.
170. El Hage, R.; Brosse, N.; Chrusciel, L.; Sanchez, C.; Sannigrahi, P.; Ragauskas, A. Characterization of milled wood lignin and ethanol organosolv lignin from miscanthus. *Polym. Degrad. Stab.* **2009**, *94*, 1632–1638, doi:10.1016/j.polymdegradstab.2009.07.007.
171. Sperling, L. H. *Introduction to Physical Polymer Science*; 4 edition.; Wiley-Interscience: Hoboken, N.J, 2005; ISBN 978-0-471-70606-9.
172. Chanda, M.; Roy, S. K. *Plastics Technology Handbook, Fourth Edition*; 4 edition.; CRC Press: Boca Raton, FL, 2006; ISBN 978-0-8493-7039-7.
173. Rogošić, M.; Mencer, H. J.; Gomzi, Z. Polydispersity index and molecular weight distributions of polymers. *Eur. Polym. J.* **1996**, *32*, 1337–1344, doi:10.1016/S0014-3057(96)00091-2.
174. Tolbert, A.; Akinosho, H.; Khunsupat, R.; Naskar, A.; Ragauskas, A. Characterization and analysis of the molecular weight of lignin for biorefining studies. *Biofuels Bioprod. Biorefining* **2014**, *8*, doi:10.1002/bbb.1500.
175. Asikkala, J.; Tamminen, T.; Argyropoulos, D. S. Accurate and Reproducible Determination of Lignin Molar Mass by Acetobromination Available online: http://pubs.acs.org/doi/abs/10.1021/jf303003d (accessed on Apr 7, 2018).
176. Pellinen, J.; Salkinoja-Salonen, M. High-performance size-exclusion chromatography of lignin and its derivatives. *J. Chromatogr. A* **1985**, *328*, 299–308, doi:10.1016/S0021-9673(01)87400-8.
177. Chua, M. G.; Wayman, M. Characterization of autohydrolysis aspen (P. tremuloides) lignins. Part 3. Infrared and ultraviolet studies of extracted autohydrolysis lignin. *Can. J. Chem.* **1979**, *57*, 2603–2611.
178. Lora, J. H.; Wayman, M. Delignification of hardwoods by autohydrolysis and extraction. *Tappi Tech. Assoc. Pulp Pap. Ind.* **1978**.
179. Felício, C. M.; Machado, A. E. da H.; Castellan, A.; Nourmamode, A.; Perez, D. da S.; Ruggiero, R. Routes of degradation of β-O-4 syringyl and guaiacyl lignin model compounds during photobleaching processes. *J. Photochem. Photobiol. Chem.* **2003**, *156*, 253–265, doi:10.1016/S1010-6030(03)00007-8.
180. Koch, H.; Hübner, K.; Fischer, K. The Influence of Light on the Molecular Mass of Lignin. *J. Wood Chem. Technol.* **1994**, *14*, 339–349, doi:10.1080/02773819408003101.
181. Gierer, J.; Nilvebrant, N.-O. Studies on the Degradation of Lignins by Oxygen in Acidic Media. *Holzforsch. - Int. J. Biol. Chem. Phys. Technol. Wood* **1994**, *48*, 51–58, doi:10.1515/hfsg.1994.48.s1.51.

182. Gierer, J.; Reitberger, T. The Reactions of Hydroxyl Radicals with Aromatic Rings in Lignins, Studied with Creosol and 4-Methylveratrol. *Holzforsch. - Int. J. Biol. Chem. Phys. Technol. Wood* **1992**, *46*, 495–504, doi:10.1515/hfsg.1992.46.6.495.
183. El-Saied, H.; Nada, A.-A. M. A. The thermal behaviour of lignins from wasted black pulping liquors. *Polym. Degrad. Stab.* **1993**, *40*, 417–421, doi:10.1016/0141-3910(93)90152-9.
184. Sun, R.; Tomkinson, J.; Lloyd Jones, G. Fractional characterization of ash-AQ lignin by successive extraction with organic solvents from oil palm EFB fibre. *Polym. Degrad. Stab.* **2000**, *68*, 111–119, doi:10.1016/S0141-3910(99)00174-3.
185. Gargulak, J. D.; Lebo, S. E. Commercial Use of Lignin-Based Materials. In *Lignin: Historical, Biological, and Materials Perspectives*; ACS Symposium Series; American Chemical Society, 1999; Vol. 742, pp. 304–320 ISBN 978-0-8412-3611-0.
186. Lora, J. H.; Glasser, W. G. Recent Industrial Applications of Lignin: A Sustainable Alternative to Nonrenewable Materials. *J. Polym. Environ.* **2002**, *10*, 39–48, doi:10.1023/A:1021070006895.
187. Sperling, L. h. Glass-Rubber Transition Behavior. In *Introduction to Physical Polymer Science*; John Wiley & Sons, Inc., 2005; pp. 349–425 ISBN 978-0-471-75712-2.
188. Jain, R. K.; Sjöstedt, M.; Glasser, W. G. Thermoplastic Xylan Derivatives with Propylene Oxide. *Cellulose* **2000**, *7*, 319–336, doi:10.1023/A:1009260415771.
189. Gröndahl, M.; Eriksson, L.; Gatenholm, P. Material Properties of Plasticized Hardwood Xylans for Potential Application as Oxygen Barrier Films. *Biomacromolecules* **2004**, *5*, 1528–1535, doi:10.1021/bm049925n.
190. *ASTM D 906-98 (2017) Standard Test Method for Strength Properties of Adhesives in Plywood Type Construction in Shear by Tension Loading*; 2017;
191. Lundquist, K. Low-molecular weight lignin hydrolysis products. *Appl. Polym. Symp.* **1976**, *28*, 1393–1407.
192. Li, J.; Gellerstedt, G. Improved lignin properties and reactivity by modifications in the autohydrolysis process of aspen wood. *Ind. Crops Prod.* **2008**, *27*, 175–181, doi:10.1016/j.indcrop.2007.07.022.
193. Roberts, R. S.; Muzzy, J. D.; Faass, G. S. Process for extracting lignin from lignocellulosic material using an aqueous organic solvent and an acid neutralizing agent. **1988**.
194. Leschinsky, M.; Zuckerstätter, G.; Weber, H. K.; Patt, R.; Sixta, H. Effect of autohydrolysis of Eucalyptus globulus wood on lignin structure. Part 2: Influence of autohydrolysis intensity. *Holzforschung* **2008**, *62*, 653–658, doi:10.1515/HF.2008.133.
195. Song, T.; Pranovich, A.; Sumerskiy, I.; Holmbom, B. Extraction of galactoglucomannan from spruce wood with pressurised hot water. *Holzforschung* **2008**, *62*, 659–666, doi:10.1515/HF.2008.131.
196. Mansouri, N. E. E.; Yuan, Q.; Huang, F. Synthesis and characterization of kraft lignin-based epoxy resins. *BioResources* **2011**, *6*, 2492–2503, doi:10.15376/biores.6.3.2492-2503.
197. Ibrahim, V.; Mamo, G.; Gustafsson, P.-J.; Hatti-Kaul, R. Production and properties of adhesives formulated from laccase modified Kraft lignin. *Ind. Crops Prod.* **2013**, *45*, 343–348, doi:10.1016/j.indcrop.2012.12.051.
198. Argyropoulos, D. S.; Sadeghifar, H.; Cui, C.; Sen, S. Synthesis and Characterization of Poly(arylene ether sulfone) Kraft Lignin Heat Stable Copolymers. *ACS Sustain. Chem. Eng.* **2014**, *2*, 264–271, doi:10.1021/sc4002998.
199. Pizzi, A. Recent developments in eco-efficient bio-based adhesives for wood bonding: opportunities and issues. *J. Adhes. Sci. Technol.* **2012**, *20*, 829–846, doi:10.1163/156856106777638635.

200. C. G. Overberger and G. Menges, Encyclopedia of polymer science and engineering, 2nd edition. *Br. Polym. J.* **1985**, *4*, 377–377, doi:10.1002/pi.4980170412.
201. Maron, R.; Crosby, C. . Interaction between fibers and phenolic Resins. *Tappi J.* **1971**, *54*, 1319–1322.

APPENDIX

Appendix IA

1. **Statistical analysis: F-test and t-test of replicate formulations**
   The results of F-test and t-test showed no significant differences between replicate resin formulations. Therefore, the data of the two duplicates was pooled.

Tensile index of adhesive (MS_F50_1A)	Tensile index of adhesive (MS_F50_1B)
10170.80962	14469.76255
12952.53226	14766.40684
14173.49149	9518.304021
12325.63602	12156.48856
13026.7191	11188.47267
11160.89951	6017.457271
12002.0981	9464.800872
9082.654137	
6135.569411	
9653.745625	

F-Test Two-Sample for Variances

	Variable 1	*Variable 2*
Mean	11068.42	11083.1
Variance	5618941	9487952
Observations	10	7
df	9	6
F	0.592219	
P(F<=f) one-tail	0.230222	
F Critical one-tail	0.296406	

t-Test: Two-Sample Assuming Unequal Variances

	Variable 1	*Variable 2*
Mean	11068.41553	11083.1
Variance	5618941.294	9487952
Observations	10	7
Hypothesized Mean Difference	0	
df	11	
t Stat	-0.010604276	
P(T<=t) one-tail	0.495864525	
t Critical one-tail	1.795884819	

P(T<=t) two-tail	0.991729051
t Critical two-tail	2.20098516

Tensile index of adhesive (SMAH_F0_1A)	**Tensile index of adhesive (SMAH_F0_1B)**
10644.44599	11248.19172
9963.457334	9584.842793
11570.71421	9940.628765
8181.281369	7080.82602
13186.41291	9967.547269
11199.58908	10886.51287
12263.52337	10229.20601
7123.265976	8717.340533
11401.84465	8449.718696
	11339.2651

F-Test Two-Sample for Variances

	Variable 1	*Variable 2*
Mean	10614.95	9487.97
Variance	3718077	2351752
Observations	9	11
df	8	10
F	1.580982	
P(F<=f) one-tail	0.244463	
F Critical one-tail	3.071658	

t-Test: Two-Sample Assuming Equal Variances

	Variable 1	*Variable 2*
Mean	10614.94832	9487.97
Variance	3718077.493	2351752
Observations	9	11
Pooled Variance	2959007.736	
Hypothesized Mean Difference	0	
df	18	
t Stat	1.457622481	
P(T<=t) one-tail	0.081085533	
t Critical one-tail	1.734063607	
P(T<=t) two-tail	0.162171067	
t Critical two-tail	2.10092204	

Tensile index of adhesive (WS_F50_1A)	Tensile index of adhesive (WS_F50_1B)
1283.131698	1915.215932
3530.729594	1378.887795
1133.332434	2885.619492
4336.364377	3066.779362
1214.161602	4248.465099
5196.624752	2130.852692
1965.609179	1939.115164
2053.817085	3907.145288

F-Test Two-Sample for Variances

	Variable 1	*Variable 2*
Mean	2589.22134	2684.01
Variance	2447045.846	1040854
Observations	8	8
df	7	7
F	2.350998143	
P(F<=f) one-tail	0.140976949	
F Critical one-tail	3.78704354	

t-Test: Two-Sample Assuming Equal Variances

	Variable 1	*Variable 2*
Mean	2589.22134	2684.01
Variance	2447045.846	1040854
Observations	8	8
Pooled Variance	1743949.928	
Hypothesized Mean Difference	0	
df	14	
t Stat	-0.143555503	
P(T<=t) one-tail	0.443948655	
t Critical one-tail	1.761310136	
P(T<=t) two-tail	0.887897309	
t Critical two-tail	2.144786688	

Tensile index of adhesive (W_F50_1A)	Tensile index of adhesive (W_F50_1B)
1699.559376	2580.318726
1468.747899	2074.224376

2640.027869	2277.254086
2939.731918	2223.191399
3977.002694	2391.414162
1648.604309	1748.005451
3203.977484	4928.97669
2526.478283	3290.311567
2246.438033	4520.943591
	3235.46172

F-Test Two-Sample for Variances

	Variable 1	*Variable 2*
Mean	2483.396	2927.01
Variance	672708.4	1135280
Observations	9	10
df	8	9
F	0.592548	
P(F<=f) one-tail	0.236329	
F Critical one-tail	0.295148	

t-Test: Two-Sample Assuming Unequal Variances

	Variable 1	*Variable 2*
Mean	2483.396429	2927.01
Variance	672708.4493	1135280
Observations	9	10
Hypothesized Mean Difference	0	
df	17	
t Stat	-1.022375686	
P(T<=t) one-tail	0.160466308	
t Critical one-tail	1.739606726	
P(T<=t) two-tail	0.320932616	
t Critical two-tail	2.109815578	

Tensile index of adhesive (NHW_F50_1A)	Tensile index of adhesive NH(W_F50_1B)
2060.17698	1553.843451
1902.46548	4413.337782

2283.830004	2250.59847
2762.882582	2493.943199
1779.951396	1574.635788
2454.961016	2287.070921
3186.222958	4532.00095
3975.051806	3515.244619
1131.725288	5717.230931
1251.908504	3434.308554
1783.506314	
1807.75588	

F-Test Two-Sample for Variances

	Variable 1	*Variable 2*
Mean	2198.37	3177.221
Variance	651291.9	1924102
Observations	12	10
df	11	9
F	0.338491	
P(F<=f) one-tail	0.047033	
F Critical one-tail	0.345277	

t-Test: Two-Sample Assuming Equal Variances

	Variable 1	*Variable 2*
Mean	2198.369851	3177.221
Variance	651291.911	1924102
Observations	12	10
Pooled Variance	1224056.396	
Hypothesized Mean Difference	0	
df	20	
t Stat	-2.016309779	
P(T<=t) one-tail	0.025997595	
t Critical one-tail	1.724718243	
P(T<=t) two-tail	0.05199519	
t Critical two-tail	2.085963447	

Tensile index of adhesive (W_F0_1A)	**Tensile index of adhesive NHW_F50_1B)**
7849.485434	7701.818755
7339.704827	7445.313162
6822.790885	6810.998587

6819.110847	9497.579605
7082.987624	7481.120233
9746.844122	7591.210297
7271.78496	8497.734001
9109.852034	9491.344324
6647.760248	8066.826667
10113.14774	9488.943276

F-Test Two-Sample for Variances

	Variable 1	*Variable 2*
Mean	7880.347	8207.289
Variance	1671576	972553.5
Observations	10	10
df	9	9
F	1.71875	
P(F<=f) one-tail	0.216059	
F Critical one-tail	3.178893	

t-Test: Two-Sample Assuming Equal Variances

	Variable 1	*Variable 2*
Mean	7880.346873	8207.289
Variance	1671576.293	972553.5
Observations	10	10
Pooled Variance	1322064.917	
Hypothesized Mean Difference	0	
df	18	
t Stat	-0.635812923	
P(T<=t) one-tail	0.266449865	
t Critical one-tail	1.734063607	
P(T<=t) two-tail	0.53289973	
t Critical two-tail	2.10092204	

2. Pearson correlation

Table 16: Data of 6 lignins (*W, SMAH, SMAH_IRR50, SMAH_IRR100, MS, WS)*

	PD	*Mw*	*Mn*	*Change in*	*Change in*	*Change in*	*S/G*	*Differenc*	*Tg*	*Total*	*ASL*	*Klason*	*Young's*	*Tensile*	*PD*	*Mw*	*Mn*	*PhOH*	*Xylan*	*Ash*
Ash																				1
Xylan																				0.92908
PhOH																				0.11572
Mn																				0.31446
Mw																				0.40273
PD																				0.46577
Tensile																				-0.16865
Young's																				0.03751
Klason																				-0.68017

										1.00000
									1.00000	0.83747
								1.00000	0.79450	0.34160
							1.00000	0.24062	-0.13302	-0.32120
						1.00000	0.99012	0.34120	-0.07552	-0.33075
					1.00000	0.86915	0.79748	0.59274	0.03030	-0.43887
				1.00000	-0.05847	0.19368	0.29778	-0.31335	-0.33862	-0.17747
			1.00000	0.59650	0.65177	0.89572	0.93709	0.17321	-0.12909	-0.24575
		1.00000	0.30908	-0.46795	0.83069	0.62141	0.51292	0.86929	0.50999	0.03023
	1.00000	0.81666	0.62600	-0.22396	0.92108	0.90702	0.84754	0.46591	0.01362	-0.33943
1.00000	0.48048	0.03215	0.53340	0.35643	0.55790	0.56679	0.57828	-0.29327	-0.80114	-0.94889
0.41853	0.99756	0.84638	0.60172	-0.26432	0.91174	0.89198	0.82844	0.50958	0.07888	-0.27859
0.59162	-0.15319	-0.27647	-0.33025	-0.02696	0.00576	-0.26375	-0.29075	-0.40464	-0.70754	-0.80757
0.07093	-0.11198	0.15558	-0.64575	-0.53196	0.05705	-0.41993	-0.52241	0.16091	-0.06729	-0.35639
-0.94893	-0.66029	-0.20971	-0.75983	-0.40398	-0.70822	-0.79017	-0.80437	0.11759	0.62983	0.80926
-0.99066	-0.58367	-0.13634	-0.62366	-0.34596	-0.64724	-0.67367	-0.68136	0.20275	0.72937	0.90717
-0.98029	-0.59730	-0.13319	-0.52155	-0.20594	-0.61123	-0.62876	-0.62981	0.26166	0.77035	0.92773
0.68026	-0.10601	-0.33917	-0.24051	0.03166	0.00249	-0.18472	-0.19345	-0.53243	-0.82765	-0.86492
-0.48929	-0.94767	-0.93158	-0.43174	0.46169	-0.96671	-0.77461	-0.67399	-0.72990	-0.00487	0.47554
-0.32388	-0.67793	-0.81205	-0.53535	-0.03731	-0.89311	-0.65942	-0.57744	-0.79800	-0.29311	0.23287
ASL	Total	Tg	Differenc	S/G	Change in	Change in	Change in	resin Mn	resin Mw	resin PD

Table 17: p values: Tensile strength column is in bold to showcase no value is <0.05

p value	Ash	Xylan	PhOH	Mn	Mw	PD	Tensile	Young's	Klason	ASL
PD	1	1	1.000	1.000	1.000	1.000	1.000	1.000	1.000	1.000
Mw	1	1	1.000	1.000	1.000	1.000	1.000	1.000	1.000	1.000
Mn	1	1	1.000	1.000	1.000	1.000	1.000	1.000	1.000	1.000
Change in	1	1	1.000	1.000	1.000	1.000	1.000	1.000	1.000	1.000
Change in	1	1	1.000	1.000	1.000	1.000	1.000	1.000	1.000	1.000
Change in	1	1	1.000	1.000	1.000	1.000	1.000	1.000	1.000	1.000
S/G	1	1	1.000	1.000	1.000	1.000	1.000	1.000	1.000	1.000
Differenc	1	1	1.000	1.000	1.000	1.000	1.000	1.000	1.000	1.000
Tg	1	1	1.000	1.000	1.000	1.000	1.000	1.000	1.000	1.000
Total	1	1	1.000	1.000	1.000	1.000	1.000	1.000	1.000	1.000
ASL	1	1	1.000	1.000	1.000	1.000	1.000	1.000	1.000	#DIV/0!
Klason	1	1	1.000	1.000	1.000	1.000	1.000	1.000	#DIV/0!	0.409
Young's	1	1	1.000	1.000	1.000	1.000	1.000	#DIV/0!	0.703	0.216
Tensile	1	1	1.000	1.000	1.000	1.000	#DIV/0!	0.096	0.831	0.894
PD	1	1	1.000	1.000	1.000	#DIV/0!	0.765	0.543	0.201	0.004
Mw	1	1	1.000	1.000	#DIV/0!	0.001	1.000	0.324	0.284	0.000
Mn	1	1	1.000	#DIV/0!	0.000	0.004	0.908	0.274	0.268	0.001
PhOH	1	1	#DIV/0!	0.175	0.226	0.413	0.198	0.001	0.762	0.137
Xylan	1	#DIV/0!	0.832	0.185	0.247	0.232	0.653	0.852	0.004	0.325
Ash	#DIV/0!	0.007	0.827	0.544	0.429	0.352	0.749	0.944	0.137	0.531

Total	Tg	**Differenc**	S/G	Change in	Change in	Change in	resin Mn	resin Mw	resin PD
1.000	1.000	**1.000**	1.000	1.000	1.000	1.000	1.000	1.000	#DIV/0!
1.000	1.000	**1.000**	1.000	1.000	1.000	1.000	1.000	#DIV/0!	0.037
1.000	1.000	**1.000**	1.000	1.000	1.000	1.000	#DIV/0!	0.059	0.508
1.000	1.000	**1.000**	1.000	1.000	1.000	#DIV/0!	0.646	0.802	0.535
1.000	1.000	**1.000**	1.000	1.000	#DIV/0!	0.000	0.508	0.887	0.522
1.000	1.000	**1.000**	1.000	#DIV/0!	0.025	0.057	0.215	0.955	0.384
1.000	1.000	**1.000**	#DIV/0!	0.912	0.713	0.567	0.545	0.511	0.737
1.000	1.000	**#DIV/0!**	0.211	0.161	0.016	0.006	0.743	0.807	0.639
1.000	#DIV/0!	**0.551**	0.349	0.041	0.188	0.298	0.025	0.301	0.955
#DIV/0!	0.047	**0.184**	0.670	0.009	0.013	0.033	0.352	0.980	0.510
0.335	0.952	**0.276**	0.488	0.250	0.241	0.229	0.573	0.055	0.004
0.000	0.034	**0.206**	0.613	0.011	0.017	0.042	0.302	0.882	0.593
0.772	0.596	**0.523**	0.960	0.991	0.614	0.576	0.426	0.116	0.052
0.833	0.769	**0.166**	0.277	0.915	0.407	0.288	0.761	0.899	0.488
0.154	0.690	**0.080**	0.427	0.115	0.061	0.054	0.824	0.180	0.051
0.224	0.797	**0.186**	0.502	0.165	0.142	0.136	0.700	0.100	0.013
0.211	0.801	**0.289**	0.695	0.197	0.181	0.180	0.616	0.073	0.008
0.842	0.511	**0.646**	0.953	0.996	0.726	0.713	0.277	0.042	0.026
0.004	0.007	**0.393**	0.357	0.002	0.070	0.142	0.100	0.993	0.340
0.139	0.050	**0.274**	0.944	0.017	0.154	0.230	0.057	0.573	0.657

Table 18*:* Values of improved strength at F0 and F50 as calculated by Equations (6) and (7), respectively.

	Improvement in tensile at F50 (%)	Improvement in tensile @ F0
W	-45.46	54.16
SMAH	99.02	723.10
MS	450.50	357.00
WS	59.28	51.69
SMAH IRR 50		7.77
SMAH IRR 100	N/A	239.36

RESUME

PRAJAKTA DONGRE, PhD Candidate

118 Harvard Place, Syracuse, NY 13210 | phone: (315)-600-6262 | email: pdongre@syr.edu

PERFORMANCE PROFILE

- Extensive understanding of polymers, wet end chemistry and green technology.
- Creative problem solver with strong attention to detail.
- Strong communication and presentation skills.
- Excellent at collaborating in team settings that involve coaching or advising.
- Exceptional time management and leadership abilities.
- Enthusiastic, adaptive and self-motivated.

EDUCATION

State University of New York-College of Environmental Science Forestry (SUNY-ESF), Syracuse, NY

Doctor of Philosophy, *Bioprocess Engineering* *May 2018*

Research Area: Lignin utilization for green thermoplastics and resins
Synthesis and testing of formaldehyde-free resins

Chulalongkorn University, Bangkok, Thailand

Bachelors of Science, *Nano-engineering* (focused in Bioengineering) *May 2010*

WORK EXPERIENCE

- **Research Assistant,** SUNY-ESF *Spring, 2011 – Fall, 2017*

  Performed polymer synthesis and processing.

  Developed and improved the process of lignin utilization for high value applications.

  Designed experiments at bench and pilot scales.

  Performed analysis of wood, pulp and black liquor using standard TAPPI methods.

  Operated equipment such as extruder, Parr reactor, M/K digester, ultrafilteration membrane, tensile tester and hydraulic press.

  Performed qualitative and quantitative characterization of polymer based materials utilizing various analytical techniques:

  - Developed and set up the SEC method at the PBE department
  - HPLC
  - UV/vis Spectrophotometry
  - NMR

  Regularly performed advanced data capturing, analysis and reporting.

- **Instructor,** SUNY-ESF

  Principles of Mass and Energy Balance *Fall, 2016*

  Professional Engineering Seminar Series - Communication *Fall, 2017*

- **Teaching Assistant,** SUNY-ESF

  Pulping and Bleaching (Lab) *Spring 2017*

  Discover Lignocellulosics (Lab) *Spring, 2017*

  Thermodynamics *Spring, 2014*

  Principles of Mass and Energy Balance *Fall, 2013*

CERTIFICATIONS, SCHOLARSHIPS & AWARDS

- Renata Marton, Graduate Student Award *2016-2017*
- Eastman Award, 2nd place *Fall, 2015*
- Six Sigma Green Belt *Spring, 2011*
- Herman Louis Joachim Graduate Fellowship *Spring, 2011-Spring, 2013*
- Vice-President of International Activities, Graduate Student Association *2012-2013*

PUBLICATIONS

1. Dongre P, Driscoll M, Amidon T.E, and Bujanovic B (2015) "Lignin-furfural based adhesives" Energies. 8:7897-7914.
2. Wang KT, Jing C, Wood C, Nagardeolekar A, Kohan N, Dongre P, Amidon T, Bujanovic B (2017) "Toward Complete Utilization of Miscanthus in a Hot-Water Extraction-Based Biorefinery" Energies, 11(1): 39-62
3. Dongre P, Nagardeolekar A, Wang K, Jing C, Wood C, Kohan N, Amidon T and Bujanovic B (2017) "Use of Angiosperm Lignocellulosics in a Biorefinery Based on Hot Water Extraction: Willow, Miscanthus, and Wheat Straw" Oral presentation at the International Conference on Biomass Conversion and Renewable Materials, August 14-17. Syracuse, NY
4. Dongre P, Driscoll M, Amidon T.E, and Bujanovic B (2015) "Increasing the value of the biorefinery: Lignin based adhesives and thermoplastics" Oral presentation at PacifiChem Conference, December 14-20. Honolulu, HI.
5. Dongre P, Driscoll M, Smith J, Amidon T.E, and Bujanovic B (2015) "Potential uses of hot-water extracted lignin – thermoplastics and adhesives" Poster presented at TAPPI-IBBC Conference, October 28-30. Atlanta, GA. *Poster competition at TAPPI-IBBC - 1st place*